BIOSYNTHESIS OF SILVER AND SELENIUM NANOPARTICLES USING EXTRACTS OF *COMMELINA AFRICANA* AND THEIR BIOLOGICAL ACTIVITY

BY

SILUNGILE PEARL MHLONGO

2019

Submitted in fulfilment of the academic requirements for the degree of Master of Science in the School of Chemistry and Physics at the University of KwaZulu-Natal, Durban

As the candidate's supervisor, I have approved this dissertation for submission

Signed: _____ Name: _____

Date: _____

ABSTRACT

Commelina africana is an indigenous medicinal plant that belongs to the Commelinacaea family. This plant is traditionally used for the treatment of venereal diseases and burns, and it is eaten as a vegetable. Despite the plants medicinal and nutritional significance, it has not been phytochemically investigated.

Nanoparticles are currently being investigated for their medicinal value. Different synthesis techniques, especially those that are less toxic, inexpensive and more environmentally friendly are being explored. The use of plant material to synthesise nanoparticles is known to be a greener and safer method. These nanoparticles have potential for applications in the biomedical sciences. Currently, silver nanoparticles (AgNPs) are being used for the dressing of wounds and prevention of infections. Selenium nanoparticles (SeNPs) are being used biologically as antioxidants.

This study aimed at extracting, isolating and characterising the secondary metabolites from *C. africana*. The crude aqueous and methanolic extracts from the plant were used to synthesise AgNPs and SeNPs at varying extract volumes. The crude extracts served as reducing agents and reduced Ag^{+} and Se^{4+} to their elemental states. The synthesised nanoparticles were tested for their antioxidant activities (using the 1,1-diphenyl-2-picrylhydrazyl (DPPH) and ferric reducing antioxidant power (FRAP) assays) and antibacterial activities relative to the extracts from which they were synthesised and known standards.

Four phytosterols (stigmasterol, ergosterol peroxide, *β*-sitosterol and campestanol) were isolated and identified from the extracts of *C. africana*. AgNPs and SeNPs were synthesised using the plant material and characterised using spectroscopic and microscopic techniques. AgNPs consisted of spheres and SeNPs showed a mixture of spheres and rods. Both types of nanoparticles had a wide particle size range.

For the antioxidant activity, ergosterol peroxide showed good radical scavenging activity by the DPPH test whilst SeNPs synthesised using the methanol extract showed good radical scavenging activity and reducing potential by the DPPH and FRAP tests, respectively. Crude extracts, phytocompounds and nanoparticles were tested against two Gram-positive bacteria (*Enterococcus faecalis* and *Staphylococcus aureus*) and four Gram-negative bacteria (*Pseudomonas aeruginosa, Escherichia coli, Klebsiella pneumoniae* and *Chromobacterium violaceum*) for their antibacterial activity. Plant synthesised AgNPs showed satisfactory inhibitory activity against the growth of all bacterial strains except *E. faecalis.* These nanoparticles also exhibited anti-quorum sensing abilities indicating their potential to block cell-to-cell signalling that is used to determine their physiological activities and for co-ordinated gene expression.

This study adds to the base of knowledge on the medicinal plant species, *C. Africana* and highlights the synergistic effects between AgNPs and SeNPs with active plant biomolecules for biological systems. The findings of this study also indicate that medicinal plants can be used as a greener and more environmentally friendly technique for the synthesis of AgNPs and SeNPs.

DECLARATION – PLAGIARISM

I, Silungile Pearl Mhlongo_____ declare that

1. The research reported in this thesis, except where otherwise indicated; is my original research.

2. This thesis has not been submitted for any degree or examination at any other university

3. This thesis does not contain other person/s data, pictures, graphs or other information, unless specifically acknowledged as being sourced from the other person/s.

4. This thesis does not contain other person/s writing, unless specifically acknowledged as being sourced from other researcher/s. Where other written sources have been quoted, then:

5. Their words have been re-written but the general information attributed to them has been referenced.

6. Where their exact words have been used, then their writing has been placed in italics and/or inside quotation marks, and referenced.

7. This thesis does not contain text, graphics or tables copied and pasted from the internet, unless specifically acknowledged, and the source being detailed in the thesis in the Reference section.

Signed: _____

PREFACE

The experimental work described in this thesis was carried out in the School of Chemistry and Physics at the University of KwaZulu-Natal, Durban, from July 2016 to December 2018 under the supervision of Dr Roshila Moodley and Dr Karin Pruessner.

These studies present original work by the author and have not otherwise been submitted in any form for any degree or diploma to any tertiary institution. Where use has been made of the work of others, it is duly acknowledged in the text.

Signed: _____ Name: _____

Date: _____

DEDICATION

This work is dedicated to the memory of my late grandparents; Apostle M.H and Mrs S.B Mhlongo.

ACKNOWLEDGEMENTS

I would like to start off by thanking God Almighty for the strength He has given me to pull through this challenging and defining moment of my life and career.

My sincere gratitude goes to my supervisor Dr R Moodley for holding my hand and guiding me through what I would describe as a maze. I am also grateful for the scientific knowledge you have imparted to me.

To my parents who have been very supportive (but not always understanding) of my studies; words fail me. Your hard work and selfless sacrifices throughout the years have not gone unnoticed. I would like to thank my grandfather Apostle M.H Mhlongo who has always wanted me to further my studies, no matter the circumstances. Though you could not live long enough to read this in print, in my heart you will remain one of my biggest cheerleaders.

I am thankful for all the support I received from my siblings (Nombulelo, Thandeka and Sphesihle), aunts (Thobekile and Zanele), uncle (Bongani), cousin (Siphumelele) and niece (Thobisa).

Thank you to Mr Mbhele for providing me with the herbs for my research.

I would like to thank the technical staff of the Chemistry (Dillip, Vuyo, Unathi, Jeremiah and Maila) and Microscopy departments (Subashen, Philip, Vishal and S'khumbuzo) for all their help. I would also like to extend my gratitude to Dr H. Y. Chenia and Farzana Mohamed for their assistance and guidance through the antibacterial testing process.

I would like to thank my colleagues and friends from UKZN Westville campus. Andiswa Ntshele, Mxolisi Sokhela, Vuyisile Mahlaba, Nonhlanhla Joyisa, Ntombizodwa Vundla, Paul Awolade, Kimona Kisten, Lamla Thungatha, Joel Mavuso, Noxolo Mqadi, Esther Ofusori, Zamokuhle Buthelezi and Valentine Uwumubyenyi; thank you for your support. Bongisiwe

Shelembe, our sleepless nights seem to have finally paid off. Dr Sunday Bodede, thank you so much for all your assistance.

A special thank you goes to Dr Nomfundo Mahlangeni, the dynamite in a small package. The unwavering academic and emotional support you have not given only to me but to everyone else in the Natural Products lab is one of the best things to bear witness of. Ngiyabonga angiphezi.

TABLE OF CONTENTS

LIST OF ABBREVIATIONS

^{1}H-NMR Proton nuclear magnetic resonance spectroscopy

^{13}C-NMR Carbon 13- nuclear magnetic resonance spectroscopy

C. violaceum *Chromobacterium violaceum*

CC Column chromatography

COSY Correlation spectroscopy

CAgNPs-A Silver nanoparticles synthesised from the aqueous extract

CAgNPs-M Silver nanoparticles synthesised from the methanol extract

CSeNPs-A Selenium nanoparticles synthesised from the aqueous extract

CSeNPs-M Selenium nanoparticles synthesised from the methanol extract

d Doublet

dd Doublet of doublets

DCM Dichloromethane

DEPT Distortionless enhancement by polarisation transfer

DPPH 2,2-diphenyl-1-picrylhydrazyl

E. coli *Escherichia coli*

EDX Energy-dispersive X-ray spectroscopy

E. faecalis *Enterococcus faecalis*

EtOAc Ethyl acetate

FTIR Fourier-transform infrared

GC-MS Gas chromatography-mass spectrometry

HMBC Heteronuclear multiple bond correlation

LRMS Low resolution mass spectroscopy

HRTEM High resolution transmission electron microscopy

HSQC Heteronuclear single quantum coherence

J Coupling constant

K. pneumonia *Klebsiella pneumonia*

m Multiplet

MeOH Methanol

NPs Nanoparticles

P. aeruginosa *Pseudomonas aeruginosa*

ppm parts per million

QSI Quorum sensing inhibition

s Singlet

S. aureus *Staphylococcus aureus*

SAED Selected area electron diffraction

SEM Scanning electron microscopy

Std Dev Standard deviation

t Triplet

TEM Transmission electron microscopy

TLC Thin-layer chromatography

UV-Vis Ultraviolet visible spectroscopy

AgNPs Silver nanoparticles

SeNPs Selenium nanoparticles

LIST OF FIGURES

LIST OF TABLES

CHAPTER ONE

1.1. Introduction

Since time immemorial, people have been using plants to meet their nutritional and medicinal needs. Traditional medicine refers to the use of medicinal methods and theories that have been passed on from generation to generation. These practices have been around for centuries but differ from country to country. Traditional medicine can be used for spiritual purposes and as herbal remedies. Asian and African communities strongly advocate the use of traditional medicine. About 80% of Africans currently use traditional medicine for their healthcare needs (Oyebode et al., 2016). In disadvantaged communities, primary healthcare services may be found on the outskirts of the area or are not readily available. Therefore, traditional medicine serves as a substitute. Plant and animal parts have been used for treatment for centuries and these practices are highly trusted, especially in rural communities. Herbalists have vast knowledge of the medicinal benefits of plants and use the aqueous extracts, decoctions or dry plant material for treatment.

Medicinal plants have been studied extensively and some isolated compounds from medicinal plants such as quercetin and curcumin are well known. Most of these phytocompounds are recognised for their biological activities such as antimicrobial, antioxidant and anti-inflammatory (Acamovic & Brooker, 2007). Some of the popular naturally occurring compounds that have been discovered include caffeine and cocaine. Caffeine is a natural stimulant used from plants since the Stone Ages. Although prehistoric man was unaware of the existence of caffeine, they used plants that contained this stimulant for both recreational and medicinal purposes. Caffeine was isolated nearly two hundred years ago from mocha beans.

Today, this naturally occurring alkaloid has been isolated from over sixty plant species and is enjoyed by many.

In this study, we conduct a phytochemical investigation on the medicinal plant species, *Commelina africana* L. This herbaceous plant has been commonly used in traditional medicine to treat venereal diseases such as gonorrhoea (Attah et al., 2012). Minimum research has been done on this species unlike *Commelina benghalensis* L. of the same genus, which is a perennial herb that is indigenous to Africa and Asia. *Commelina benghalensis* is used to treat mouth thrush, snakebites, burns and is used as a laxative (Khan et al., 2011). Research conducted on the extracts from *C. benghalensis* indicated good antibacterial activity against *Salmonella typhi, Escherichia coli, Staphylococcus aureus* and *Enterococcus faecalis* (Khan et al., 2011). This provides a scientific basis for the traditional use of this plant to treat infections caused by burns.

Plants have also displayed the ability to accumulate heavy metals (Iravani, 2011). This ability to take up and reduce metal ions indicates that plant material (extracts, tissues or whole plants) are good natural reducing agents. This phenomenon is exploited in the synthesis of nanoparticles (Mittal et al., 2013). The use of plant material for the formation of nanoparticles has many advantages when compared to traditional chemical methods. These advantages include the use of less toxic solvents and materials. The process is also less expensive and readily scalable. Interest in biosynthesis of nanoparticles has grown in recent years because of these advantages (Iravani, 2011; Mittal et al., 2013).

The use of medicinal plants to synthesise nanoparticles falls under the nanomedicine structure. Due to potential application in the medical field, nanomaterials are also being researched for their anticancer properties due to the side effects of current drugs that are in use (Iravani, 2011; Mittal et al., 2013). This field of research has recently begun to gain momentum. The aqueous

leaf extract of *Diospyros montana* was used to synthesise selenium nanoparticles which were then examined for their antioxidant and antibacterial properties (Kokila et al., 2017). The nanoparticles were shown to possess good antimicrobial activity against *Staphylococcus aureus* and *Escherichia coli*, as well as substantial antioxidant activity that was particle size dependent (Kokila et al., 2017). A study on the synergistic antibacterial effects of silver nanoparticles synthesised using the extracts of the leaves of *Capparis spinosa* and antibiotics was conducted against *Escherichia coli*, *Staphylococcus aureus*, *Salmonella typhimurium* and *Bacillus cereus* (Benakashani et al., 2016). The study revealed the antibacterial activity of the synthesised nanoparticles, especially against *E. coli* (Benakashani et al., 2016).

1.2. Problem statement

For centuries, plants have been used by traditional healers in African communities for the treatment of various illnesses. Research into active biomolecules has sparked interest in this field of science as these phytocompounds have been shown to possess pharmaceutical and medicinal properties (Cooper & Nicola, 2014). Modern medicine has a large array of pharmaceuticals at their disposal but, despite these scientific breakthroughs, new challenges develop such as drug resistance. Natural products are being explored to overcome these challenges. Additionally, scientific approaches to improving the activity of natural products are being explored such as combinations with metal nanoparticles. Some of these metals include selenium and silver. Investigations into biosynthesised nanoparticles may lead to the discovery of more efficient and environmentally friendly pharmaceuticals, including antibiotics. This could lead to the replacement of conventional drugs, especially antibiotics such as those that contain fluoroquinolines, which have disabling and potentially permanent side effects.

1.3. Aims and objectives

The aim of this study was to conduct a phytochemical investigation on the medicinal plant species, *Commelina africana* L., to synthesise metal nanoparticles using the plant-mediated synthesis route and to evaluate their biological activity.

The objectives were:

1. The extraction, isolation and identification of secondary metabolites from the leaves of *Commelina Africana* using spectroscopic techniques including nuclear magnetic resonance spectroscopy (NMR).

2. The synthesis of selenium and silver nanoparticles from the crude extracts (aqueous and methanol) of the leaves.

3. Characterisation of nanoparticles by scanning electron microscopy (SEM), ultraviolet–visible spectroscopy (UV-Vis), transmission electron microscopy (TEM) and Fourier-transform infrared spectroscopy (FTIR).

4. Investigation of nanoparticles, plant extracts and pure phytocompounds for biological activity (antibacterial and antioxidant).

CHAPTER TWO

LITERATURE REVIEW

2.1. Traditional medicine

The World Health Organization (WHO) defines traditional medicine as being the bulk of knowledge, ability and applications that are unique to different cultures based on their different theories and beliefs (World Health Organization, 2000). Traditional medicine is used to maintain health as well as prevent, diagnose and treat various physical and mental illnesses (World Health Organization, 2000). There is great diversity in traditional medicine, with practices differing from country to country, and from region to region (World Health Organization, 2000; World Health Organization 2005). One of the advantages of using traditional medicine is that it has a long history. These practices have been passed down from generation to generation. The people who have inherited these cultural practices have a vast knowledge and understanding of the properties of medicinal plants. In as much as traditional medicine has been around for centuries, there is still a great need for scientific research to provide additional evidence in terms of its safety and efficacy (World Health Organization, 2005). Research can help developing and developed countries introduce traditional medicine as part of their primary healthcare services. This could greatly benefit underprivileged communities that depend solely on these treatments because of the expensive costs of modern medicine.

Reduced access to basic healthcare is the reality for majority of the population in African countries. According to Statistics South Africa, the top five rated killers in South Africa in 2015 were tuberculosis, diabetes, strokes, heart related diseases and HIV. These diseases

spread more rapidly in vulnerable communities as patients are either unaware of their affliction or there is lack of treatment and hospital facilities. In most cases, the only option is to seek alternative medical advice from local herbalists. In the Kwahu District of Ghana, the ratio of traditional practitioner to patient is one to two hundred patients and one to twenty thousand patients for a medical practitioner (Rukangira, 2001). This results in long waiting periods at public clinics and hospitals with patients being turned away before receiving treatment. As a result, afflicted patients including those infected with HIV, rely less on modern medicine and more on traditional medicine. Medicinal plants such as *Hypoxis hemerocallidea* and *Sutherlandia* are used by traditional healers for the treatment of HIV in sub-Saharan Africa (Mills et al., 2005). The South African Ministry of Health has since recommended these two species for the treatment and management of HIV (Mills et al., 2005). Phytochemical studies on *H. hemerollidea* revealed the presence of hypoxides, sterols, stanols and sterol glycosides in the plant that could be responsible for the medicinal effects (Mills et al., 2005).

2.2. A South African view on traditional medicine

In a study conducted by WHO, an estimated 80% of South Africans make use of traditional medicine as part of their primary healthcare (World Health Organization, 2005; Street et al., 2012). This equates to approximately forty million South Africans (Street et al., 2012). The trade of traditional medicine is estimated to contribute about R 2.9 billion to the country's economy (Mander et al., 2007). The general perception with people who consume traditional medicine is that majority are uneducated. However, this is not the case, as a survey conducted in Durban, South Africa indicated a greater diversity of consumers (Fig 2.1) (Mander et al., 2007).

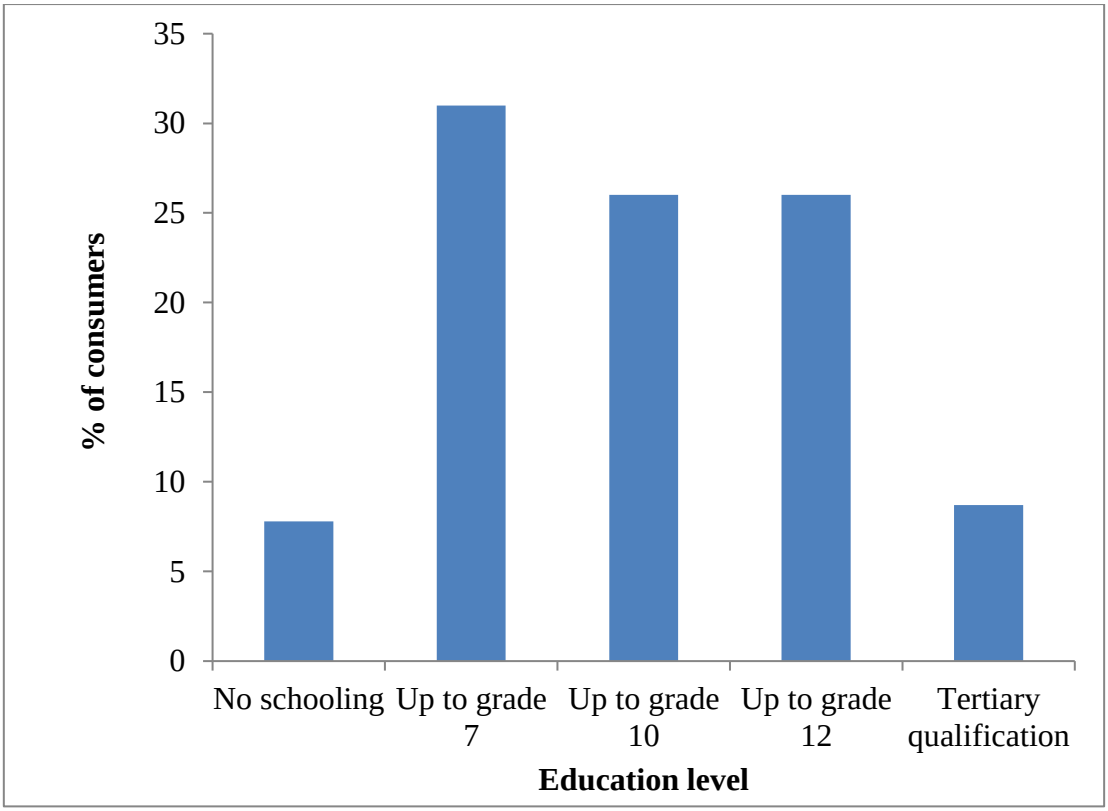

Figure 2.1: Depiction of levels of education of medicinal plant consumers in Durban (Mander et al., 2007)

Traditional medicine consumption in South Africa, which is one of the most developed countries in the African continent, is similar to less developed countries such as Ethiopia (Mander et al., 2007). On average, a South African consumer purchases traditional medicine approximately five times per year compared to six times for an Ethiopian consumer (Mander et al., 2007). The medicinal plant trade in South Africa has between 400 000 to 500 000 traditional practitioners with approxinately 1000 medicinal plant species traded in both urban and rural areas of the country (Mahlangeni, 2012). It is also estimated that 133 000 households earn a living through this trade (Mander et al., 2007). These medicines are dispensed as both herbal decoctions and crude herbs using different plant parts (Fig 2.2 and 2.3).

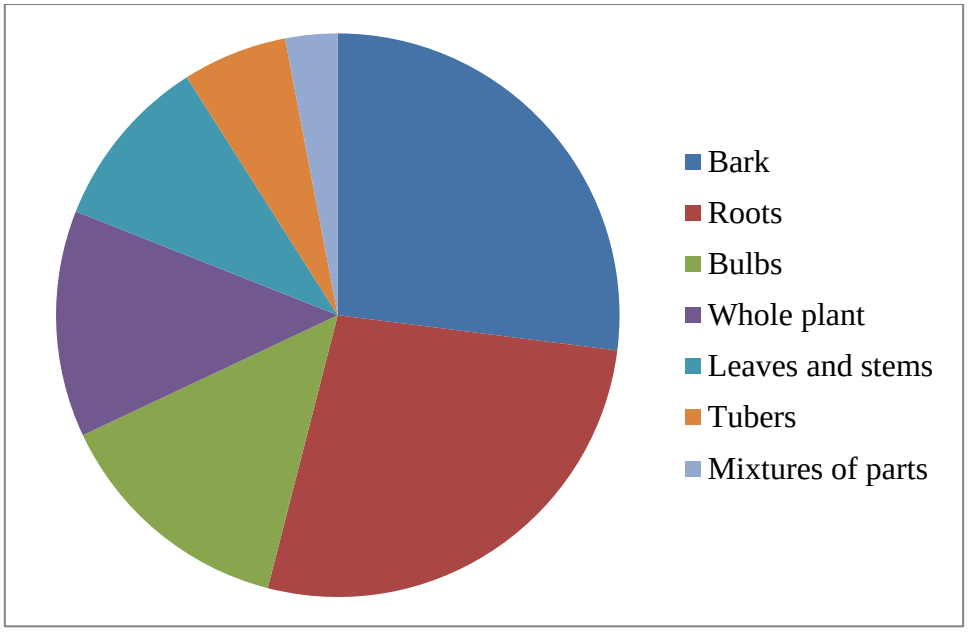

Figure 2.2: Various parts of the plant used by traditional practitioners (Mander et al., 2007; Bouayad et al, 2012)

Figure 2.3: Various plant parts traded at the Durban Muthi Market

There is increasing concern about the safety and efficacy of traditional medicine due to the use of unlabelled decoctions and mixtures. This has led to WHO enforcing proper labelling of herbal remedies that should include a list of all active ingredients, the plant name, the manufacturing and expiry date, the dosage recommendations and therapeutic indications (World Health Organization, 2005).

2.3. Use of plants and natural products in healthcare

2.3.1. Primary and secondary metabolites

Natural products are the products given to us by nature including plants, sand, fungi, bacteria etc. Natural products from plants can be divided into two major classes, namely, primary and secondary metabolites. Metabolites are usually found as small molecules that act as intermediates in the metabolic processes in nature (Cooper & Nicola, 2014). Primary metabolites are the molecules that have a direct involvement in the development, growth and reproduction of the natural species (Cooper & Nicola, 2014). Examples of primary metabolites include vitamins, amino acids, lipids, carbohydrates and proteins. Secondary metabolites are often derived and modified from primary metabolites and are produced by organisms for survival in their environment. Secondary metabolites are grouped into various classes based on the functionality of the molecule (Cooper & Nicola, 2014). These include, but are not limited to, alkaloids, saponins, sterols, terpenes and flavonoids. Plant secondary metabolites are also known as phytocompounds.

2.3.1.1. Phytosterols

Phytosterols are secondary metabolites that are found in the fat soluble parts (or extractions) of plants. These secondary metabolites are present in all plant foods and animals and are formed as by-products in the biosynthesis of isoprenoids. The structural backbone of phytosterols

includes three infused six membered rings (A, B and C) and a five membered ring (D) (Fig 2.4). Phytosterols consist of the hydroxyl group (-OH) at carbon 3 and they are divided into two categories which are Δ^5-sterols and stanols. Δ^5-sterols are the common phytosterols that have a double bond between the carbons at position 5 and 6, and stanols would lack the double bond at that position (Fig 2.5). With over 250 phytosterols reported to date, the three most abundant phytosterols are *β*-sitosterol, stigmasterol and campesterol. Phytosterols are structurally similar to cholesterol. Cholesterol has an eight carbon side chain, while the majority of common phytosterols have a side chain with nine or ten carbons (Kritchevsky & Chen, 2005).

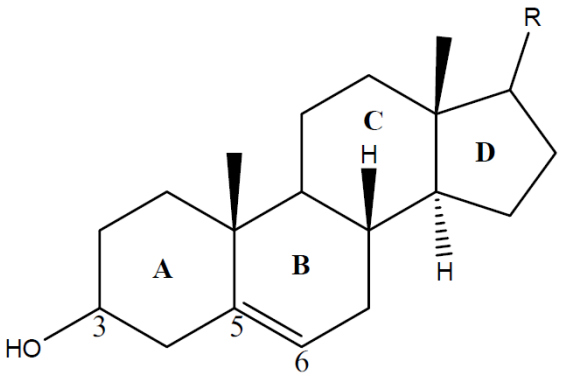

Figure 2.4: Basic skeleton of sterols

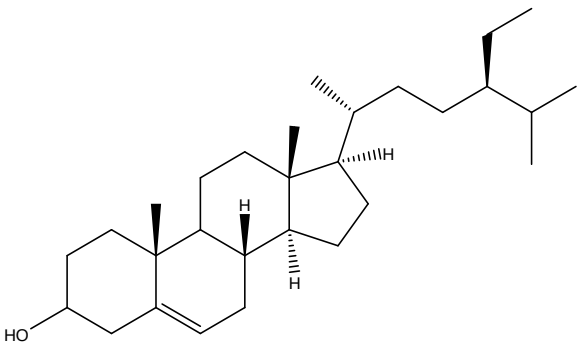

***β*-Sitosterol**

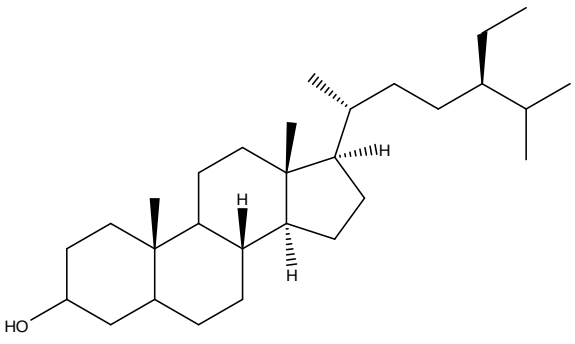

Sitostanol

Figure 2.5: Phytosterols (*β*-sitosterol and sitostanol)

Phytosterols can exist as freestanding compounds, esters or glycosides (Harborne, 1984). The esterification of phytosterols makes them more fat-soluble, which then allows integration into fat-containing foods (Ogbe et al., 2015). In plants, phytosterols ensure and regulate the permeability of the cell membranes. For decades phytosterols have been used for the treatment of hypercholesterolemia to lower cholesterol levels in the blood by promoting the absorption of cholesterol in the lumen of the intestines (Kritchevsky & Chen, 2005; Panpipat et al., 2015). Phytosterols competitively replace cholesterol in mixed micelles, even when the human body only absorbs about 5% of ingested phytosterols against the net absorption of 60% cholesterol (Rocha et al., 2011). The lowering of serum cholesterol helps to decrease the chances of cardiovascular and coronary heart disease (Rocha et al., 2011). Of the 5% of phytosterols absorbed, only 1% is retained in the liver (Rocha et al., 2011).

The effects of a phytosterol-poor (126 mg/day) and phytosterol-rich (449 mg/day) diet, on cholesterol absorption, was investigated (Lin et al., 2011). The results showed phytosterols to lower cholesterol absorption and increase cholesterol excretion rate (Lin et al., 2011). Phytosterols have been incorporated in foods such as yoghurts, fat spreads and salad dressings to reduce serum cholesterol levels. Phytosterols, sitosterol in particular, have gained prominence for their ability to induce apoptosis in cancerous cells and decrease the likelihood of cancer (Ogbe et al., 2015; Shahzad et al., 2017). A study on the effects of a phytosterol/sterolin mixture on healthy individuals, patients living with HIV without treatment and patients living with HIV and taking the phytosterol/sterolin mixture was conducted (Breytenbach et al., 2001). The results of the study showed treated patients to exhibit a Th-1 cytokine pattern of secretion in the cells (Breytenbach et al., 2001). Th-1 is a tumour suppressor; these findings highlight a preventative method for cancer in HIV patients (Grattan, 2013).

2.3.1.2. Alkaloids

Alkaloids that occur in nature contain at least one nitrogen atom usually located in a cyclic ring (Cooper & Nicola, 2014; Evans & Evans, 2009). Alkaloids were first isolated in the nineteenth century and they were among the first natural products to have been isolated (Cooper & Nicola, 2014; Evans & Evans, 2009). They are alkali-like which means that they are basic in nature (Evans & Evans, 2009). The isolation of alkaloids involves a series of acid – base extractions. Plants produce alkaloids to defend themselves against animals and pathogens (Bouayad et al., 2012). These properties have been exploited for use as pesticides and rat (or human) poison, for example, strychnine. They are also used medicinally. Alkaloids are divided into six major groups:

a) Alkaloids that contain the nitrogen atom in the heterocycle and originate from amino acids
b) Polyamine alkaloids
c) Protoalkaloids from amino acids
d) Pseudoalkaloids
e) Purine-like alkaloids
f) Peptide and cyclopeptide alkaloids

The first documented alkaloid from a plant species was morphine (Fig 2.6) that was isolated from *Papaver somniferum* (opium poppy).

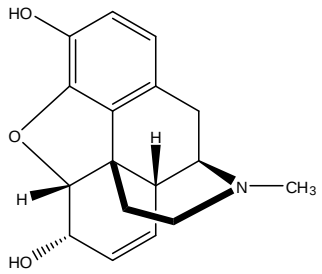

Figure 2.6: Chemical structure of morphine

2.3.1.3. Saponins

Saponins are naturally occurring groups of phytocompounds found in a large array of plant species. These secondary metabolites are normally characterised by their ability to create foam in aqueous solution, hence the name saponins (Milgate & Roberts, 1995). Structurally, saponins can be seen as glycosides and can be classified into two major groups (triterpenes and steroids). Steroid saponins are usually found in monocotyledons and triterpene saponins are found in dicotyledons (Bone, 2013). Triterpene saponins are more common. The uses of saponins range from food and beverages to pharmaceuticals. Due to their ability to create a soapy lather, they have been used traditionally as natural detergents (Tamura et al., 2012). Biologically, they are known to exhibit anti-inflammatory, cytotoxic, antifungal and haemolytic activity (Negri & Tabach, 2013).

2.4. An overview of the Commelinaceae family

Commelinaceae is a family of herbaceous flowering plants. These plants are terrestrial herbs that are also tree climbers. Plants of the Commelinacaea family are botanically characterised by their jointed stems with sheathing leaves. The plants in this family are represented by 50 genera and about 600 species, worldwide (Wilson, 1981). Of the fifty genera, the most common ones include *Tradescantia*, which is a class of spiderworts, and *Commelina*, which consists of dayflowers. The most common species from the Commelinaceae family are *Commelina benghalensis*, *Commelina diffusa* and *Murdannia nudiflora* (Wilson, 1981).

2.4.1. The genus Commelina

The *Commelina* genus comprises 170 known flowering species that have a short life span. The plants in this genus are creeping herbs that mostly grow in moist areas but are tolerant of dry conditions. This genus consists of plants such as *C. benghalensis*, *C. diffusa*, *Commelina*

nudiflora and *Commelina robusta*. These plants can be found as weeds around plantations. The listed species are widespread and are native to the African and Asian continents.

2.4.2. Medicinal uses of Commelina plants

Depending on the geographical location, species from this genus may be used to treat a variety of ailments. *C. benghalensi*s is used in African traditional medicine to treat sore throat, eye infections, burns, infertility and sore feet (Ibrahim et al., 2010). In Asia, it is used as a laxative and anti-depressant, as well as for the treatment of leprosy, mouth thrush and psychosis (Khan et al., 2011a). Other species in this genus have common traditional uses that include treatment of urinary tract infection, influenza, abscess, backache, diarrhoea, laryngitis and boils (Ibrahim et al., 2010; Khan et al., 2011a; Khan et al., 2011b).

2.4.3. Phytochemical studies of Commelina species

A phytochemical screening of *C. nudiflora* extracts yielded positive results for sterols, terpenoids, tannins, flavonoids and cardiac glycosides (Suganya & Jothi, 2014). The extracts of this plant showed good radical scavenging antioxidant activity that was concentration dependent (Suganya & Jothi, 2014). The ethanolic extract from *C. benghalensis* was profiled for its phytochemical constituents by GC-MS. The identified compounds included 1-hexadeconol, 9-eicosene, 3-dodecene, tetracosane, 13-docosenamide, 11-decyltetracosane, 9,10-anthracenedione and phenol 2,4-bis(1,1-dimethylethyl) (Sumithra & Purushothaman, 2017). These compounds are known to have biological activity therefore, it was concluded that their presence justified the traditional use of this plant for the treatment of various ailments (Sumithra & Purushothaman, 2017).

2.4.4. Commelina africana

Commelina africana (Fig 2.7) is indigenous to Africa and is widespread around the continent. It is mostly found in countries including Ethiopia, Senegal and South Africa, but it also occurs in Australia, Yemen and Saudi Arabia. *C. africana* (known as 'iNdangabane' in isiZulu and yellow wandering jew or dayflower in English) is a small herbaceous, perennial plant with stems that trail along moist ground with some erect branches (Ruffo et al., 2002). *C. africana* differs from the rest of the genus by its small, canary-yellow flowers instead of the usual blue flowers the rest of the plants in its genus possess.

Figure 2.7: Photographic image of *Commelina africana*

2.4.5. Medicinal uses of Commelina africana

In Kenya, South Africa and Zimbabwe, an infusion of the plant is used as a wash to treat fever, colds and coughs. The locals apply the fluid from the stem directly into the eye to cure eye infections (or diseases) (Attah et al., 2012). Kenyans use the extract of the entire plant as a dip to reduce fever (Attah et al., 2012). The stems are pounded and the fluid is ingested to treat colds and coughs. Children take a bath in a cold infusion of the plant to help with restlessness (Kiguba et al., 2016). In many parts of the African continent, the root extract is used to treat infertility, menstrual cramps, pelvis pains and venereal diseases (Nikolajsen et al., 2011). Tanzanian women insert the pounded plant leaves and stem in their vagina to induce abortion (Nikolajsen et al., 2011).

2.4.6. Phytocompounds from Commelina africana

A phytochemical screening of the crude extracts from the plant gave positive results for alkaloids, cardenolides, saponins and tannins (Agunbiade et al., 2012). The plant was also found to contain a high magnesium concentration which is reported to be helpful in fighting heart-related conditions and strokes, and may also assist in cell repairment (Agunbiade et al., 2012). Extracts of the plant were assessed for their ability to induce uterine contractions, and it was found to have a positive response thereby validating the use of the plant to promote abortion (Nikolajsen et al., 2011). Except for phytochemical screening, there have been no phytochemical investigations on *C. africana*.

2.5. Nanotechnology and nanomedicine

Nanotechnology is the study of materials that are between 1 and 100 nanometres (nm) in size (Bhatia, 2016). Nanotechnology manipulates material at the microscopic scale (Bhatia, 2016).

Recently, the demand for nanoparticles has increased due to its use in a number of applications including nanomedicine (Edison & Sethuraman, 2012). Nanoparticles are applicable in catalysis, medicine, materials and energy (Edison & Sethuraman, 2012). Several factors such as size, shape and surface morphology of nanoparticles influence the chemical, physical, electronic and optical properties of the nano-scaled material (Edison & Sethuraman, 2012). Nanotechnology is currently being included in biomedical applications (Anu et al., 2017). Recent developments in this field of research has shown nanoparticles to have potential as drug carriers (Bhatia, 2016). There are certain size reduction methods that are able to produce different types of structures at the nano-scale that display distinctive physicochemical and biological properties. An added advantage to these reduction methods is improved bioavailability, reduced toxicity and efficient drug release (Bhatia, 2016). The advantages of using nano-scaled material include enhanced solubility, increased surface area, lower dosage requirements and more rapid therapeutic action (Bhatia, 2016; Sahoo, 2005).

Nanomedicine refers to nanostructures that are used specifically as medicine with intent to improve the health and well-being of humans (Bhatia, 2016). Nanomedicine aims to repair, monitor, construct and control the human biological systems at the molecular level, using nanostructures (Sahoo, 2005). Nanomedicine has been categorised into the following five sub-disciplines by the European Science Foundation (ESF) (Bhatia, 2016).

a) Analytical tools
b) Nanomaterials and nanodevices
c) Nano-imaging tools
d) Novel therapeutics and drug delivery systems
e) Clinical and toxicological issues

Current commercial drugs are small molecules that fail to reach target cells or tissues and thus are unsuccessful. Nanomedicine focuses on creating drugs that can permeate through any membrane by selectively targeting the affected cell. A well-known example of nanomedicine is Doxil, which is a nano-drug that attacks cancer cells during chemotherapy. Doxil was the first nano-drug to be approved by the Food and Drug Administration (FDA).

2.6. Nanomedicine in South Africa

South Africa is still in its developmental stage when it comes to research on nanomedicine. Currently, there is on-going research at the Council for Scientific and Industrial Research (CSIR) on the reformulation of the tuberculosis (TB) drugs into nano-drugs that slowly release into the bloodstream at lower dosage (Dube & Ebrahim, 2017; Muthupandian et al., 2018; Saidi et al., 2018). Development of nano-scaled antiretrovirals (ARVs) and antimalarial drugs is also being conducted (Dube & Ebrahim, 2017; Muthupandian et al., 2018; Saidi et al., 2018). There is still a big window of opportunity when it comes to nanomedicine research in South Africa.

2.7. Plant-mediated synthesis of nanoparticles

The formation of nanoparticles can occur through several scientific routes (Fig 2.8). These include physical, chemical and biological procedures with the chemical approach being the most common. The major drawback to using chemical methods is the use of harsh, toxic, costly and environmentally unfriendly chemicals (Edison & Sethuraman, 2012). Green synthesis routes (using plant extracts and microorganisms) have emerged and are preferred for the formation of nanoparticles. These routes produce nanoparticles that are reliable, stable, cost effective and environmentally friendly (Anu et al., 2017). The secondary metabolites found in plants and microorganisms have redox capacity and are good for the biosynthesis of

nanoparticles (Ahmad & Sharma, 2012). The noble metals that are commonly studied include silver, gold, zinc, copper and selenium. Gold nanoparticles are used in medicine, optics, catalysis and optoelectronics (Edison & Sethuraman, 2012).

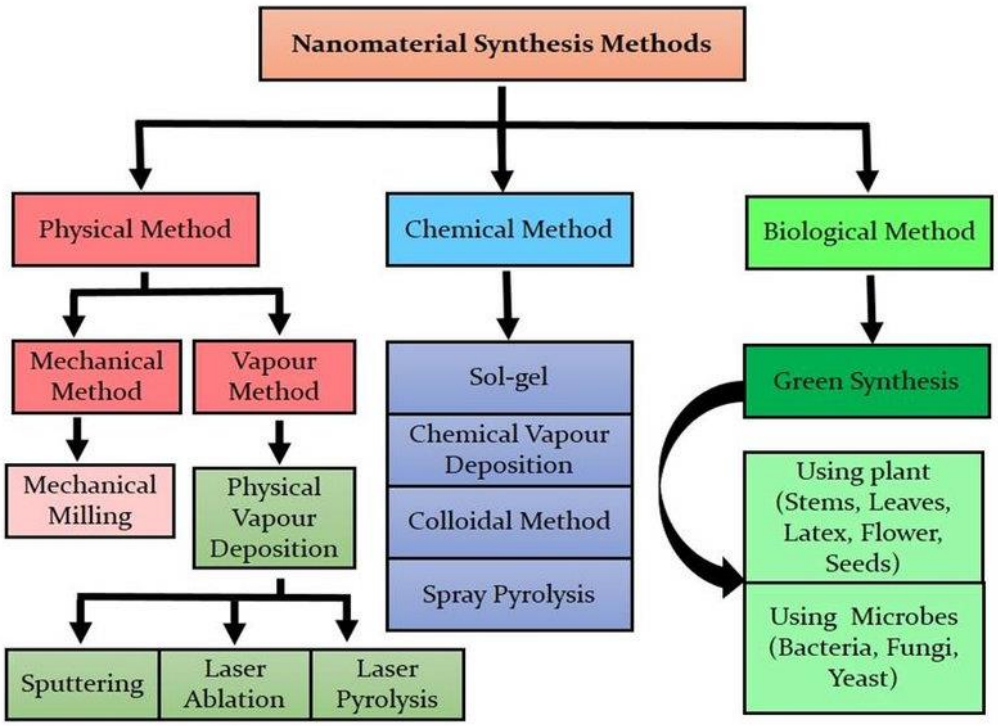

Figure 2.8: Different methods employed for the synthesis of nanoparticles

2.7.1. Selenium and silver metals for the formation of nanoparticles

In nature, selenium is found in both organic and inorganic states. There are three inorganic states of selenium that are found in nature and these are selenide (Se^{2-}), selenite (SeO_3^{2-}) and selenate (SeO_4^{2-}) with the oxidation state of selenium in each ion being -2, +4 and +6, respectively (Sarkar et al., 2015). In its organic form it is found in selenomethionine (Fig 2.9) and selenocysteine (Fig 2.10) which are both amino acids with selenomethionine being the most preferred form of selenium for nutritional value (Sarkar et al., 2015).

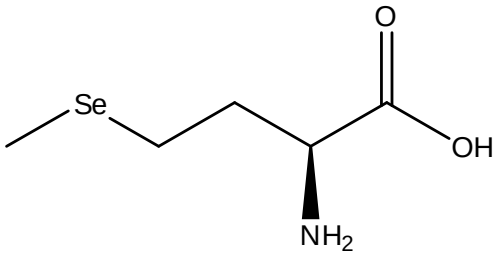

Figure 2.9: Chemical structure of selenomethionine

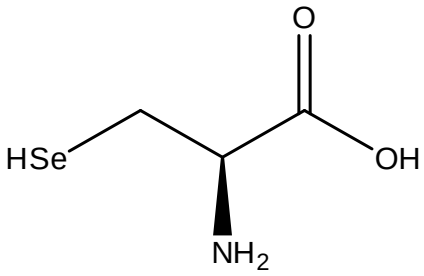

Figure 2.10: Chemical structure of L-selenocysteine

Selenium is generally viewed as a cofactor for a few enzymatic structures. Glutathione peroxidase (GSHPx) was the first selenoprotein to have been identified and it is used as a catalyst in the reduction of hydrogen peroxide to alcohol (Sarkar et al., 2015). Selenium is an essential micronutrient; its deficiency may result in the development of either the Keshan disease, which is a cardiomyopathy, or the Kashin-Beck disease, which affects bones and joints (Weekley & Harris, 2013). Selenium uptake by plants is dependent on its bioavailability in the soil. The recommended average daily intake of selenium for adults is approximately 55 µg (Weekley & Harris, 2013).

Selenium nanoparticles (SeNPs) are used as dietary supplements. The size of the particles affect their biological properties; smaller particles have higher cellular uptake hence greater activity (Honesdlova et al., 2018). SeNPs can be synthesised by the use of ascorbic acid (Malhotra et al., 2014). Ascorbic acid or vitamin C (Fig 2.11), $C_6H_8O_6$, is a plant-derived vitamin that is known for its excellent antioxidant properties. Selenium nanoparticles were

formed using the aqueous extracts from *Spirulina*, where sodium selenite (Na_2SeO_3) was used as a precursor with ascorbic acid to reduce selenium (Yang et al., 2012). When ascorbic acid is at high concentrations, the toxicity of inorganic selenium is reduced. The sequential addition of plant material and ascorbic acid to sodium selenite allows the selenite ion (SeO_3^{2-}) to form hydrous ions when dissolved in water (Yang et al., 2012). The remaining hydroxyl ions (-OH) from water form hydrogen bonds with the hydroxyl groups of the phytocompounds. The free selenite is then reduced to elemental selenium by ascorbic acid. The formation of elemental selenium is proportional to the population of SeNPs (Yang et al., 2012). The average size of SeNPs using *Spirulina* and ascorbic acid ranged from 4 to 6 nm with the particles being mostly spherical (Kokila et al., 2017). These particles were shown to have strong antioxidant properties with the scavenging properties being highly dependent on concentration and particle size (Kokila et al., 2017).

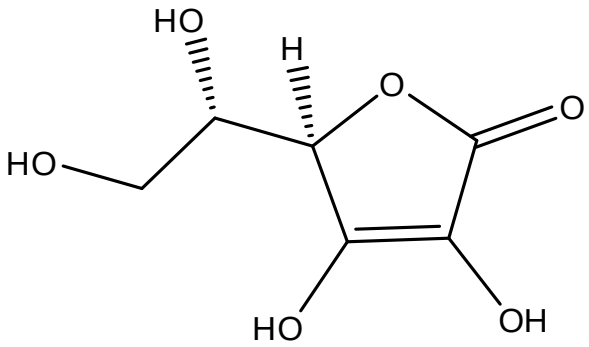

Figure 2.11: Structure of ascorbic acid

Silver has been used medicinally for many years with its most common use being in wound dressings (Alexander, 2009). Silver has the ability to suppress microbes and, for this reason, is incorporated in ointments that are used for open wounds and burns (Ponarulselvam et al., 2012). A silver sulfadiazine antibacterial ointment formed by combining silver nitrate and sulfonamide is also used to treat burns (Rai et al., 2009).

Similar to silver, silver nanoparticles (AgNPs) are generally active against microbes. The surface area of AgNPs is directly proportional to their biological effectiveness (Song & Kim, 2009; van den Wildernberg, 2005). AgNPs are able to attach onto the cell membrane of microbes affecting its porosity and they can also penetrate bacterial biofilms (Radzig et al., 2013).

The synthesis of AgNPs using the aqueous extract of the *Terminalia chebula* fruit was confirmed visually by an immediate colour change to yellow-brown and by UV/Vis where absorbances for AgNPs were observed between 400-500 nm (Edison & Sethuraman, 2012). The results also showed the absorbance to increase with pH indicating that the formation of AgNPs favours basic conditions. The particles were found to be stable at an optimum temperature of 5 °C. AgNPs were observed to be spherical with capping by phytoconsituents using HR-TEM (Edison & Sethuraman, 2012). A similar study on the synthesis of AgNPs using the aqueous extracts of *Catharanthus roseus* showed the average particle size of the spheres to be between 35-55 nm (Ponarulselvam et al., 2012).

2.8. Extraction, isolation and structure elucidation of phytocompounds

The initial step for the phytochemistry of medicinal plants is extraction. Extraction helps in obtaining the different chemical components from the plant material. Prior to extraction, there are a series of basic operational steps that need to be taken including pre-washing, drying and grinding of the plant material. The most commonly used method of extraction is exhaustive extraction where different solvents of increasing polarity are used (Doughari, 2012). Lipophilic compounds (non-polar) are extracted by hexane and dichloromethane, while hydrophilic compounds (polar) are extracted by ethyl acetate and methanol.

2.9. Chromatographic techniques

To isolate pure phytocompounds from crude plant extracts, separation techniques such as thin-layer chromatography (TLC), column chromatography (CC) and high-performance liquid chromatography (HPLC) needs to be employed. Chromatography relies on the separation of compounds based on their polarity and boiling points. This method requires the presence of a stationary phase and a mobile phase.

2.9.1. Thin-layer chromatography (TLC)

This is a basic chromatography technique that is quick, simple and cheap. It is generally used to determine the number of components in a mixture. Separation is based on polarity. The solvent system that effects separation on TLC informs the mobile phase needed for column chromatography. The ratio between the distance travelled by a compound and by the solvent is called retardation factor (R_f) (IUPAC, 1997).

$$R_f = \frac{Distance\ travelled\ by\ the\ solute}{Distance\ travelled\ by\ the\ solvent}$$

Compounds that possess the same R_f value are considered to be the similar.

2.9.2. Column chromatography (CC)

Similar to TLC, separation by column chromatography (CC) is based on polarity. The stationary phase, which in most cases is silica gel that can be packed dry or wet, is held by a narrow glass tube (column). Separation is driven by gravity (Fig 2.12). This technique requires very large volumes of solvent.

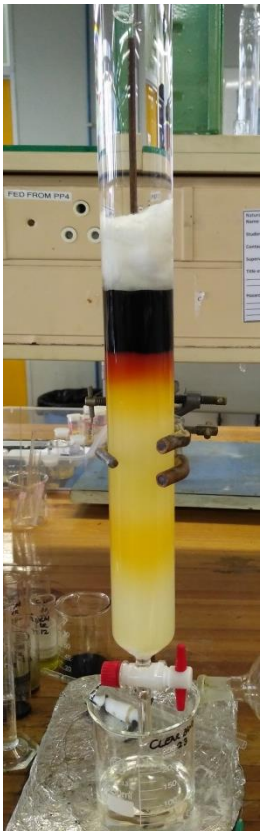

Figure 2.12: Column chromatography used to separate compounds from a crude extract

2.9.3. Spectroscopic techniques

Spectroscopy is the study of the relationship between matter and radiation (Bruice, 2006). Spectroscopic techniques are qualitatively used for structure elucidation and quantitatively used to determine concentrations. Different techniques use different kinds of electromagnetic radiation (Bruice, 2006).

2.9.3.1.Nuclear magnetic resonance spectroscopy (NMR)

Nuclear magnetic resonance (NMR) is a powerful spectroscopic tool that detects the nuclei of an atom and where they are placed within the organic molecule. The electrically charged atomic nuclei have a spin that has a magnetic moment that results in a magnetic field. The nuclei generates a magnetic field that is similar to that of a bar magnet. For nuclei to have a magnetic

moment, it needs to have a $\frac{1}{2}$ spin. When there is an absence of an external magnetic field, the magnetic moment is disorderly arranged, but when there is an external magnetic field the magnetic moment will either align with (lowest energy state) or against (highest energy state) it. The difference in energy states is supplied by radiation. A signal is generated by the nucleic absorption of the electromagnetic radiation. This interaction results in a NMR spectrum. A stronger magnetic field generates a greater energy difference, therefore, giving a stronger signal on the NMR spectrum. The NMR spectrometer can be tuned to produce spectra of different nuclei (^{1}H and ^{13}C). Molecules can be analysed by one-dimensional NMR (1D NMR) or two-dimensional NMR (2D NMR) spectroscopy.

2.9.3.2.Fourier-transform infrared spectroscopy (FTIR)

Fourier-transform infrared spectroscopy (FTIR) is a qualitative technique used to determine different functional groups and chemical bonds present in a sample by detecting the stretching and bending of bonds. The FTIR spectrometer makes use of the infrared (IR) region (4000 to 600 cm^{-1}) in the electromagnetic spectrum. IR radiates at a lower frequency and is unable to emit electrons, thus, absorption is a result of vibrations between atoms in a sample. IR radiation passes through a sample to give an IR spectrum which is a plot of percentage transmission versus the wavenumber on the transmitted radiation.

2.9.3.3.Ultraviolet-visible spectroscopy (UV-Vis)

Ultraviolet-visible (UV-Vis) spectroscopy is used to study electronic energy level changes of an organic molecule. These energy changes are brought on by a transfer of electrons. The UV-Vis spectrophotometer (Fig 2.13) has a beam of light in the UV-Vis region, to provide lighting for the sample. The incoming light is filtered by the monochromator and monochromatic light is directed to the sample. The double beam spectrometer compares the absorbance of both the

reference and the test sample concurrently to ensure background correction for the solvent (reference). The absorbance spectrum is a plot of absorbance versus wavelength in nm. For compounds to be detected in the absorption band, they need to have conjugated pi-electrons (Kumar, 2006). For the analysis of nanoparticles, the peak broadness is dependent on the particle size, shape and distribution.

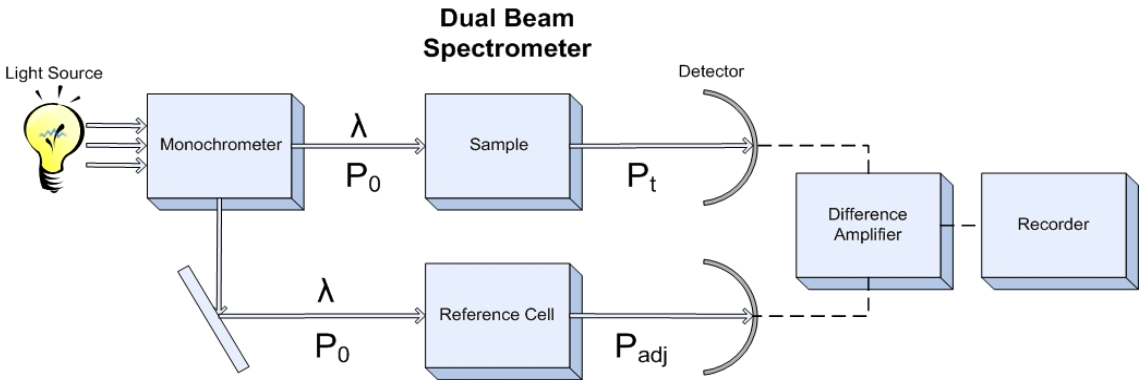

Figure 2.13: Schematic diagram of a UV-Vis spectrophotometer

2.9.3.4.Gas chromatography-mass spectrometry (GC-MS)

Gas chromatography-mass spectrometry (GC-MS) is a technique that is typically used for the separation of mixtures and subsequent identification of their masses. This technique bases the separation of components on their boiling points and, for this reason, it is a technique used for the analysis of volatile compounds. GC-MS has a stationary phase and mobile phase that is an inert carrier gas such as helium or argon. The sample is introduced into the GC by injection into the heated injector port. The sample is then moved to the column for separation by the carrier gas. The components with lower boiling points (the most volatile) are eluted first. The time in which the compound takes to elute the column is called the retention time. As the components are eluted, they are sent to a detector for a read out. Figure 2.14 demonstrates the different components of a GC.

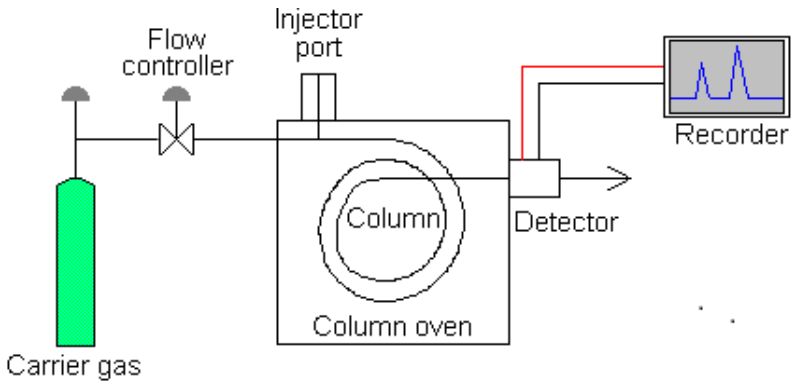

Figure 2.14: Different components of a GC instrument

A mass spectrometer is mostly coupled with the GC instrument to ionise, accelerate, deflect and detect a beam of ions thereby measuring the mass-to-charge (*m/z*) ratio of a compound relative to the ions in the sample. The molecule from the GC gets ionised by an electron beam of very high energy, resulting in the formation of a molecular ion and other fragmented ions (Fig 2.15). The outcome is displayed as a mass spectrum.

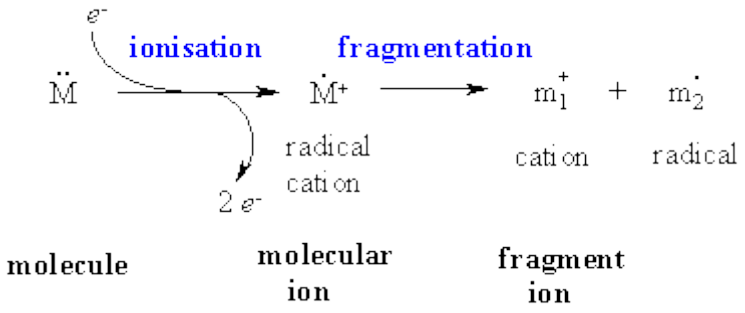

Figure 2.15: Ionisation of a molecule

2.10. Characterisation of nanoparticles

2.10.1. Transmission electron microscopy (TEM) and selected area electron diffraction (SAED)

Transmission electron microscopy (TEM) is a technique that is used for the determination of particle shape, size and morphology. The kinds of samples that can be examined by TEM include metals, polymers, plant and animal tissue, ceramics, viruses, alloys and bacteria. These may come in the form of nanoparticles, nanotubes and catalysts. This technique transmits an electron beam by penetrating a thin specimen. The TEM instrument can be divided into three main sections which are the illumination system, the specimen stage (or holder) and the imaging system (Lin et al., 2014; Williams & Carter, 1996) (Fig 2.16).

The illuminating system houses the electron gun which is responsible for the production of the electron beam, together with condenser lenses which focus the beam of electrons onto the sample. The electron beam typically accelerates at 100-200 kV (Lin et al., 2014). A sample that has been suspended on a carbon-coated copper grid is held in place by the specimen stage. The specimen stage can be kept stationery, moved around, inserted or removed from the TEM instrument to suit the needs of the user. When the incident beam interacts with the sample, the electrons get scattered and diffracted, resulting in an image of the sample (Lin et al., 2014). In the case of nanoparticles, the resulting TEM images show their dispersion and distribution. A further analysis of a crystalline specimen can be performed on this instrument via the selected area electron diffraction (SAED) function which produces electron diffraction patterns (Fultz & Howe, 2012).

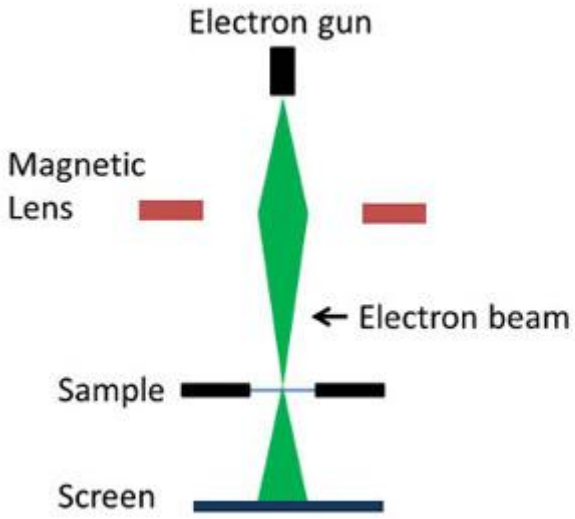

Figure 2.16: Schematic diagram of the principles of a transmission electron microscope

SAED is a crystallographic technique that can be carried out within a conventional TEM. The main function of the SAED component is to enable the identification and characterisation of different phases and crystal structures of materials, similar to X-ray powder diffraction (XRD). The wavelength in the electron beam of the SAED is smaller in comparison to that of the XRD. SAED is able to analyse and examine for a diffraction pattern at specific sample areas (approximately 100 nm in diameter) and this is one of the advantages electrons have over x-rays (Fultz & Howe, 2012).

The operational principle for the SAED is that the electrons from the electron gun are treated as a wave as opposed to particles like in a typical TEM instrument. This beam of electrons of parallel high energy is focused onto the specimen where, on interaction, some electrons will be scattered and some will pass through the sample. For this interaction (diffraction) to occur, the electrons need to adhere by Bragg's law which states that when electrons at a fixed wavelength at a particular angle are focussed onto a crystalline sample, there should be a resultant reflection of electrons that are produced by the constructive interference of the scattered wavelengths. The constructive interference is described as the beam of electrons that are diffracted from the

crystal at an angle that is equal to the initial beam and the result of this is a diffraction pattern that may show the presence of either polycrystalline, single crystalline or amorphous material (Fultz & Howe, 2012).

Polycrystalline material (Fig 2.17 A) which is composed of many crystallites (grains) is identified by fine spots arranged in rings. Single crystalline material (Fig 2.17 B) has brighter spots that are not arranged in distinctive rings. Particles with larger sizes have bigger spots and those of smaller sizes will results in smaller diffraction spots. An amorphous diffraction pattern (Fig 2.17 C) means the selected sample area is not crystalline and this results from a random arrangement of atoms in the unit cell. The indexing of the SAED patterns is done by measuring the diameter (2R) for each of the rings, then calculating the radius (R). A reciprocal of these values was calculated in order to obtain the interplanar distance (d) which was compared to the d-values in literature for phase identification (Jyoti et al., 2016; Kora et al., 2012; Mehta et al., 2017).

$$d = 1/R$$

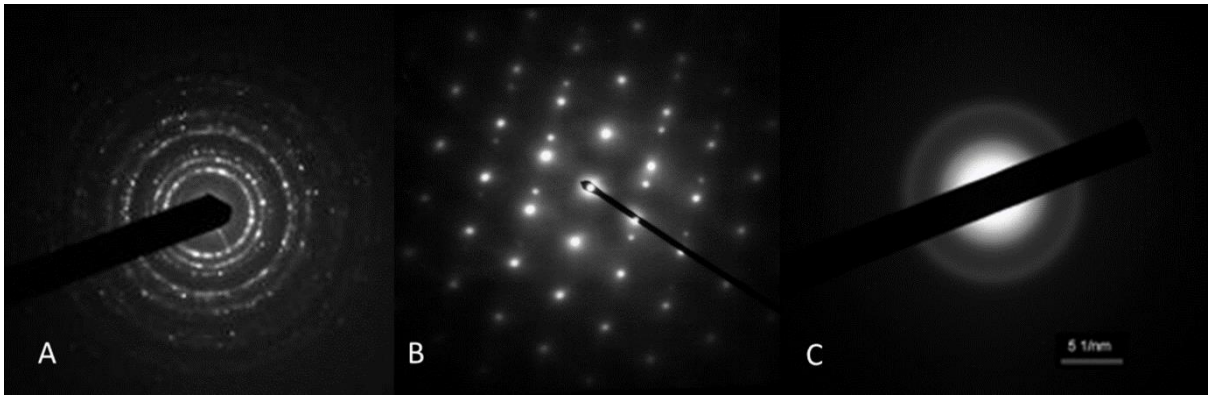

Figure 2.17: Diffraction patterns from polycrystalline material (A), single crystalline material (B) and amorphous material (C)

2.10.2. Scanning electron microscopy (SEM) and energy-dispersive x-ray spectroscopy (EDX)

Scanning electron microscopy (SEM) was invented after TEM and so operational principles are similar with minor variations. Sample preparation methods for this technique requires sample to be dried to a powder, placed on a carbon tape on a sample holder then coated with gold or other conductive metals. SEM (Fig 2.18) uses a tungsten filament as its source of electrons and the maximum voltage these accelerate at is typically 30 kV. This is less than that of TEM, meaning SEM would have a smaller electron gun. The beam of electrons passes through electromagnetic lenses which focus the beam onto the specimen. SEM is able to examine specimens that are relatively thicker than those analysed by TEM and for this reason, the incident beam scans over the surface of the specimen, as opposed to penetrating the specimen. The electron beam strikes and interacts with the sample atoms which generate scattered electrons (secondary electrons) and these are identified by a detector and an image is displayed on the monitor. Characteristic x-ray images give information on the sample composition and topography. SEM is also able to give images at very high resolutions (Lin et al., 2014).

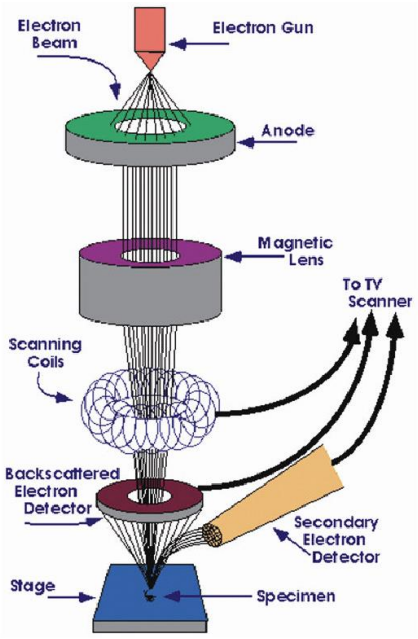

Figure 2.18: Schematic diagram of the principles of a scanning electron microscope (Walock, 2012)

Energy-dispersive x-ray spectroscopy (EDX) is a technique that qualitatively and quantitatively analyses for the chemical composition of a sample. This technique is commonly used in combination with either SEM or TEM because of their use of an electron beam. The beam of electrons excites the electrons within atoms of a sample. The electron is ejected, leaving behind an unoccupied hole. An electron from a higher energy outer shell fills the hole. The difference in energies is released as x-rays and x-ray energies are unique to each element. This interaction is measured by an energy-dispersive spectrometer and the spectrum is a plot of intensity over the x-ray energy (keV). Figure 2.19 is an example of an EDX spectrum.

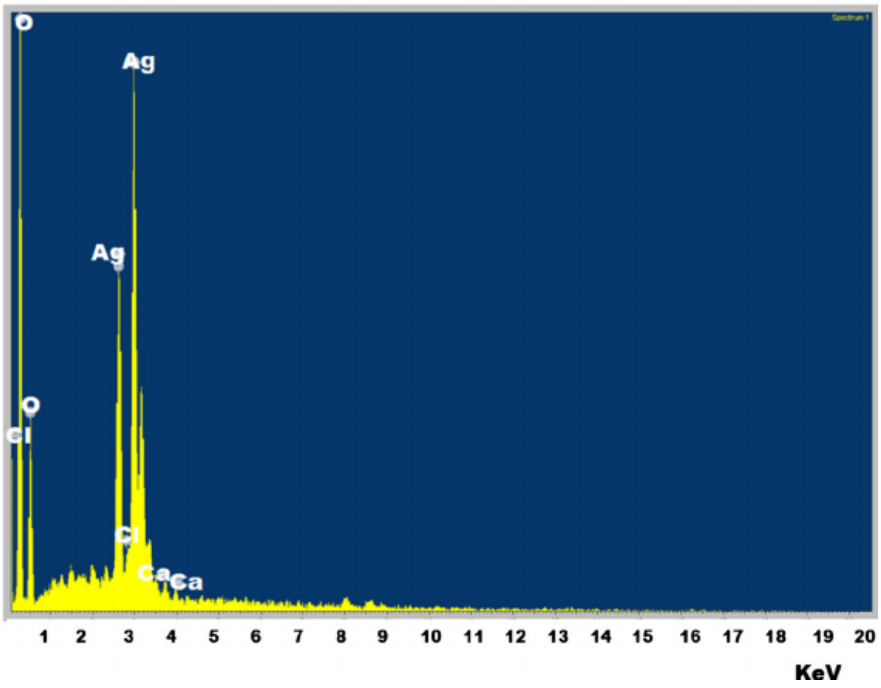

Figure 2.19: EDX spectrum of AgNPs synthesised from the *Vitis vinifera* fruit (Gnanajobitha et al., 2013)

2.11. Biological activity

2.11.1. Secondary metabolites and nanoparticles as antioxidants

There are a number of biological processes that occur within the human body. Unfortunately, these processes produce unwanted by-products including reactive oxygen species (ROS). These ROS can be present as both radical (hydroxyl radical) and non-radical (hydrogen peroxide) species. Our bodies have natural antioxidant systems such as enzymes and lipids that fight off these species. They do this by donating electrons to radicals to prevent an attack on healthy cells for extra electrons by ROS (Fig 2.20). When biological processes produce more free radicals than the natural antioxidants can contain, oxidative stress results, which brings about severe damage to biomolecules such as DNA and proteins (Ndhlala, 2009). Oxidative stress leads to the progression of diseases such as diabetes, cancer, cardiovascular disease and neurodegenerative diseases (Ndhlala, 2009; Shelembe, 2014).

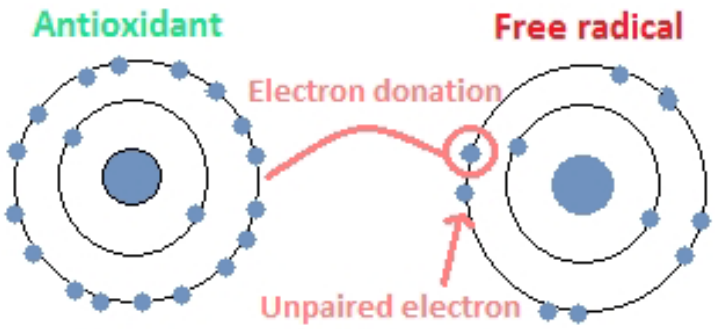

Figure 2.20: Electron donation by the antioxidant to the free radical

Secondary metabolites such as flavonoids, alkaloids, terpenoids and vitamins have defensive effects against the scavenging ROS. Antioxidants need to be able to react against the oxidation in its small quantities. The reaction between hydrogen from secondary metabolites and ROS stabilises these ROS which can then form stable complexes with proteins and lipids (Ndhlala, 2009; Shelembe, 2014). The secondary metabolites then become resonance stabilised due to delocalisation of pi electrons.

Some of the methods used to assess the scavenging power of plants and their compounds include the 2,2-diphenyl-1-picrylhydrazyl (DPPH) and ferric reducing antioxidant power (FRAP) assays. The DPPH method is the most common for assessing the antioxidant properties of natural products. The DPPH radical is quite stable in solution and absorbs at 517 nm when dissolved in methanol (Mishra et al., 2012). The working principle of this assay is that the DPPH radical accepts a proton from an antioxidant and, in turn, the DPPH radical will be reduced to (DPPH):H (Mishra et al., 2012). This reaction can be visually observed as the purple DPPH radical turns to yellow upon reduction. The proposed mechanism for the reaction between the DPPH radical and an antioxidant (RH) is given in Figure 2.21. As the radical gets reduced, the absorbance is decreased (Mishra et al., 2012). The absorbance changes are measured using a spectrophotometer.

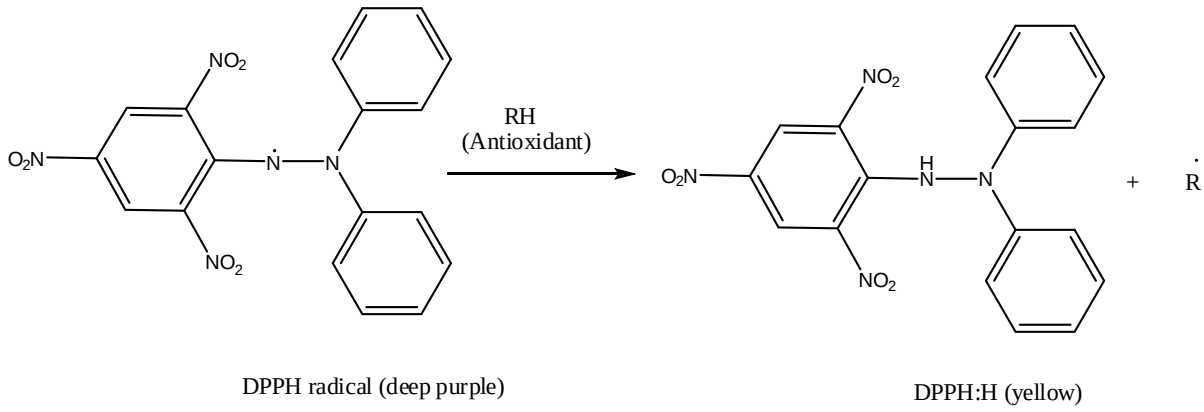

Figure 2.21: Mechanism for the reduction of the DPPH radical

The FRAP method is based on the reduction of the complex ferric-2,4,6-tri(2-pyridyl)-1,3,5-triazine (Fe^{3+}-TPTZ) ion to the ferrous (Fe^{2+}) ion by an antioxidant. Optimum reduction is achieved at low pH levels (Benzie & Strain, 1996). This reaction can also be visually observed as the solution changes from yellow (Fe^{3+}) to a deep blue complex (Fe^{2+}), and the absorbance change can be measured at 700 nm (Antolovich et al., 2002). The proposed mechanism for the reaction is given below.

Fe^{3+} + Antioxidant $\longrightarrow$ Fe^{2+} + Oxidised antioxidant

A linear response between the concentration of analytes and the absorbance of analytes have been observed indicating that an increase in concentration will also result in an increase in absorbance (Antolovich et al., 2002).

2.11.2. Secondary metabolites and nanoparticles as anti-bacterial agents

There is a growing concern about bacterial infections since bacteria have developed resistance to antibiotics that are commonly available. There is therefore need for more research to focus on the development of antibiotics that can inhibit or kill bacterial cells that are responsible for infectious diseases. The first discovery of an antibacterial agent (penicillin) in 1928 by Sir

Alexander Fleming was isolated from the *Penicillium notatum* mold (Ullah & Ali, 2017). The discovery of penicillin showed natural products to be capable of acting as antibacterial agents.

Antibacterial agents are grouped into different classes according to the type of action, spectrum of activity, primary function, chemical structure and source (Fig 2.22). Type of action can either be bacteriostatic or bactericidal (Calderón & Sabundayo, 2007; Ullah & Ali, 2017). Bacteriostatic agents restrain bacterial growth and bactericidal agents kill bacteria by attacking its cell wall. Penicillin is an example of a bactericidal agent. Grouping antibiotics based on their chemical structure helps identify those that behave similarly. Such structural classifications can be broken down into β-lactams and aminoglycosides (Ullah & Ali, 2017). *β*-lactams contain a four-membered lactam ring (Fig 2.23 A) and are active against Gram-positive bacteria. Aminoglycosides consist of two amino sugars that are joined to an aminocyclitol by a glycoside bond (Fig 2.23 B). They are active against Gram-negative bacteria and are used to inhibit the synthesis of proteins (Calderón & Sabundayo, 2007).

The source of antibiotics is important because synthetic antibiotics are less toxic than those found in nature. The spectrum of activity can be sub-divided into two categories which are broad or narrow (Ullah & Ali, 2017). Broad spectrum antibiotics can be effective on a wide range of pathogenic bacteria and are not limited to Gram-positive or Gram-negative bacteria as narrow spectrum agents (Ory & Yow, 1963). The most important classification would be the functionality of the antibacterial agent. Some antibacterial agents may inhibit cell wall synthesis, and some may inhibit nucleic acid synthesis (Calderón & Sabundayo, 2007; Ullah & Ali, 2017).

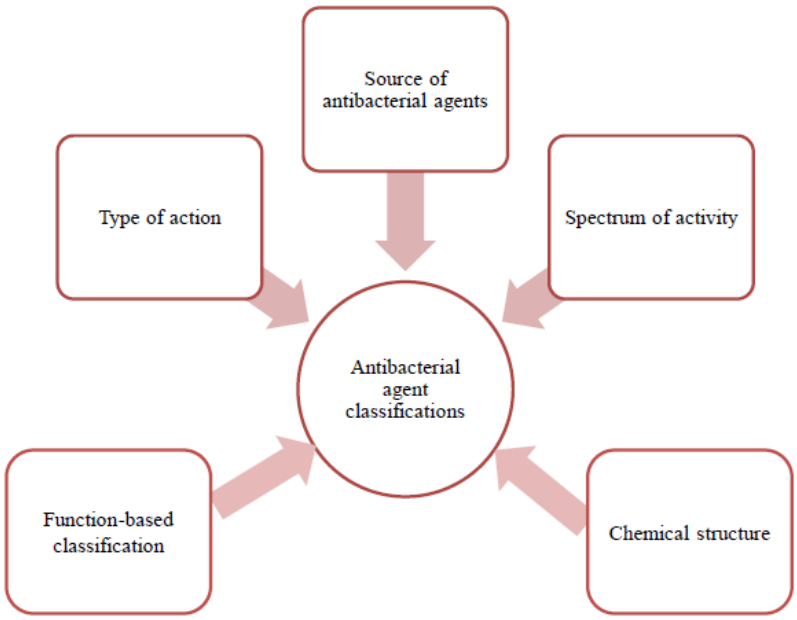

Figure 2.22: Classification of antibacterial agents

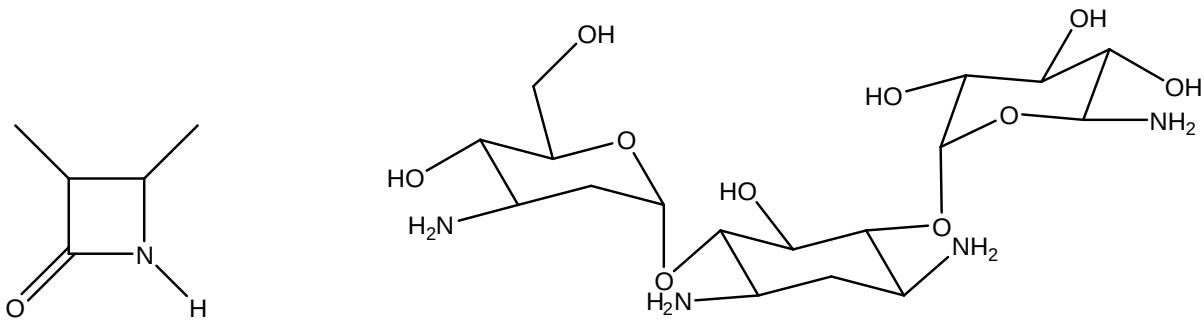

β-lactam ring (A) kanamycin A (B)

Figure 2.23: β-lactam ring (A) and kanamycin A (an example of an aminoglycoside) (B)

Bacteria are classified as Gram-negative or Gram-positive organisms. Gram-positive bacteria have bigger and thicker membranes than their counterparts. Gram-positive bacteria include *Staphylococcus aureus* and *Enterococcus faecalis*. Examples of Gram-negative bacteria include *Escherichia coli*, *Klebsiella pneumonia*, *Pseudomonas aeruginosa* and *Chromobacterium violaceum*.

Natural products play an integral role in the discovery of new antibacterial agents and in some regions (especially in Africa and Asia) they are still used as a primary source for bacterial treatments. There is an array of laboratory methods that screen extracts for antibacterial activity. The most commonly used ones are the agar (broth) dilution and the disc-diffusion methods (Balouiri et. al, 2016). The agar disc-diffusion method is the standard and official method for most industrial and pharmaceutical companies and institutions. This method quantifies the ability of the antibacterial agent to inhibit the growth of bacteria (Bonev et al., 2008). The pathogenic organism is introduced on the agar containing plate by means of the swabbing technique. The potential antibacterial organism is then introduced to the plate via disc holes and the plate is left to incubate for about 24 hours (Fig 2.24).

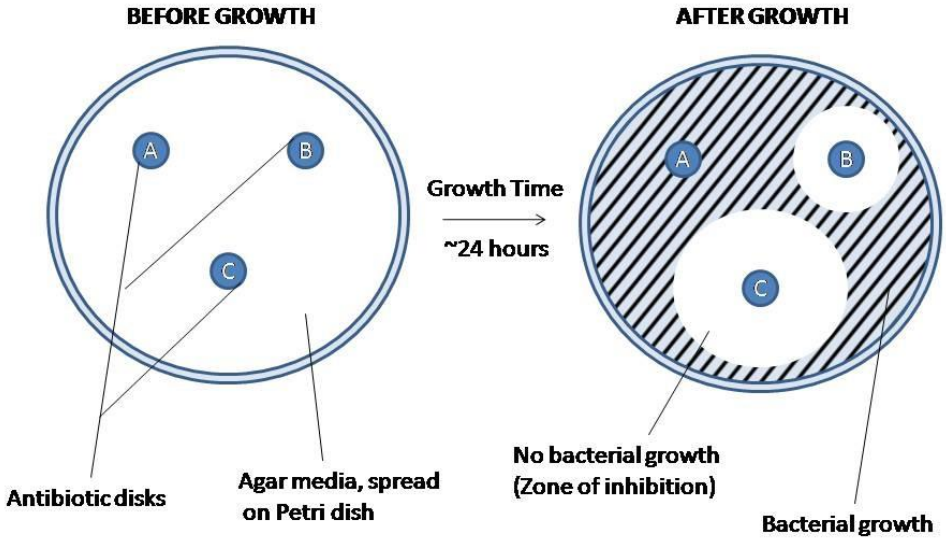

Figure 2.24: Agar disc-diffusion method for the quantification of inhibition zones by the antibacterial agent

A typical petri dish with set agar that has been swabbed with a bacterial organism and with discs that are filled with the potential antimicrobial agent is shown in Figure 2.24. The impregnated agar is left to incubate for approximately 24 hours, the average time it takes for bacteria to fully grow. After incubation, test samples are observed to either not have any

activity, have a moderate response or have strong activity against the bacterial strain (Balouiri et al., 2016). Antimicrobial activity may be recognised visibly and the area showing activity is known as the zone of inhibition. The diameter of the zone of inhibition is measured using a standard ruler in millimetres from one edge of the circle to the other. The size of the zone of inhibition can be affected by the concentration of the sample and the depth of the agar. Higher concentrations and shallower depths would result in larger inhibition diameters. The ideal activity would be to have a larger zone of inhibition at very low concentrations of samples (Balouiri et al., 2016).

Metal and plant-based nanoparticles have also been investigated for their ability to inhibit the growth of microbials. SeNPs were investigated for their antimicrobial abilities against *Aspergillus niger*, *Staphylococcus aureus* and *Escherichia coli* (Kokila et al., 2017). Their zones of inhibition were found to increase with increasing concentration with the highest activity observed against *A. niger* and lowest against *E. coli* (Kokila et al., 2017). SeNPs may be used to limit common contamination in food at lower temperatures. At temperatures higher than 37 °C the particles will not be able to inhibit the growth of *E. coli*.

The stem and root extracts from *Acacia rigula* were used in a one-pot synthesis of AgNPs that were subsequently analysed for their antimicrobial activity against *E. coli, P. aeruginosa* and *Bacillus subtilis* (Escárcega-González et al., 2018). *P. aeruginosa* is a multidrug resistant bacterial species however, the AgNPs were found to moderately inhibit the growth of this strain. Therefore, AgNPs from *A. rigula* extracts could be an alternative non-toxic antimicrobial treatment (Escárcega-González et al., 2018).

CHAPTER THREE

MATERIALS AND METHODS

3.1. Plant material collection

Commelina africana leaves and stems were purchased from the Durban Berea Muthi Market. These had been collected by Mr Mbhele and the herbalist gave an insight into the common traditional uses of this plant. The plant was identified by Mr E.N Khathi, University of KwaZulu-Natal (UKZN), School of Health Science's herbarium on the Westville campus where a voucher specimen (Mhlongo S 01) was deposited.

3.2. Reagents

All chemicals and reagents were purchased from Sigma-Aldrich, Fluka and Merck. All reagents were analytical reagent grade and any further dilutions were performed using double distilled water.

3.3. Plant extraction and compound isolation

Both the leaves and stems were sun dried for four weeks and they were then separated. Leaves were powdered separately using a disk mill. Crushed leaves and stems were exhaustively extracted sequentially by placing on an orbital shaker for three days at room temperature. The solvents used were hexane, followed by dichloromethane (DCM) and methanol (MeOH). The concentrated MeOH extract was mixed with water and subjected to further partitioning with equal volumes of DCM then ethyl acetate (EtOAc) in a separating funnel (2 L). Each of the collected extracts had their volumes reduced to almost dryness on the rotary evaporator and the

remaining residue was kept at lower temperatures until further use. The concentrated extracts were subjected to column chromatography using a silica gel column (Merck Kieselgel 60, 0.063-0.200 mm, 70-230 mesh ASTM) for separation and isolation of compounds. The extracts were separated using a hexane: EtOAc solvent system starting from 100% hexane that was stepped by 10% to 90% EtOAc. The purity of the collected fractions were monitored by thin layer chromatography (TLC) (Merck silica gel 60, 20 x 20 cm F254 aluminium sheets) where the spots were analysed under UV (254 nm) and visualized using anisaldehyde spray reagent (97: 2: 1; MeOH: conc. H_2SO_4: anisaldehyde).

3.4. Characterisation of phytocompounds

The Bruker Avance III 400 and 600 MHz spectrometers were used for nuclear magnetic resonance (NMR) spectroscopy. Samples were dissolved in deuterated chloroform ($CDCl_3$) or methanol (MeOD). Infrared spectra were recorded using a Perkin-Elmer Universal ATR Spectrometer, while ultraviolet-visible (UV-Vis) spectra were recorded on a UV-Vis-NIR Shimadzu UV-3600 Spectrophotometer. The Agilent GC-MSD instrument was used for gas chromatography mass spectroscopy (GC-MS). This apparatus was equipped with a DB-5SIL MS (30 m x 0.25 mm inner diameter, 0.25 μm film thickness) fused silica capillary column and helium (2 mL min^{-1}) was used as the carrier gas. The GC-MS samples were dissolved in EtOAc or DCM. The injector was kept at 250 °C whilst the transfer line was at 280 °C. The column temperature was held at 50 °C for 2 min, and then ramped up to 280 °C at 20 °C min^{-1} where it was held for 15 min.

3.5. Synthesis of silver and selenium nanoparticles

Commelina africana leaves (10 g) were homogenized in double distilled water (50 mL) at 50 °C for 2 hours then filtered by vacuum after it had been cooled to room temperature. Sodium selenite (10 mM) was prepared by dissolving Na_2SeO_3 (0.173 g) in double distilled water (100 mL). Ascorbic acid (50 mM) was used as the initiator of the reaction and it was prepared by dissolving 0.440 g in double distilled water (50 mL) (Yang et al., 2012). Different volumes of the aqueous and methanolic extract (1-5 mL) were added dropwise to sodium selenite (5 mL) at room temperature, with stirring. To the mixture, 4 mL of the initiator was added to form a brick red solution. The mixture was agitated on the orbital shaker for 24 hours, centrifuged and washed with distilled water or ethanol and dried at 60 °C for 48 hours. The resulting nanoparticles were stored at 3-5 °C until further analysis.

The silver nitrate ($AgNO_3$) standard was prepared by dissolving 0.169 g of the salt in double distilled water (100 mL) to form a concentration of 10 mM. Different volumes of the aqueous and methanolic extract (1-5 mL) were added to a silver nitrate (10 mL) solution at room temperature. The mixture was agitated on the orbital shaker for 24 hours, centrifuged and washed with distilled water or ethanol and dried at 60 °C for 48 hours. The resulting nanoparticles were stored at 3-5 °C until further analysis.

Freestanding nanoparticles were synthesised using sodium borohydride ($NaBH_4$) as the reducing agent. $NaBH_4$ (5 mL, 20 mM) was added in equal parts with the $AgNO_3$ and Na_2SeO_3 standards with reaction parameters similar to the previously synthesised NPs.

3.6. Characterisation of nanoparticles

The nanoparticle mixtures (1 mL) were individually taken for UV-Vis analysis. The instrument was set to run at 200-700 nm and double distilled water was used as a reference sample to correct the baseline using a 10 mm quartz cuvette. The functional groups present in these NPs were investigated using FTIR. Particle size, distribution, morphology and crystallinity of NPs were analysed by the means of transmission electron microscopy (TEM). The dried NPs were re-suspended in absolute ethanol and agitated in a water bath at room temperature for at least 15 minutes. The sample (µL) was deposited on a carbon grid, left to dry at room temperature for a minimum of 10 minutes then analysed on the JEOL TEM 2100 equipped with SAED for the determination of crystallinity. Scanning electron microscopy (SEM) was performed on a ZEISS LEO 1450 instrument equipped with an EDX detector and was used to determine the elemental composition of the nanoparticles. Prior to analysis, the dried samples were prepped by depositing a very small amount of the nanoparticles on a stub layered with carbon tape. The stub was then coated with gold to ensure conductivity.

3.7. Antioxidant activity

3.7.1. 2,2-diphenyl-1-picrylhydrazyl (DPPH) assay

The free radical scavenging activity of the extracts, phytocompounds and nanoparticles were assessed by the method adapted from Murthy et al. (2012) with minor adjustments. Solutions were dissolved in MeOH and standards at different concentrations (1000, 800, 500, 200, 100 and 50 µg mL^{-1}) and were made up in 10 mL volumetric flasks. From each of these solutions, a volume of 150 µL was pipetted and mixed with 0.1 mM DPPH in methanol (2850 µL). The mixtures were left to react in the dark at room temperature for 30 minutes. After the reaction period, the individual absorbances of these mixtures were measured at 517 nm using a UV-Vis

spectrophotometer. The readings were taken in triplicate and the average absorbance was used for calculations and analysis. Ascorbic acid was used as a positive control. The scavenging activity of the sample against the control used can be calculated using the following equation:

$$\% \text{ Scavenging activity} = \frac{\text{Ac} - \text{As}}{Ac} \times 100$$

Where Ac is the absorbance of the control and As the absorbance of the sample.

3.7.2. Ferric reducing antioxidant power (FRAP) assay

The reducing power of the sample was assessed by the method adapted from Murthy et al. (2012) with minor adjustments. In a test tube, 2.5 mL of sample at different concentrations (1000, 800, 500, 200, 100 and 50 µg mL^{-1}) was mixed with a 0.2 M phosphate buffer (2.5 mL) at pH 6.5 and 1% potassium ferricyanide (2.5 mL). The mixture was left to react in a water bath at 50 °C for 20 minutes. After the reaction, 10% trichloro-acetic acid (2.5 mL) was added to each mixture and mixed thoroughly. The above-mentioned mixture (2.5 mL) was then mixed with distilled water (2.5 mL) and 0.1% iron(III)chloride (0.5 mL) and this was left to stand at room temperature for 10 minutes. After the reaction period, the individual absorbances of these mixtures were measured at 700 nm using a UV-Vis spectrophotometer. The readings were taken in triplicate and the average absorbance was used for calculations and analysis. Ascorbic acid was used as a positive control.

4. Antibacterial activity of phytocompounds, extracts and nanoparticles

The Kirby-Bauer disc diffusion method was used for this test. The Mueller-Hinton petri dishes containing agar were uniformly swabbed with bacterial strains under sterile conditions. These consisted of *Staphylococcus aureus* ATCC 43300 and *Enterococcus faecalis* ATCC 51299 which are Gram-positive bacteria as well as *Pseudomonas aeruginosa* ATCC 27853,

Escherichia coli ATCC 35128, *Klebsiella pneumonia* ATCC 700603 and *Chromobacterium violaceum* ATCC 12472 which are Gram-negative. The agar containing the bacteria was impregnated with 20 and 40 µL of the 10 mg mL^{-1} sample and incubated for 24 hours at 30 °C except the *C. violaceum* plates which were incubated at 25 °C. The zone of inhibition was observed and measured (mm) as the clear region around the disc. An overlay assay known as the anti-quorum sensing (QS) method was used with the *C. violaceum* strain. Molten soft agar (5 mL) was inoculated with 150 µL of *C. violaceum* and thoroughly mixed and poured on agar plates then allowed to solidify at room temperature. The agar was impregnated with 20 and 40 µL of the 10 mg mL^{-1} sample and incubated for 24 hours at 25 °C. The halo around the disc confirmed the inhibition of the bacteria by the sample.

CHAPTER FOUR

RESULTS AND DISCUSSION

4.1. Characterisation of Phytocompounds

4.1.1. Spectroscopic data of phytocompounds

This section summarises the NMR, GC-MS, LRMS, and UV-Vis results obtained for each of the isolated compounds while highlighting the significant peaks and chemical shifts that led to the concluded structures. Various spectra for all the isolated compounds can be found in Appendix A.

Stigmasterol (1) GC-MS: *m/z* (rel %): 412 $[M]^+$, ^{1}H NMR (400 MHz, $CDCl_3$) δ_H (ppm): 5.33 (1H, d, J=5.20 Hz) , 5.13 (1H, q, J=7.88 Hz) , 4.99 (1H, q, J=7.92 Hz) , 3.50 (1H, m, J=5.24 Hz), 2.30 (1H, d, J=1.60 Hz), 2.28 (1H, d, J=2.08 Hz), 2.26 (1H, d, J=1.44 Hz), 2.25 (1H, d, J=2.20 Hz), 2.24 (1H, d, J=2.20 Hz), 2.21 (1H, d, J=2.12 Hz), 2.18 (1H, d, J=2.36 Hz), 2.15 (1H, s), 1.98 (1H, q, J=5.32 Hz), 1.82 (1H, m, J=4.40 Hz), 1.65 (1H, d, J=1.84 Hz), 1.63 (1H, d, J=2.04 Hz), 1.61 (1H, t, J=3.14 Hz), 1.57 (1H, s), 1.55 (1H, t, J=4.54 Hz), 1.51 (1H, d, J=3.88 Hz), 1.49 (1H, s), 1.47 (1H, t, J=2.84 Hz), 1.45 (1H, s), 1.42 (1H, d, J=4.84 Hz), 1.27 (1H, m, J=5.22 Hz), 0.99 (1H, s), 0.96 (1H, s), 0.94 (1H, s), 0.93 (1H, s), 0.89 (1H, q, J=4.60 Hz), 0.80 (1H, m, J=4.39 Hz), 0.67 (1H, d, J=7.36 Hz).

^{13}C-NMR (400 MHz, $CDCl_3$) δ_c (ppm): 140.76 (1C, s), 138.30 (1C, s), 129.30 (1C, s), 121.72 (1C, s), 71.82 (1C, s), 56.88 (1C, s), 56.78 (1C, s), 56.08 (1C, s), 50.15 (1C, s), 45.86 (1C, s), 42.31 (1C, s), 42.23 (1C, s), 39.79 (1C, s), 39.69 (1C, s), 37.26 (1C, s), 36.51 (1C, s), 36.15 (1C, s), 33.96 (1C, s), 31.92 (1C, s), 31.67 (1C, s), 29.69 (1C, s), 29.18 (1C, s), 28.24 (1C, s),

26.11 (1C, s), 24.30 (1C, s), 23.08 (1C, s), 21.21 (1C, s), 21.09 (1C, s), 19.81 (1C, s), 19.39 (1C, s), 19.04 (1C, s), 18.98 (1C, s), 18.78 (1C, s), 11.98 (1C, s), 11.86 (1C, s).

Ergosterol peroxide (2) LR-ESI-MS: *m/z* (rel %): 451.3705 $[M + Na]^+$ (calculated for $C_{28}H_{44}O_3Na$, 451.318), ^1H NMR (400 MHz, $CDCl_3$) δ_H (ppm): 6.57 (1H, d, J=8.48 Hz), 6.48 (1H, d, J=8.48 Hz), 6.26 (1H, d, J=8.60 Hz), 6.22 (1H, d, J=8.48 Hz), 5.79 (1H, s), 5.16 (1H, m, J=8.03 Hz), 4.13 (1H, t, J=5.62 Hz), 3.94 (1H, m, J=5.48 Hz), 2.30 (1H, m, J=6.85 Hz), 2.24 (1H, s), 2.07 (1H, d, J=5.16 Hz), 1.99 (1H, d, J=7.44 Hz), 1.97 (1H, s), 1.93 (1H, d, J=6.20 Hz), 1.89 (1H, d, J=4.04 Hz), 1.83 (1H, q, J=7.06 Hz), 1.23 (1H, s), 1.07 (1H, s), 0.97 (1H, d, J=6.60 Hz), 0.89 (1H, s), 0.83 (1H, m, J=6.08 Hz), 0.71 (1H, s).

^{13}C-NMR (400 MHz, $CDCl_3$) δ_C (ppm): 135.41 (1C, s), 135.20 (1C, s), 132.31 (1C, s), 130.74 (1C, s), 82.16 (1C, s), 79.43 (1C, s), 66.48 (1C, s), 56.20 (1C, s), 51.68 (1C, s), 51.08 (1C, s), 44.56 (1C, s), 42.77 (1C, s), 39.73 (1C, s), 39.34 (1C, s), 36.93 (1C, d, J=5.87 Hz), 34.69 (1C, s), 33.06 (1C, s), 31.93 (1C, s), 29.70 (1C, s), 28.64 (1C, s), 23.40 (1C, s), 22.69 (1C, s), 20.88 (1C, s), 20.63 (1C, s), 19.94 (1C, s), 19.64 (1C, s), 18.17 (1C, s), 17.56 (1C, s), 14.12 (1C, s), 12.87 (1C, s).

***β*-sitosterol (3)** GC-MS: *m/z* (rel %): 414 $[M]^+$, ^1H NMR (400 MHz, $CDCl_3$) δ_H (ppm): 5.33 (1H, d, J=5.20 Hz), 3.50 (1H, m, J=5.29 Hz), 2.32 (1H, t, J=7.52 Hz), 1.99 (1H, m, J=3.95 Hz), 1.82 (1H, m, J=4.48 Hz), 1.60 (1H, q, J=7.40 Hz), 1.50 (1H, m, J=4.38 Hz), 1.24 (1H, d, J=32.90 Hz), 1.09 (1H, m, J=5.22 Hz), 0.99 (1H, s), 0.90 (1H, t, J=3.28 Hz), 0.87 (1H, s), 0.85 (1H, d, J=2.08 Hz), 0.84 (1H, d, J=1.76 Hz), 0.82 (1H, s), 0.80 (1H, d, J=1.48 Hz), 0.78 (1H, s), 0.68 (1H, s), 0.66 (1H, s).

^{13}C-NMR (400 MHz, $CDCl_3$) δ_C (ppm): 140.76 (1C, s), 121.72 (1C, s), 71.84 (1C, s), 56.78 (1C, s), 45.86 (1C, s), 39.79 (1C, s), 37.26 (1C, s), 36.51 (1C, s), 36.15 (1C, s), 33.74 (1C, s), 31.92 (1C, s), 31.65 (1C, s), 29.38 (1C, m, J=12.58 Hz), 28.25 (1C, s), 26.10 (1C, s), 24.71

(1C, s), 23.08 (1C, s), 22.68 (1C, s), 19.81 (1C, s), 19.04 (1C, s), 18.78 (1C, s), 14.10 (1C, s), 11.98 (1C, s), 11.86 (1C, s).

Campestanol (4) GC-MS: *m/z* (rel %): 402 $[M]^+$, ^{1}H NMR (400 MHz, $CDCl_3$) δ_H (ppm): 3.50 (1H, m, J=5.24 Hz), 2.31 (1H, t, J=7.50 Hz), 2.14 (1H, s), 2.10 (1H, s), 1.83 (1H, s), 1.82 (1H, s), 1.81 (1H, s), 1.80 (1H, s), 1.79 (1H, s), 1.78 (1H, s), 1.28 (1H, t, J=2.76 Hz), 1.25 (1H, s), 1.22 (1H, s), 1.16 (1H, s), 1.12 (1H, d, J=4.96 Hz), 1.08 (1H, s), 1.04 (1H, d, J=4.96 Hz), 1.00 (1H, s), 0.98 (1H, s), 0.90 (1H, s), 0.88 (1H, d, J=2.20 Hz), 0.86 (1H, s), 0.84 (1H, d, J=1.96 Hz), 0.83 (1H, d, J=2.48 Hz), 0.81 (1H, s), 0.79 (1H, d, J=1.72 Hz), 0.77 (1H, s), 0.76 (1H, s), 0.74 (1H, d, J=2.92 Hz), 0.67 (1H, s), 0.65 (1H, s).

^{13}C-NMR (400 MHz, $CDCl_3$) δ_C (ppm): 71.83 (1C, s), 56.76 (1C, s), 56.05 (1C, s), 51.23 (1C, s), 50.13 (1C, s), 45.83 (1C, s), 42.26 (1C, d, J=11.69 Hz), 40.48 (1C, s), 39.77 (1C, s), 39.67 (1C, s), 39.36 (1C, s), 37.24 (1C, s), 36.50 (1C, s), 36.14 (1C, s), 33.92 (1C, d, J=4.04 Hz), 31.90 (1C, s), 31.57 (1C, s), 30.91 (1C, s), 29.69 (1C, s), 29.59 (1C, s), 29.26 (1C, m, J=9.08 Hz), 28.91 (1C, s), 28.24 (1C, s), 27.97 (1C, s), 26.07 (1C, s), 24.72 (1C, s), 24.29 (1C, s), 23.06 (1C, s), 22.68 (1C, s), 21.07 (1C, s), 19.80 (1C, s), 19.38 (1C, s), 19.02 (1C, s), 18.77 (1C, s), 14.10 (1C, s), 12.23 (1C, s), 11.91 (1C, d, J=11.84 Hz).

4.1.2. Structure elucidation of phytocompounds

The isolated compounds (**1**, **2**, **3** and **4**) were identified as stigmasterol, ergosterol peroxide, *β*-sitosterol and campestanol (Fig 4.1), respectively, by comparison of their respective ^{1}H and ^{13}C NMR data to that in literature. Compound **1** was isolated from the DCM extract whilst compounds **2, 3** and **4** were obtained from MeOH extract. All compounds indicated a basic steroidal skeletal structure with similar upfield chemical shifts in their ^{1}H NMR spectra. A similar multiplet resonance (δ_H 3.46 - 3.54) was observed for the hydroxylated proton at position 3 for compounds **1**, **3** and **4**. However, a downfield shift to δ_H 3.94 was observed for

this proton in compound **2** (ergosterol peroxide), due to the close proximity of the additional electronegative atoms (peroxide between C-5 and C-8) in Ring B. With the exception of compound **4** (campestanol), the other phytosterols have double bonds within their structures; at positions 5 (δ_H 5.32, H-6) and 22 (δ_H 4.96 – 5.16, H-22&23) for compound **1** (stigmasterol); 6 (δ_H 6.48, H-6) and 7 (δ_H 6.46, H-7) for compound **2** (ergosterol peroxide) and 5 (δ_H 5.32, H-6) for compound **3** (*β*-sitosterol). This unsaturation was confirmed by ^{13}C NMR resonances at δ_C 121.71 (C-6) and 140.76 (C-5) in stigmasterol and *β*-sitosterol. Additionally, resonances at δ_C 129.27 (C-23) and 138.30 (C-22) were observed for stigmasterol confirming the presence of the second double bond.

In compound **3** (ergosterol peroxide), the bicyclic linkage was confirmed by resonances at δ_C 82.15 (C-5) and 79.43 (C-8) which were oxygenated quaternary carbons (as resolved by DEPT experiments). The structure of ergosterol peroxide was further confirmed by HMBC correlations. The olefinic protons (H-6 and 7) and the angular methyl protons (H-19) correlated with C-5, thereby justifying the position of the peroxide in the second ring. Strong correlations were also observed between the methyl doublet (H-21) and C-17, C-22 and C-20, supporting the placement of the second double bond on the side chain at C-22. The molecular mass of stigmasterol, *β*-sitosterol and *β*-sitostanol were obtained by GC-MS as 412 [M^+], 414 [M^+] and 402 [M^+], respectively while the mass of ergosterol peroxide was obtained by LR-ESI-MS as 451.3705 for $[M+Na]^+$ (calculated for $C_{28}H_{44}O_3Na$, 451.318). Spectra-guided structural assignments of all compounds were consistent with literature data (Chaturvedula and Prakash 2012; Nowak et al., 2016; Horník et al., 2013).

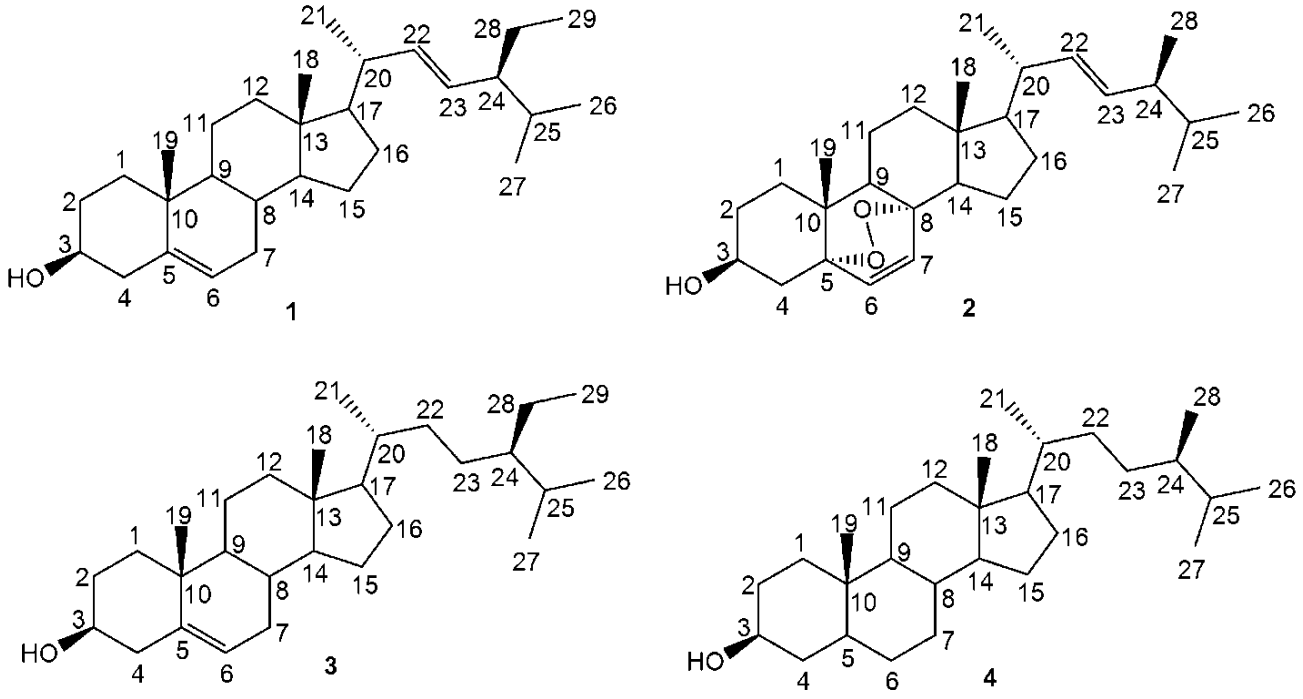

Figure 4.1: Isolated compounds from *Commelina africana*

4.2. Characterisation of nanoparticles

The aqueous and methanolic extracts of *Commelina africana* were used to synthesise silver nanoparticles (CAgNPs) and selenium nanoparticles (CSeNPs). Freestanding silver nanoparticles (AgNPs) and selenium nanoparticles (SeNPs) were synthesised using chemical means. This was done to compare the effects (if any) of extracts on nanoparticle properties. The influence of different volumes of extracts on nanoparticle properties was also investigated.

4.2.1. UV-Vis and FTIR spectroscopy

The formation of nanoparticles was observed visually by means of a colour change, upon reaction (Fig 4.2) and by measurement of the absorption peak using UV-Vis spectroscopy at wavelengths between 200 and 600 nm.

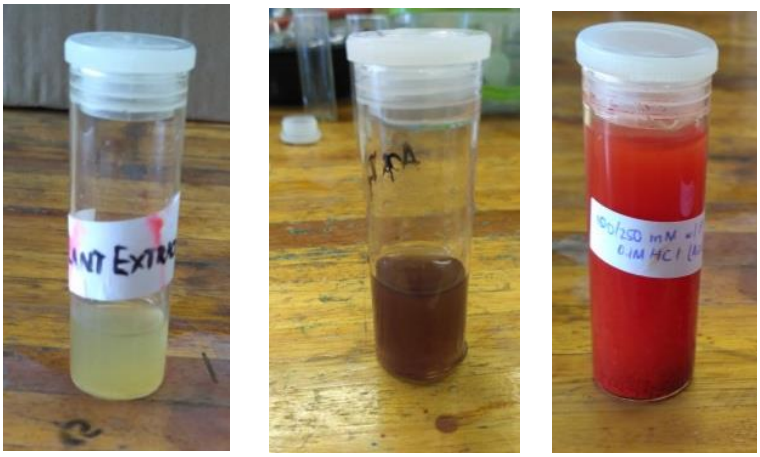

Figure 4.2: Plant extract (left), CAgNPs (centre) and CSeNPs (right)

The reduction of Ag^{+} to Ag^{0} by the aqueous and MeOH extracts is shown in Figures 4.3 and 4.4, respectively. The formation of AgNPs was observed by the development of brown particles in the reaction flask. The presence of the absorption peaks at 429 nm and 427 nm for CAgNPs (aqueous and MeOH extract) confirmed the formation of the particles as the characteristic maximum absorbance for AgNPs is between 400 and 500 nm (Edison & Sethuraman, 2012). There was no shift in absorbance maxima between CAgNPs (aqueous extract) and CAgNPs (MeOH extract) meaning that the particles formed by both methods were of similar size. The absorbance observed at 267 nm is due to compounds present in the plant extract (Edison & Sethuraman, 2012).

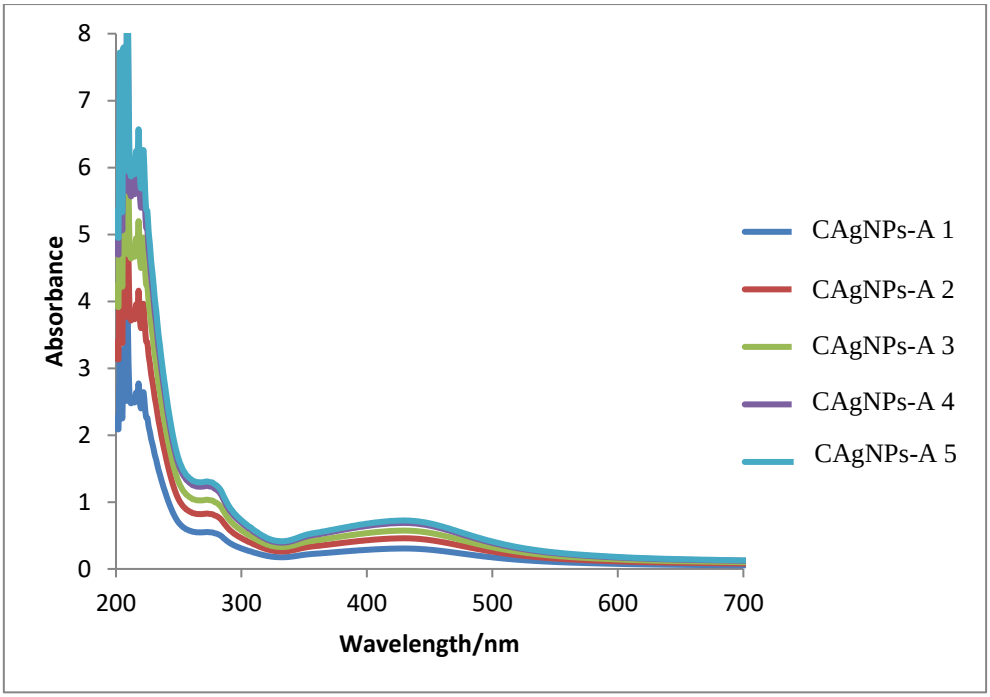

Figure 4.3: UV-Vis spectra of CAgNPs synthesised from the aqueous extract (A)

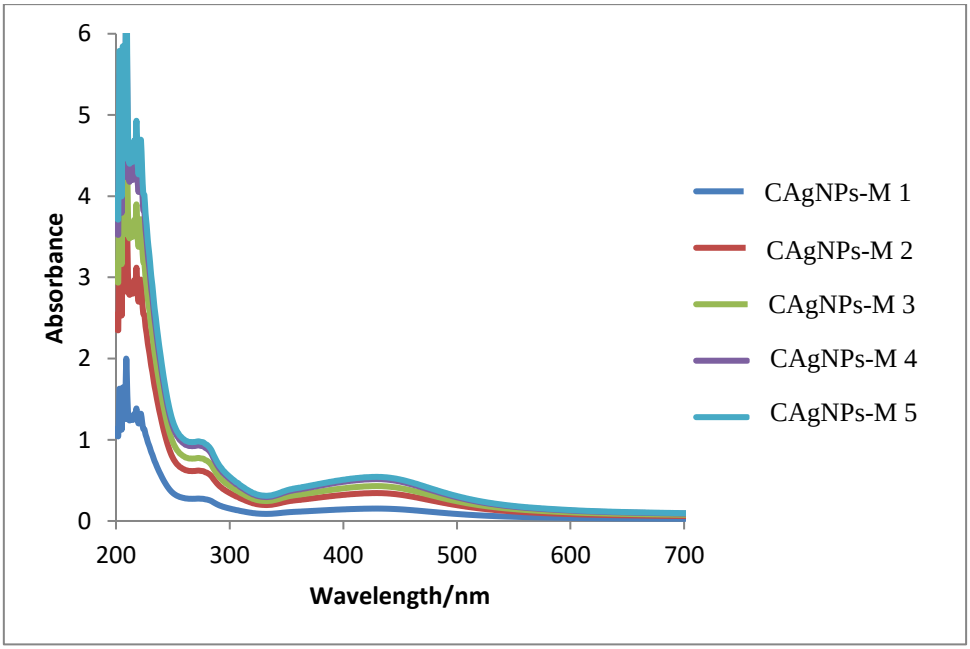

Figure 4.4: UV-Vis spectra of CAgNPs synthesised from the MeOH extract (M)

The synthesis of CSeNPs was observed by the formation of brick red particles in the reaction flask, characteristic of SeNPs (Sarkar et al., 2011). The observed absorption for CSeNPs (aqueous extract) (Fig 4.5) and CSeNPs (MeOH extract) (Fig 4.6) at 267 nm was typical of

SeNPs (Kokila et al., 2017; Srivastava & Mukhopadhyay, 2013). CSeNPs (MeOH extract) experienced a blue-shift because of the slightly larger particle sizes (Fleger & Rosenbluh, 2009).

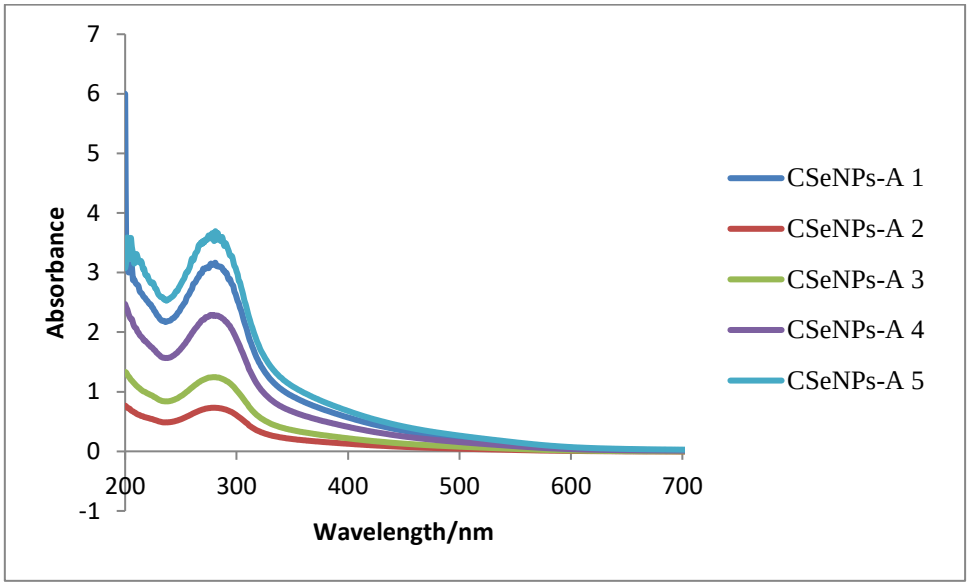

Figure 4.5: UV-Vis spectra of CSeNPs synthesised from the aqueous extract (A)

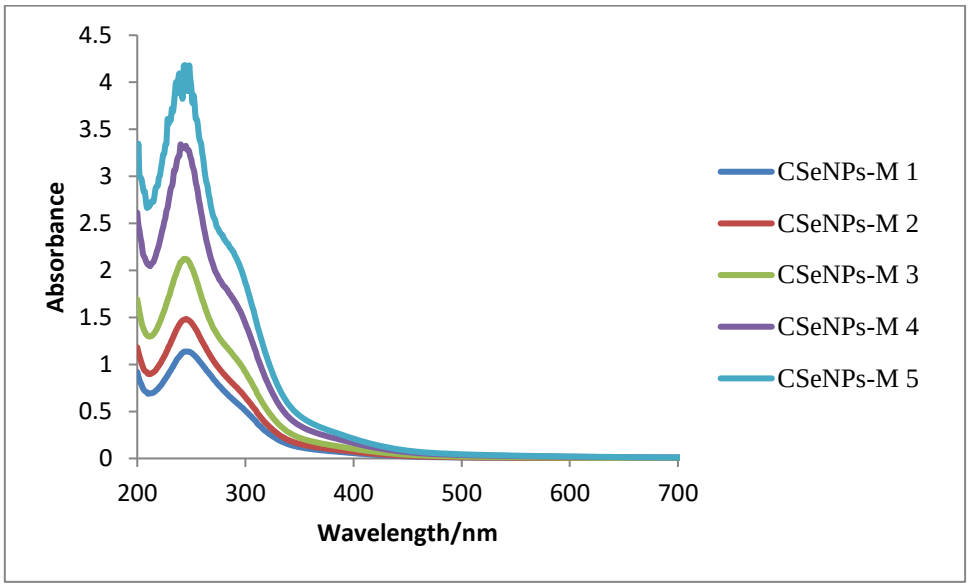

Figure 4.6: UV-Vis spectra of CSeNPs synthesised from the MeOH extract (M)

FTIR was used to determine the functional groups present in the crude aqueous and MeOH extracts of *C. africana* as well as CAgNPs, and CSeNPs synthesised from these two extracts.

The aqueous and MeOH extracts (Fig 4.7) both show the band stretches that are characteristic of the hydroxyl (-OH) group at 3245 cm^{-1} and 3296 cm^{-1}, respectively. The aqueous extract further has three distinct broad peaks at 1635 cm^{-1}, 1034 cm^{-1} and 559 cm^{-1}. These frequencies can be attributed to the alkene (C=C) bonds, the C-O group and alkyl halide or bending =C-H group, respectively. The MeOH extract has peaks at 2918 cm^{-1} and 2850 cm^{-1} (C-H stretch), 1780 cm^{-1} (C=O), 1628 cm^{-1} and 1545-1535 cm^{-1} (C=C), 1456 cm^{-1} (C-H bend) and 1036 cm^{-1} (C-O).

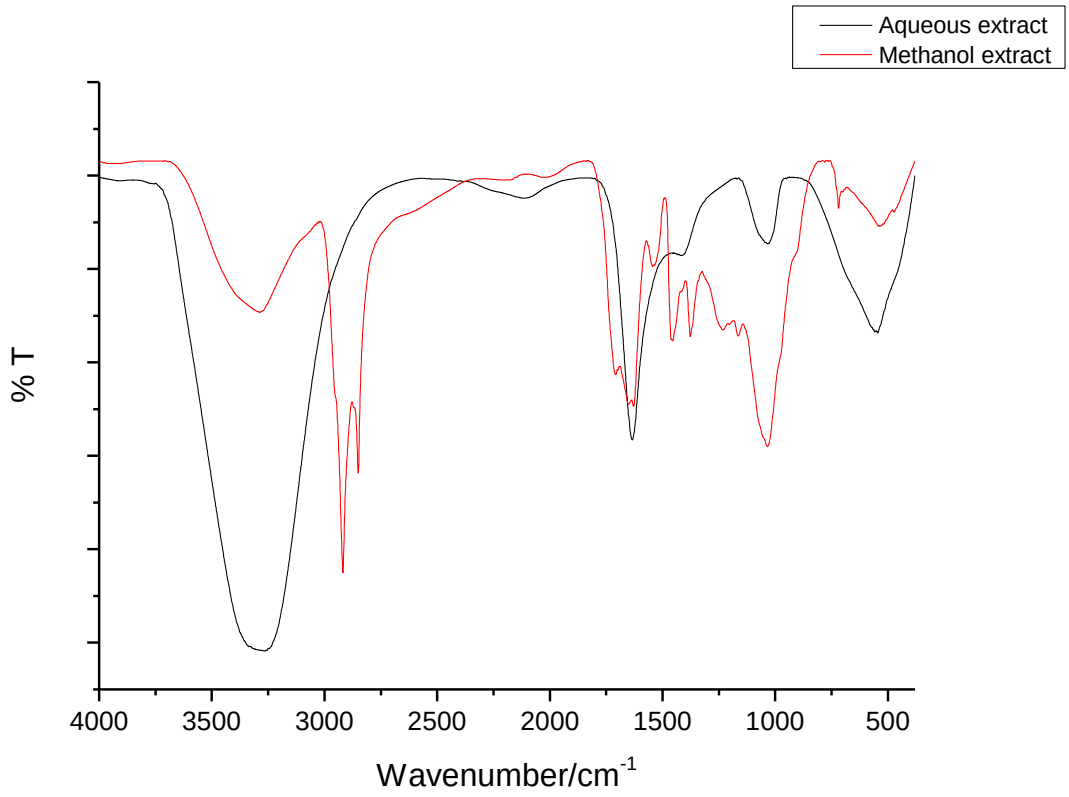

Figure 4.7: FTIR spectra of the aqueous and MeOH extracts of *Commelina africana*

The CAgNPs and CSeNPs synthesised with the aqueous and MeOH extracts (Appendix B) show similar spectral patterns including distinctive broad peaks due to the OH and C-H groups.

4.2.2. TEM and SEM analysis

4.2.2.1. Silver nanoparticles

Freestanding AgNPs showed an agglomeration of spheres with an average particle size of 72.89 ± 21.84 nm. Sodium borohydride as a reducing agent does not produce particles of sizes less than 40 nm (Agnihotri et al., 2014). The predominant shape of CAgNPs as observed by TEM images was spheres for both the aqueous and MeOH extracts. The particles were not uniform in size; both small and large particles were observed (Fig 4.8 A and B). Particle sizes ranged from 2.79 to 30.05 nm for those synthesised from the aqueous extract, and from 2.98 to 30.98 nm for those synthesised from the MeOH extract. CAgNPs from the aqueous extract exhibited more agglomeration than CAgNPs from the MeOH extract. Type of extract did not have a considerable effect on the shape and distribution of CAgNPs.

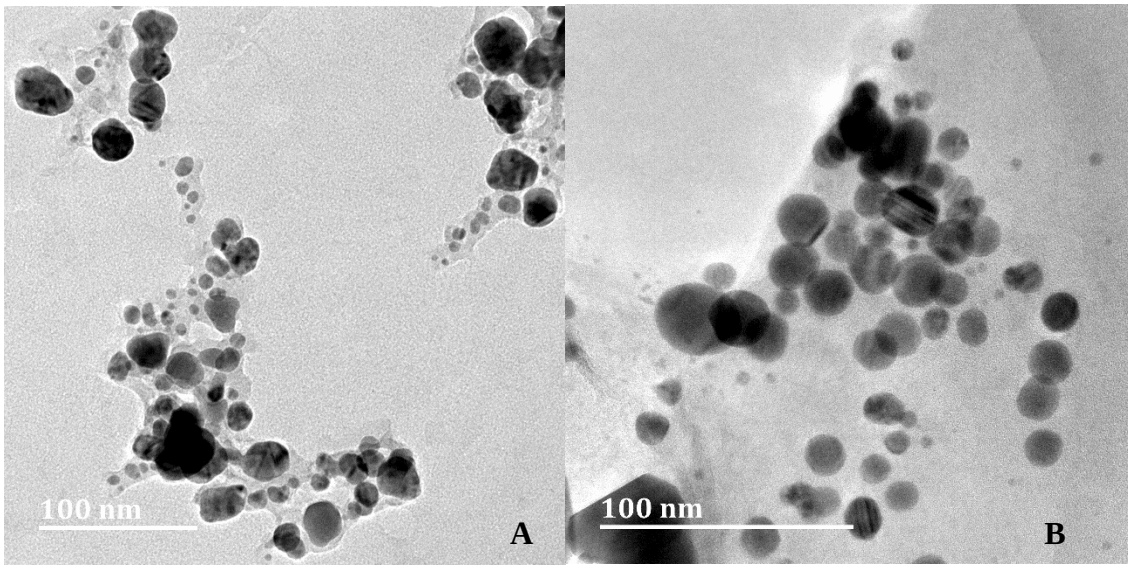

Figure 4.8: TEM images of CAgNPs synthesised using the aqueous extract (A) and the MeOH extract (B)

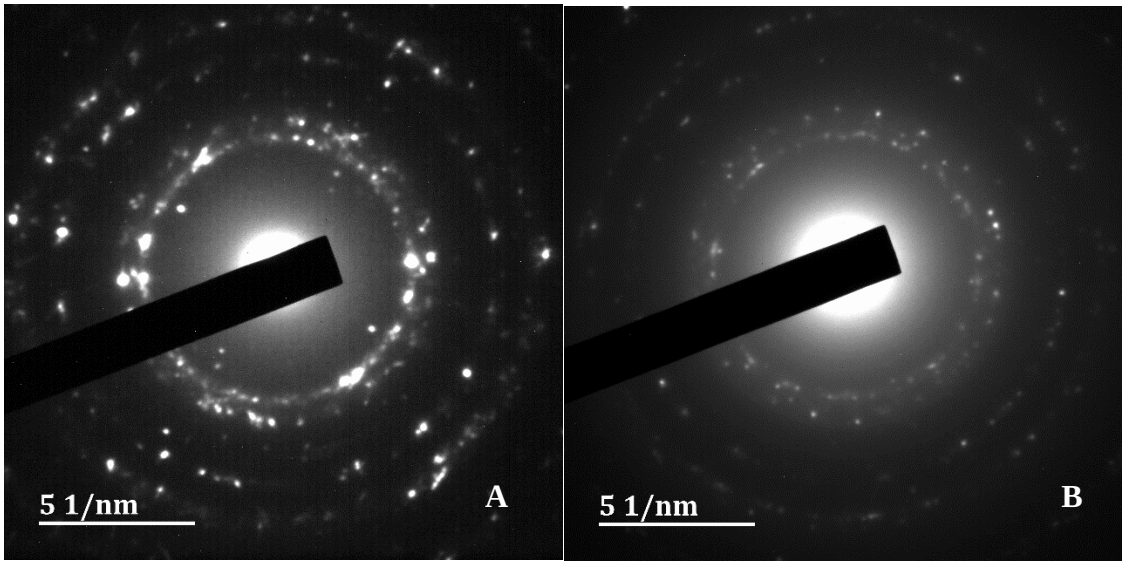

Figure 4.9: SAED images of CAgNPs synthesised using the aqueous extract (A) and the MeOH extract (B)

Figure 4.9 shows the SAED patterns for CAgNPs. The images display bright spots that are arranged within rings, which indicate that the CAgNPs are crystalline in nature. The lattice spacing 0.238 nm, 0.204 nm, 0.144 nm and 0.188 nm for CAgNPs (Fig 4.9 A) corresponded to the presence of (111), (200), (220) and (222) which are the planes of the face centred cubic (FCC) structure of AgNPs (Jyoti et al., 2016; Kora et al., 2012; Mehta et al., 2017). The observed lattice spacing 0.239 nm, 0.205 nm, 0.141 nm and 0.121 nm for CAgNPs synthesised from the MeOH extract (Fig 4.9 B) corresponded to the presence of (111), (200), (220) and (311) planes of the FCC structure. This confirms the formation of CAgNPs with the FCC crystal structure.

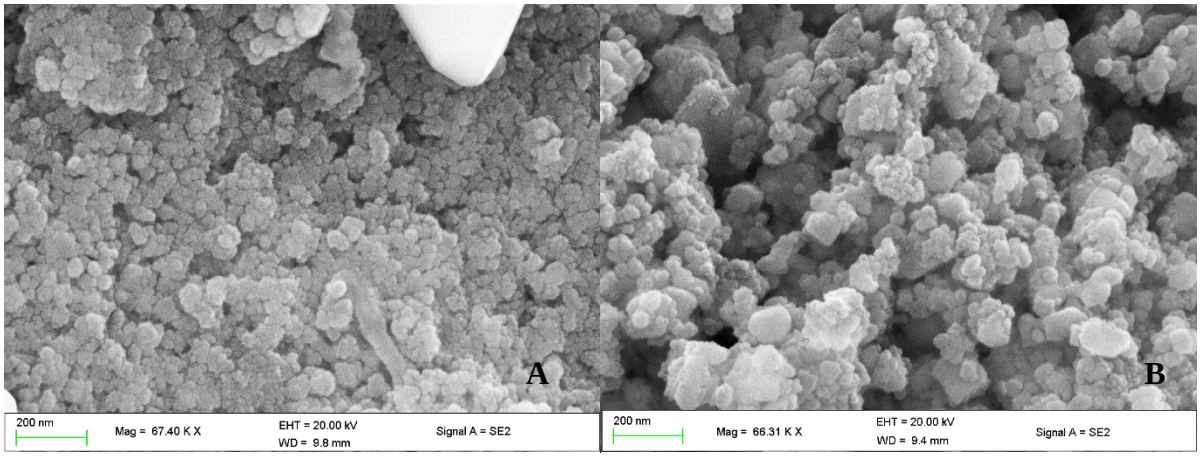

Figure 4.10: SEM images of CAgNPs synthesised using the aqueous extract (A) and the MeOH extract (B)

Figure 4.10 A and B shows the morphology, agglomeration and shapes of CAgNPs. The agglomerated spheres are in agreement with the TEM results (Fig 4.9). The structure of CAgNPs from the MeOH extract (Fig 4.10 B) is more defined than that from the aqueous extract (Fig 4.10 A).

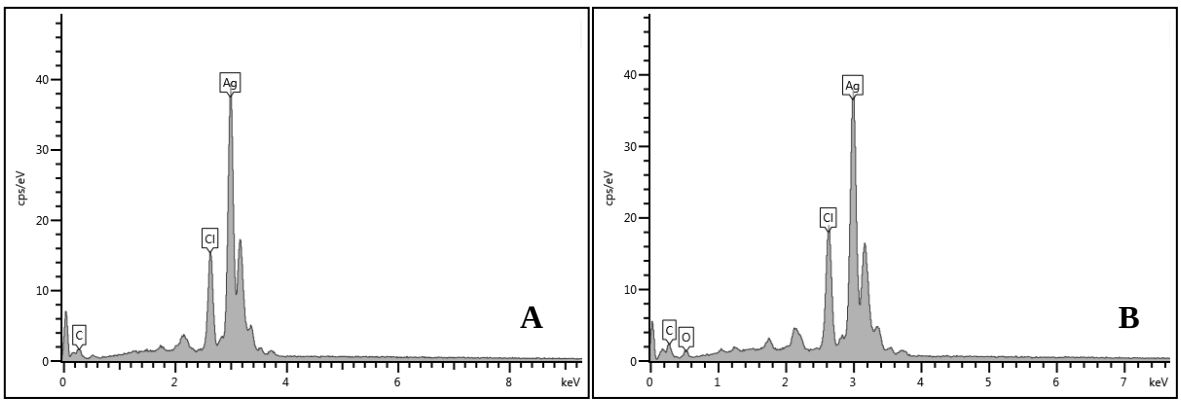

Figure 4.11: EDX spectra of CAgNPs synthesised using the aqueous extract (A) and the MeOH extract (B)

The EDX spectra (Fig 4.11) recorded from the SEM images confirm the prominence of the CAgNPs by the large peak (Ag) at 3 keV. The Ag peak at 3 keV is characteristic of AgNPs. The EDX spectra also indicate the presence of C, Cl and/or O peaks, which could be attributed

to the phytocompounds present in the extracts. Carbon sticky tape was also used to mount samples during sample preparation. Chlorine may also have resulted due to sputtering during sample preparation.

4.2.2.2. Selenium nanoparticles

The synthesis of CSeNPs yielded large particles that were a mixture of spheres and fibrous rods (Fig 4.12 A and B). The TEM image obtained for CSeNPs synthesised using the aqueous extract (Fig 4.12 A) indicated particle sizes ranging from 23.41 to 232.69 nm. CSeNPs from the MeOH extract showed particle sizes ranging from 23.62 to 275.49 nm. These particles were not well dispersed and agglomerated to form larger particles.

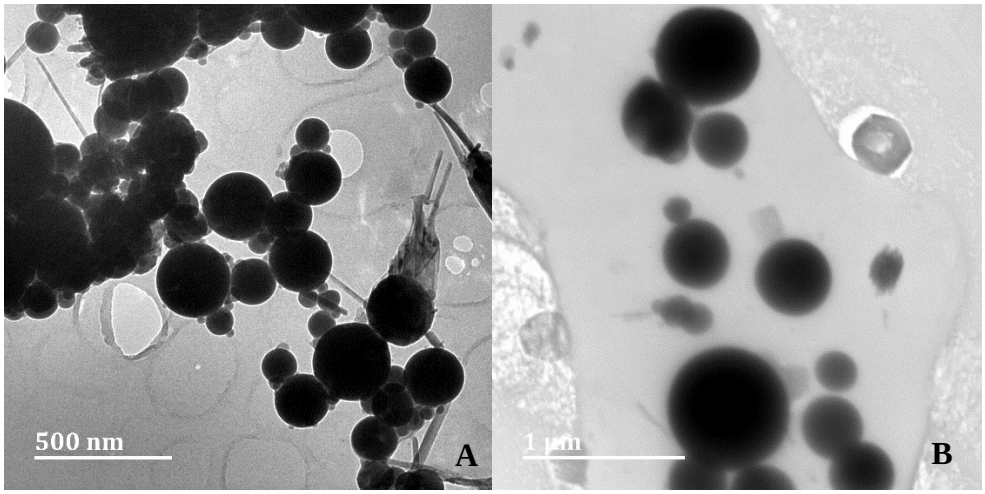

Figure 4.12: TEM images of CSeNPs synthesised using the aqueous extract (A) and the MeOH extract (B)

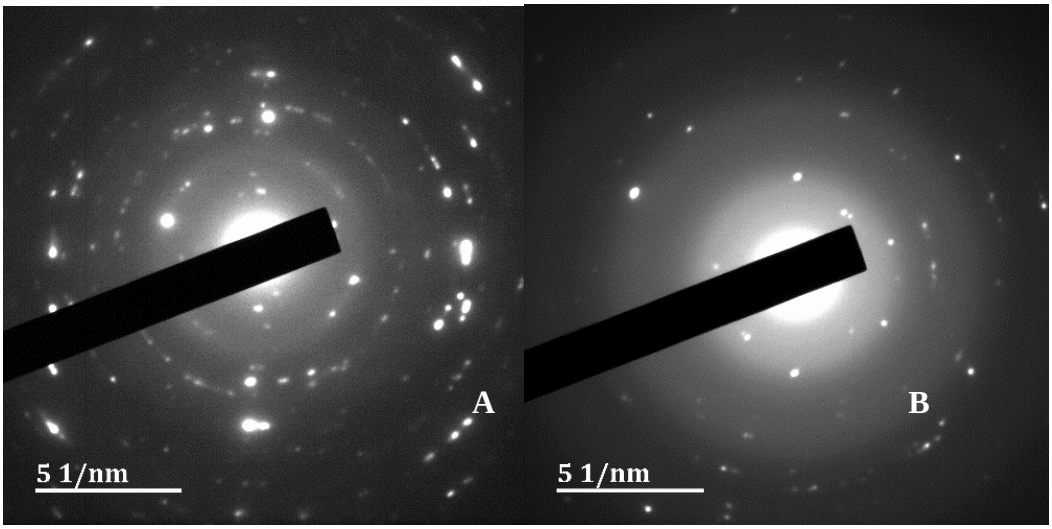

Figure 4.13: SAED images of CSeNPs synthesised using the aqueous extract (A) and the MeOH extract (B)

From the SAED patterns of CSeNPs (Fig 4.13), it is observed that the particles are of single crystallinity and the large spots on the pattern confirm their larger particle size. The diffraction grain spacing of 0.370 nm, 0.294 nm, 0.199 nm, 0.175 nm and 0.146 nm corresponds with (100), (101), (111), (201) and (103) (Fig 4.13 A); 0.300 nm, 0.288 nm, 0.155 nm and 0.146 nm corresponds with (100), (102), (201) and (202) (Fig 4.13 B). These patterns confirm the hexagonal phase of Se which is in agreement with literature (Kannan et al., 2014; Serra et al., 2014). Figure 4.14 A and B shows the different shapes produced by CSeNPs, as observed by the SEM images. The presence of spheres and rods is in agreement with the results obtained from the TEM images (Fig 4.12).

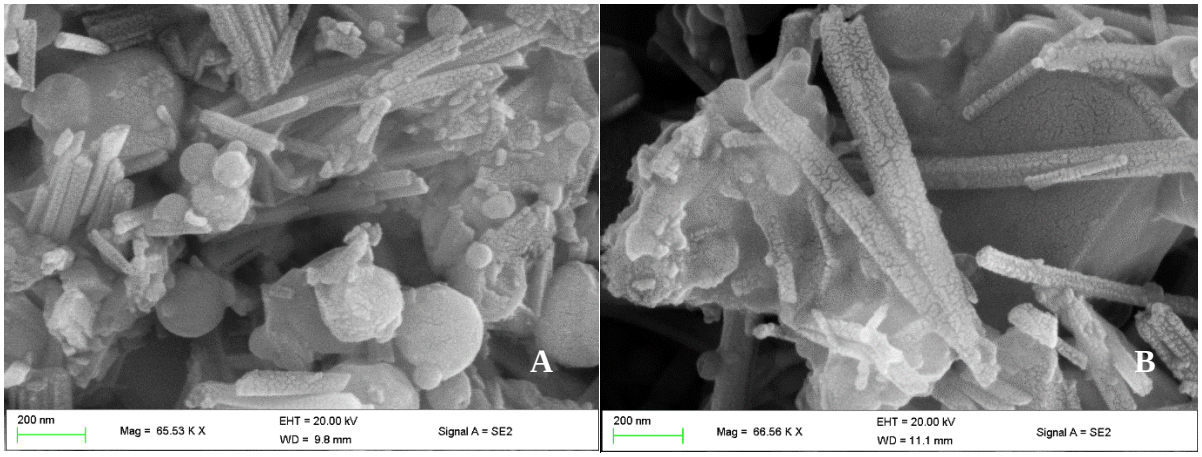

Figure 4.14: SEM images of CSeNPs synthesised using the aqueous extract (A) and the MeOH extract (B)

The EDX spectra (Fig 4.15) recorded from the SEM images confirms the presence of Se with strong characteristic peaks at 1.5, 11.2 and 12.5 keV (Kazempour et al., 2013). The carbon and oxygen peaks can be attributed to the biomolecules in the plant material.

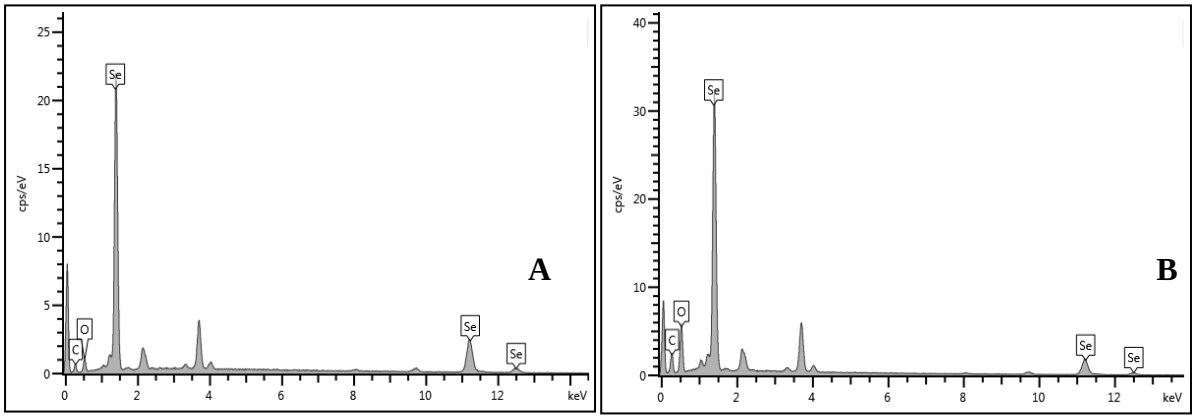

Figure 4.15: EDX spectra of CSeNPs synthesised using the aqueous extract (A) and the MeOH extract (B)

4.3. Antioxidant activity

This section discusses the results obtained for the antioxidant activity of the isolated phytocompounds (with the exception of campestanol due to insufficient sample mass), MeOH extract, aqueous extract, CAgNPs (aqueous extract), CAgNPs (MeOH extract), CSeNPs (aqueous extract), CSeNPs (MeOH extract), freestanding AgNPs and freestanding SeNPs. The highest volume (5 mL) across all synthesised NPs was used for the following tests.

4.3.1. Phytocompounds

4.3.1.1. 2,2-diphenyl-1-picrylhydrazyl (DPPH) assay

The scavenging ability of the isolated phytocompounds and ascorbic acid (standard) against the DPPH radical is summarised in Fig 4.16. The antioxidant activity of the phytosterols was relatively low, compared to the standard. The results show the scavenging activity of phytosterols to be in decreasing order of ergosterol peroxide > *β*-sitosterol > stigmasterol. Considering structure-activity relationships, it is clear that the peroxide bond in Ring B of ergosterol peroxide increases the radical scavenging activity of the phytosterol. Previous studies on the antioxidant activity of *β*-sitosterol from *Parinari curatellifolia* also showed very low to no scavenging activity relative to ascorbic acid (Halilu et al., 2013). The antioxidant activity of stigmasterol was also shown to be low using the DPPH, FRAP and phosphomolydenum assays (Sethiya et al., 2014).

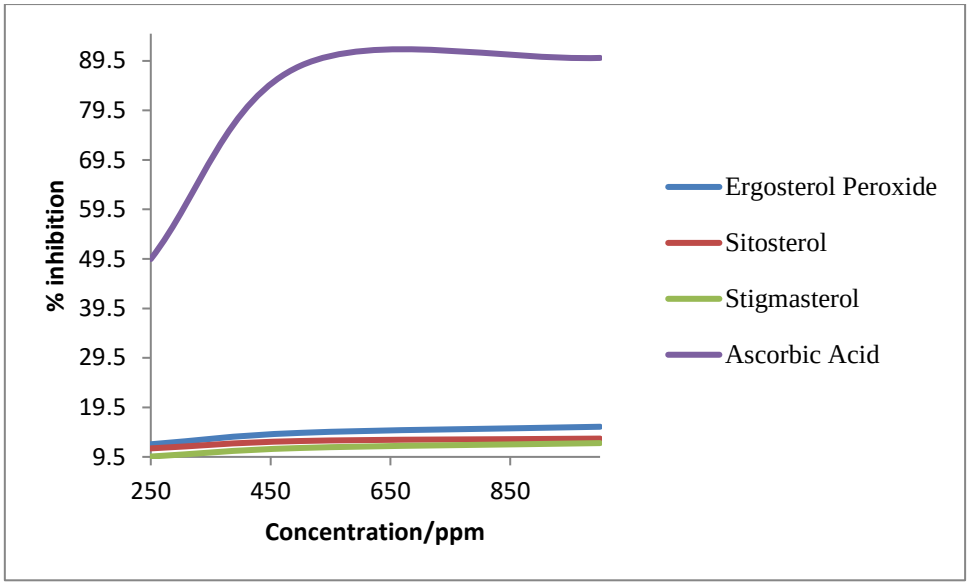

Figure 4.16: Antioxidant activity of the isolated phytocompounds and ascorbic acid standard, as measured by the DPPH method

4.3.1.2. Ferric reducing antioxidant power (FRAP) assay

The ferric reducing ability (Fe^{3+} to Fe^{2+}) of the phytosterols and ascorbic acid using the FRAP assay is presented in Figure 4.17. The order of activity for the FRAP assay is similar to the DPPH assay with ergosterol peroxide > *β*-sitosterol > stigmasterol. Similarly, the reducing powers of the phytosterols are also found to be concentration dependent. However, ergosterol peroxide had greater Fe^{3+} reducing potential, which was comparable to the standard, ascorbic acid. Previous reports on ergosterol peroxide isolated from *Armillariella mellea* showed good antioxidant activity on lipid peroxidation using the FRAP assay which also increased with concentration (Kim et al., 1999). The study showed ergosterol peroxide to have lower activity than butylated hydroxyl toluene (BHT) and butylated hydroxy anisole (BHA) but higher than that of α-tocopherol and thiourea (Kim et al., 1999).

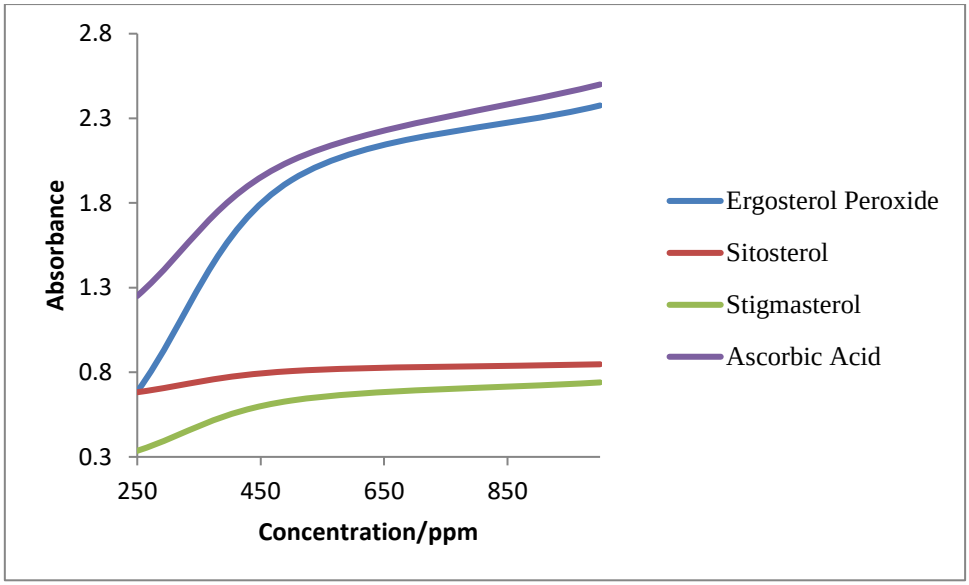

Figure 4.17: Antioxidant activity of the isolated phytocompounds and ascorbic acid standard, as measured by the FRAP method

Structure activity relationship amongst the isolated phytosterols provides a logical explanation to the observed differences in antioxidant potential. All of the compounds share the same "6-6-6-5" tetracyclic, phytosterol, ring pattern. However, there is a slight difference in the side chain of the twenty-fourth carbon methyl and ethyl branches, often resulting from the enzymatic activities of sterol methyltransferases (Valitova et al, 2016). Introduction of bicyclic peroxidation in ergosterol peroxide could be responsible for its enhanced antioxidant potential compared to stigmasterol and *β*-sitosterol. The slight difference in the antioxidant activity of stigmasterol and *β*-sitosterol proves that the double bond in position 22 has a negative influenced on antioxidant activity of stigmasterol compared to *β*-sitosterol. This is in agreement with a previous report on *β*-sitosterol as a better antioxidant than stigmasterol (Yoshida & Niki, 2003).

4.3.2. Nanoparticles

4.3.2.1. 2,2-diphenyl-1-picrylhydrazyl (DPPH) assay

The radical scavenging ability of the MeOH extract, aqueous extract, ascorbic acid (standard), freestanding AgNPs and CAgNPs (aqueous and MeOH extracts) is presented in Figure 4.18 and that of the MeOH extract, aqueous extract, ascorbic acid (standard), freestanding SeNPs and CSeNPs (aqueous and MeOH extracts) is presented in Figure 4.19.

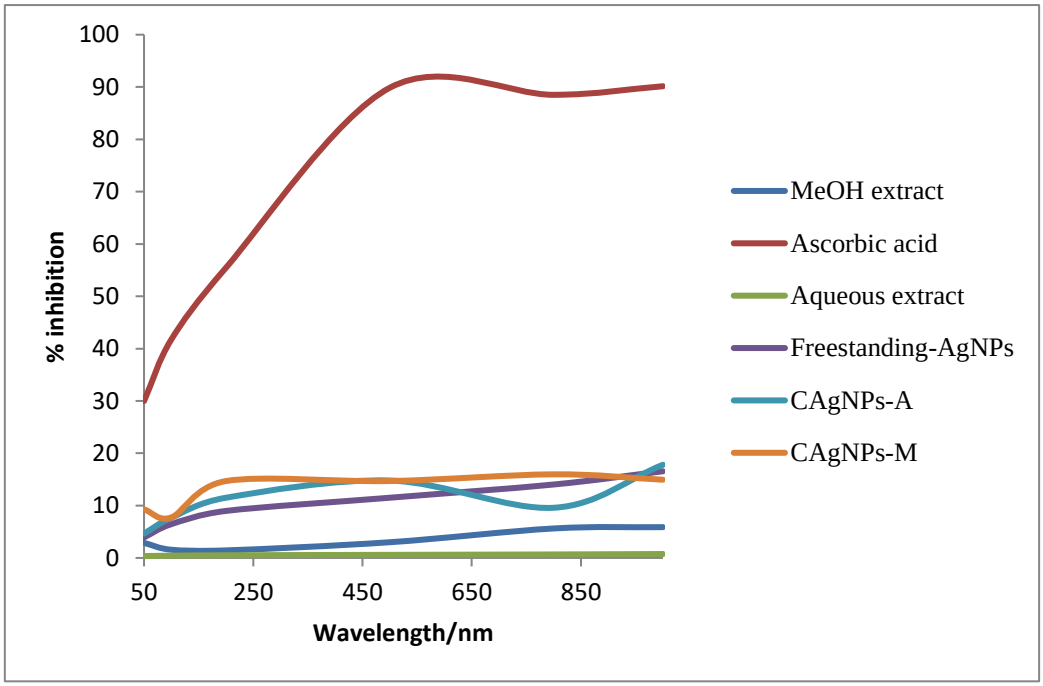

Figure 4. 18: Antioxidant activity of the MeOH and aqueous extracts, ascorbic acid (standard), freestanding AgNPs and CAgNPs (aqueous (A) and MeOH (M) extract) as measured by the DPPH assay

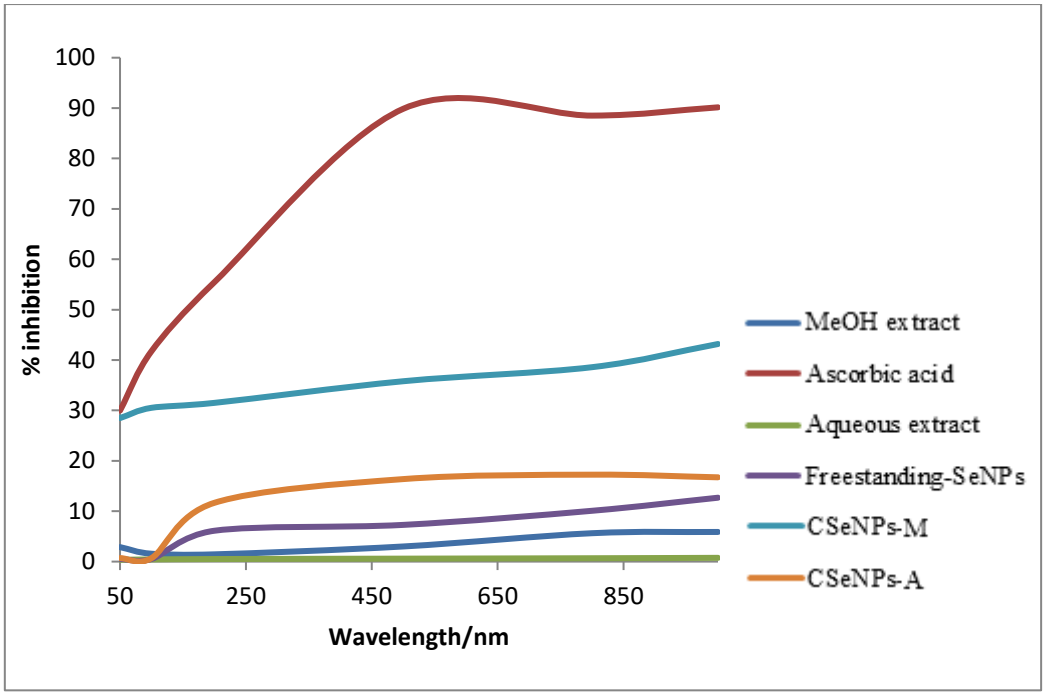

Figure 4.19: Antioxidant activity of the MeOH and aqueous extracts, ascorbic acid (standard), freestanding SeNPs and CSeNPs (aqueous (A) and MeOH (M) extract) as measured by the DPPH assay

Freestanding AgNPs and SeNPs showed similar antioxidant activity, which was slightly higher than that of the aqueous and MeOH extracts, which showed minimal activity. The results show the radical scavenging activity of CAgNPs and CSeNPS to be enhanced relative to their freestanding counterparts and extracts alone. This indicates a synergistic antioxidant effect between the metal nanoparticles and adsorbed biomolecules (Fig 4.18 & 4.19). The antioxidant activity of CSeNPs (MeOH extract) (Fig 4.19) was also found to be relatively high and comparable to the standard, ascorbic acid. The DPPH radical scavenging activity was found to be in decreasing order of ascorbic acid > CSeNPs (MeOH extract) > CAgNPs (MeOH extract) ~ CAgNPs (aqueous extract) ~ CSeNPs (aqueous extract) > freestanding SeNPs and AgNPs > MeOH extract > aqueous extract.

4.3.2.2. Ferric reducing antioxidant power (FRAP) assay

The ferric reducing ability of the aqueous and MeOH extracts, nanoparticles and ascorbic acid are presented in Figure 4.20 and Figure 4.21. Unlike the radical scavenging activity, the MeOH extract showed greater reducing ability, comparable to the standard. Similar to the radical scavenging activity, CSeNPs (MeOH extract) showed better reducing ability than the other tested nanoparticles. The reducing ability of samples steadily increased with an increase in concentration. The antioxidant activity by the FRAP assay was found to be in decreasing order of ascorbic acid > MeOH extract > CSeNPs (MeOH extract) > CSeNPs (aqueous extract) > CAgNPs (MeOH extract) > Aqueous extract > CAgNPs (aqueous extract) > freestanding AgNPs and SeNPs.

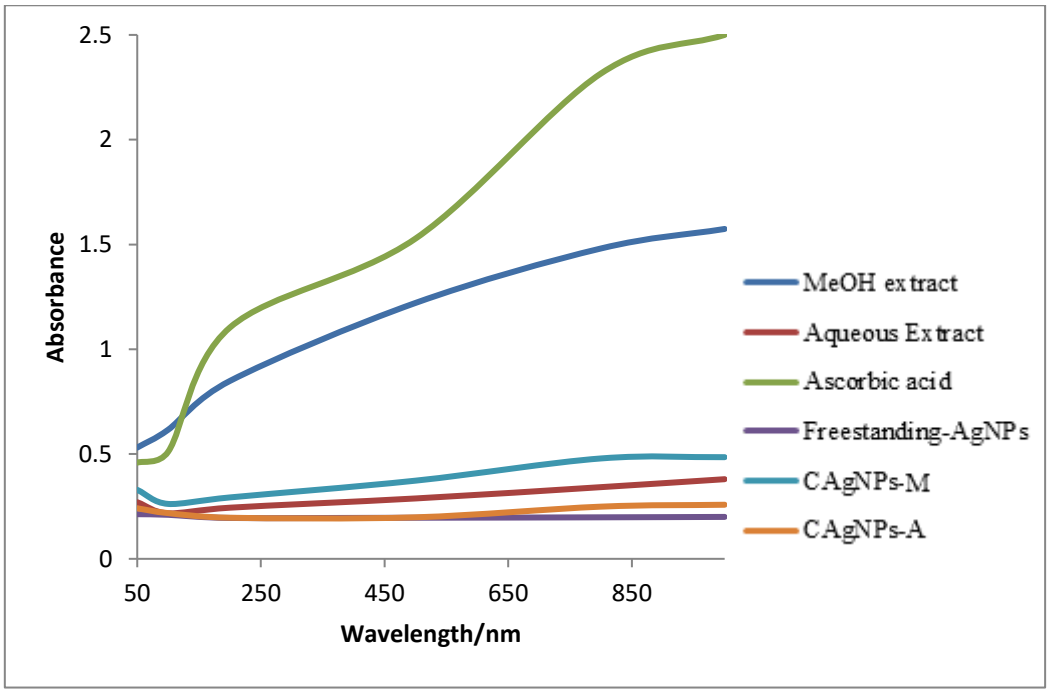

Figure 4.20: Antioxidant activity of the MeOH and aqueous extracts, ascorbic acid (standard), freestanding AgNPs and CAgNPs (aqueous (A) and MeOH (M) extract) as measured by the FRAP assay

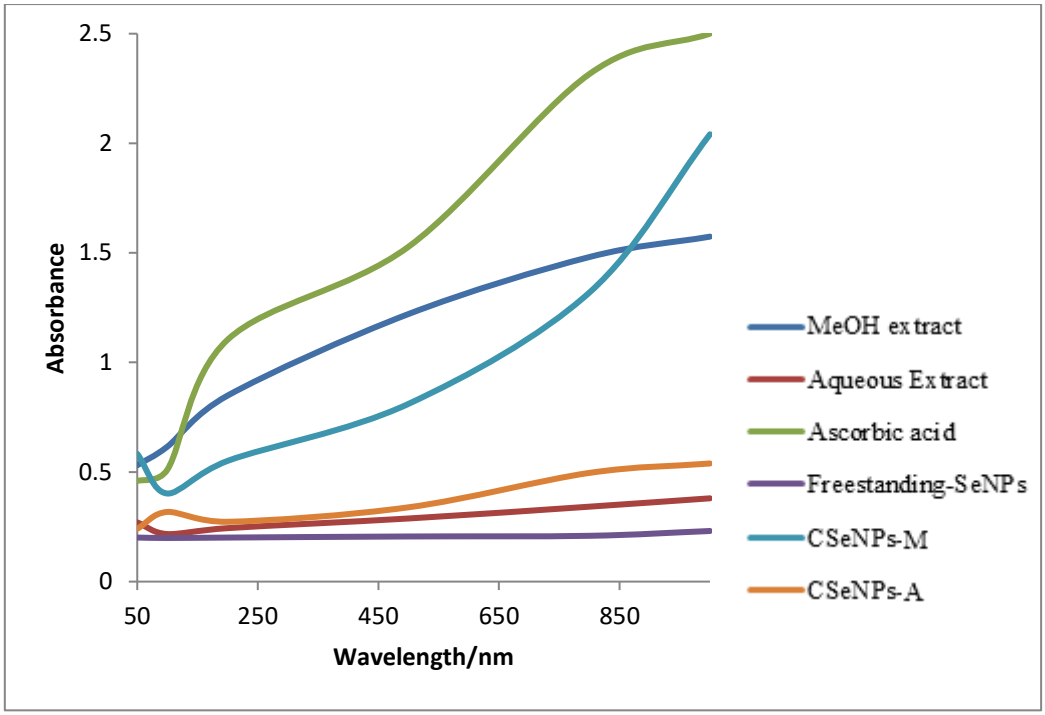

Figure 4.21: Antioxidant activity of the MeOH and aqueous extracts, ascorbic acid (standard), freestanding SeNPs and CSeNPs (aqueous (A) and MeOH (M) extract) as measured by the FRAP assay

4.4. Antibacterial activity

The phytosterols, crude extracts (aqueous and MeOH) from the leaves of *Commelina africana*, CAgNPs and CSeNPs as well as freestanding AgNPS and SeNPs were tested for their inhibitory activity against Gram-positive (*Staphylococcus aureus* and *Enterococcus faecalis*) and Gram-negative (*Escherichia coli, Klebsiella pneumonia, Pseudomonas aeruginosa* and *Chromobacterium violaceum*) bacterial strains. These results are summarised in Table 4.1 and Table 4.2. Only those results that showed activity are presented.

Table 4.1: Zones of inhibition (mm) of silver nanoparticles synthesised using *Commelina africana* aqueous extract (CAgNPs-A) and MeOH extract (CAgNPs-M) against Gram-positive bacteria at 20 µL and 40 µL concentrations

Sample identity	*S. aureus*	
	20 µL	40 µL
	Inhibition / mm	
CAgNPs-A (1 mL)*	12	12
CAgNPs-A (5 mL)**	12	13
CAgNPs-M (1 mL)	11	11
CAgNPs-M (5 mL)	8	9

*, ** 1 and 5 mL are the extract volumes used to form nanoparticles

Phytocompounds, crude plant extracts and freestanding nanoparticles were inactive against all the Gram-positive bacterial strains tested. No tested samples were active against *E. faecalis*, a common bacterial strain responsible for human infections. This bacterial stain has developed resistance to various antibiotics including vancomycin, the drug that is used as the last line of therapy for many Gram-positive infections (Kau et al., 2005). Except for CAgNPs (aqueous and MeOH extracts), all other test samples did not exhibit any activity against *S. aureus*. A previous study showed stigmasterol and *β*-sitosterol to have strong activity against Gram-positive bacteria and modest activity against Gram-negative bacteria (Sharma, 1993). However, the acetates of *β*-sitosterol and stigmasterol were shown to have lower activity against Gram-positive bacteria with no difference against Gram-negative bacteria compared to their unacetylated counterparts (Sharma, 1993). In this study, stigmasterol and *β*-sitosterol showed no activity against the bacterial strains tested.

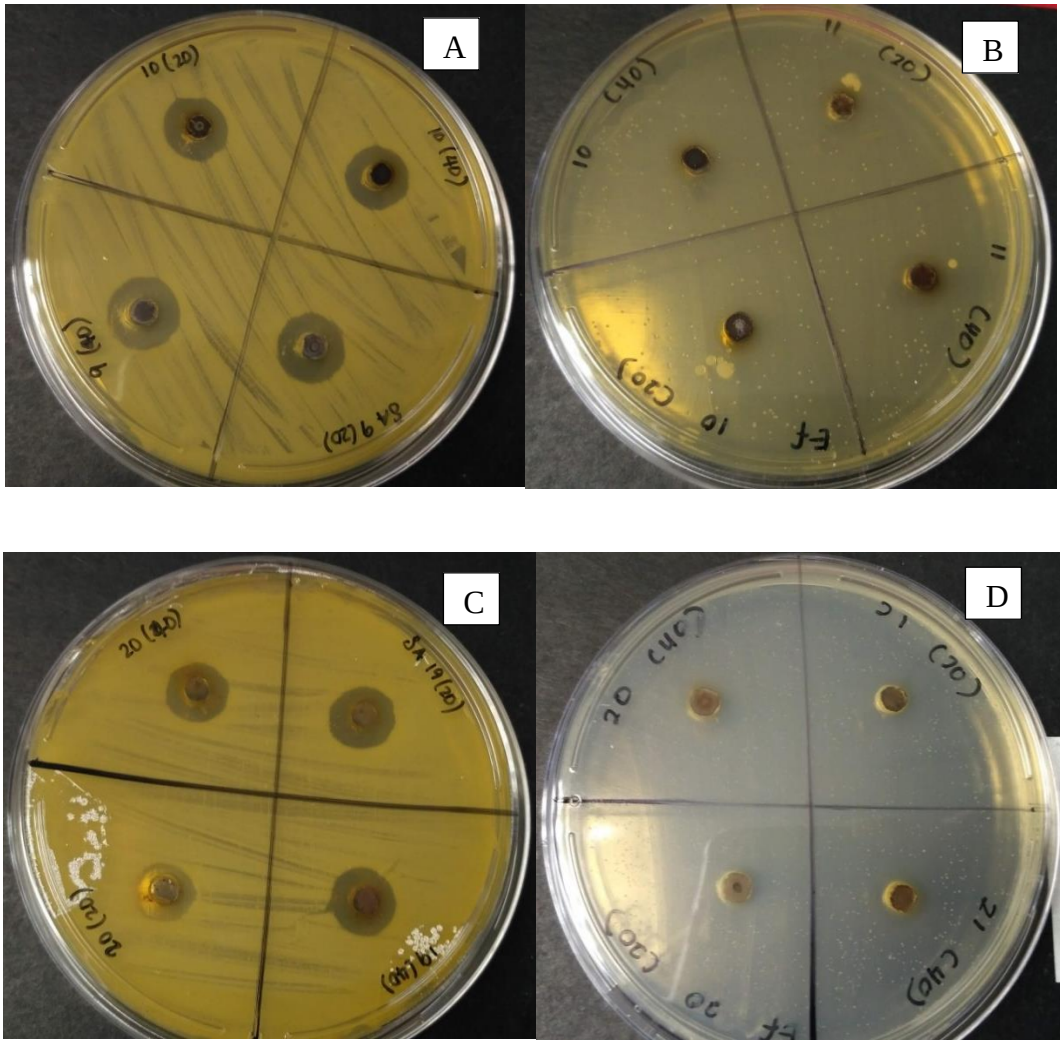

Figure 4.22: Inhibition zones of CAgNPs (aqueous extract) against *S. aureus* (A) and *E. faecalis* (B) and CAgNPs (MeOH extract) against *S. aureus* (C) and *E. faecalis* (D)

CAgNPs (aqueous and MeOH extracts) showed positive results against *S. aureus* at all tested concentrations with activity being independent of concentration (Table 4.1 & Fig 4.22). In a reaction between a soft acid (silver) and a soft base (phosphorus and sulfur compounds contained in the bacterial cells), free oxygen species may be generated, resulting in the termination of the bacteria (Jyoti et al., 2016). The inhibitory potential of the plant-synthesised AgNPs was higher than those synthesised using chemical methods (freestanding AgNPs) (no activity). This could be due to the presence of adsorbed biomolecules that produce synergistic antibacterial effects with the silver metal core.

Table 4.2: Zones of inhibition (mm) of silver nanoparticles synthesised using *Commelina africana* aqueous extract (CAgNPs-A) and MeOH extract (CAgNPs-M) against Gram-negative bacteria at 20 µL and 40 µL concentrations

Sample identity	*E. coli*		*K. pneumoniae*		*P. aeruginosa*		*C. violaceum*	
	20 µL	40 µL	20 µL	40 µL	20 µL	40 µL	20 µL	40 µL
	Inhibition / mm		Inhibition / mm		Inhibition / mm		Inhibition / mm	
CAgNPs-A (1 mL)*	11	11	7	8	14	16	16	16
CAgNPs-A (5 mL)**	8	11	9	9	13	13	14	15
CAgNPs-M (1 mL)	11	11	7	8	11	13	15	15
CAgNPs-M (5 mL)	8	8	9	13	12	11	14	15

*, ** 1 and 5 mL are the extract volumes used to form nanoparticles

Phytocompounds, crude plant extracts and freestanding nanoparticles were inactive against all the Gram-negative bacterial strains tested. CAgNPs (aqueous and MeOH extracts) showed substantial inhibitory activity against all the tested Gram-negative bacteria. The choice of plant extract used as a reductant to synthesise AgNPs did not have an observable impact on antibacterial activity, as there was no significant change in the inhibitory diameters. SeNPs (both freestanding and plant synthesised) did not prevent the growth of the *E. coli*, *K. pneumonia* and *P. aeruginosa*. However, freestanding SeNPs were active against *C. violaceum*, indicating anti-quorum sensing ability (Fig 4.23). Larger particles have a smaller surface area therefore, a small number of biomolecules can adsorb onto the surface of the particle. AgNPs were smaller in particle size; this improves their ability to perforate bacterial cell membranes (Albanese et al., 2012). They also would have the ability to adsorb more active biomolecules per volume, which could increase antibacterial activity. On the other hand, SeNPs had larger particle sizes which would adsorb less active biomolecules per volume and would not easily be taken up by the bacterial strains (Albanese et al., 2012).

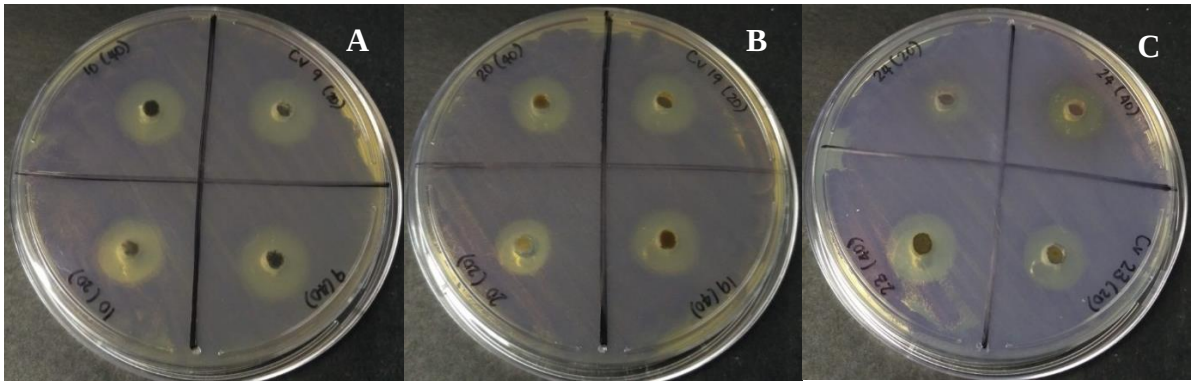

Figure 4.23: Zones of inhibition against *C. violaceum* by CAgNPs (aqueous extract) (A), CAgNPs (MeOH extract) (B) and CSeNPs (MeOH extract) (C)

The anti-quorum sensing ability of nanoparticles that produced promising results is summarised in Table 4.3. Isolated compounds, crude extracts and nanoparticles were tested for their quorum sensing (QS) inhibitory activity against the Gram-negative *C. violaceum*. The samples were added at two different concentrations (20 µL (200 µg) and 40 µL (400 µg)). With the previous antibacterial tests, isolated compounds exhibited no inhibitory activity against the tested strains; however, with the overlay test, ergosterol peroxide and *β*-sitosterol were promising in their inhibitory potential though the observed zones which were quite faint meaning that they are not strong inhibitors. CAgNPs (aqueous extract) displayed the strongest inhibition at 20 µL (200 µg) injection concentration with an 18 mm inhibition diameter. All freestanding AgNPs showed satisfactory activity with the strongest inhibition displayed by freestanding AgNPs (5 mL) at both injection concentrations with both having a 13 mm diameter of inhibition. SeNPs also showed promise, but its ability to break down communication between bacteria was relatively low, compared to CAgNPs.

Table 4.3: Anti-quorum sensing inhibition zones (mm) by AgNPs against *Chromobacterium violaceum* at 20 µL and 40 µL concentrations

Sample identity	*C. violaceum* overlays	
	20 µL	40 µL
	Inhibition / mm	
CAgNPs-A (1 mL)	18	13
CAgNPs-A (5 mL)	13	14
CAgNPs-M (1 mL)	14	15
CAgNPs-M (5 mL)	12	12
Freestanding-AgNPs (5 mL)	13	13

CHAPTER FIVE

SUMMARY AND CONCLUSIONS

In this study, four phytosterols from the medicinal plant species, *Commelina africana*, were successfully isolated, characterised and identified. They were stigmasterol, ergosterol peroxide, β-sitosterol and campestanol. The crude plant extracts were used to synthesise silver and selenium nanoparticles and their antioxidant and antibacterial activities were tested relative to the extracts, freestanding counterparts and known standards.

The general shape of the plant synthesised AgNPs was spherical with maximum sizes averaging approximately 30 nm. The formation of AgNPs was confirmed by EDX. All plant synthesised AgNPs were found to be crystalline by SAED and they have the FCC crystal structure characteristic of AgNPs. Plant synthesised SeNPs were a mixture of spheres and fibrous rods with maximum sizes averaging approximately 250 nm. The formation of SeNPs was confirmed by EDX, and SAED showed them to be crystalline with the hexagonal crystal structure.

For the biological tests, crude extracts, phytocompounds, and all synthesised SeNPs were inactive against all tested bacteria. Plant synthesised AgNPs were relatively active against the *S. aureus*, *E. coli*, *K. pneumoniae*, *P. aeroginosa* and *C. violaceum* bacterial strains. Ergosterol peroxide showed good antioxidant activity by the DPPH assay. Plant synthesised SeNPs using the MeOH extract showed good radical scavenging ability and reducing potential by the DPPH and FRAP assays, respectively.

This is the first report on the isolation of phytocompounds from the plant species, *Commelina africana*, and the use of these extracts for the synthesis of silver and selenium nanoparticles that were further tested for biological activity.

RECOMMENDATIONS FOR FUTURE STUDIES

Future work can look at the attempts to isolate more biologically active secondary metabolites from *C. africana*. The more biologically active phytocompounds could then be used synthesise NPs that could have increased antibacterial and antioxidant activities. Different parameters such as temperature, pH and time should be explored in the synthesis of NPs. Phytocompounds and NPs should be screened for anticancer, antidiabetic and antiviral activities.

Analytical studies on the different edible parts of the plant can be conducted. The study could focus on quantifying essential and non-essential (toxic) metals in the plant. This information would help at setting dietary recommendations for this plant as it is consumed by some communities.

REFERENCES

Acamovic, T., & Brooker, J. D. (2007). Biochemistry of plant secondary metabolites and their effects in animals. Proceedings of the Nutrition Society, 64(3), 403-412.

Agnihotri, S., Mukherji, S. and Mukherji, S. 2014. Size-controlled silver nanoparticles synthesized over the range 5-100 nm using the same protocol and their antibacterial efficacy. RSC Advances, 4, 3974-3983.

Agunbiade, O. S., Ojezele, O. M., Ojezele, J. O., & Ajayi, A. Y. (2012). Hypoglycaemic activity of *Commelina africana* and *Ageratum conyzoides* in relation to their mineral composition. African Health Sciences, 12(2), 198-203.

Ahmad, N., & Sharma, S. (2012). Green synthesis of silver nano particles using extracts of *Ananas comosus*. Green Sustainable Chemistry, 2(4), 141-147.

Albanese, A., Tang, P. S., & C W Chan, W. (2012). The effect of nanoparticle size, shape, and surface chemistry on biological systems. Annual Review of Biomedical Engineering, 14(1), 1-16.

Alexander, J. W. (2009). History of the medical use of silver. Surgical Infections, 10(3), 289-292.

Antolovich, M., Prenzler, P. D., Patsalides, E., Mcdonald, S., & Robards, K. (2002). Methods for testing antioxidant activity. Analyst, 127(1), 183-198.

Anu, K., Singaravelu, G., Murugan, K., & Benelli, G. (2017). Green-synthesis of selenium nanoparticles using garlic cloves (*Allium sativum*): Biophysical characterization and cytotoxicity on Vero cells. Journal of Cluster Science, 28(1), 551-563.

Attah, A. F., O'brien, M., Koehbach, J., Sonibare, M. A., Moody, J. O., Smith, T. J., & Gruber, C. W. (2012). Uterine contractility of plants used to facilitate childbirth in Nigerian ethnomedicine. Journal of Ethnopharmacology, 143(1), 377-382.

Balouiri, M., Sadiki, M., & Ibnsouda, S. K. (2016). Methods for in vitro evaluating antimicrobial activity: A review. Journal of Pharmaceutical Analysis, 6(2), 71-79.

Benakashani, F., Allafchian, A. R., & Jalali, S. A. H. (2016). Biosynthesis of silver nanoparticles using *Capparis spinosa* L. leaf extract and their antibacterial activity. Karbala International Journal of Modern Science, 2(4), 251-258.

Benzie, I. F. F., & Strain, J. J. (1996). The ferric reducing ability of plasma (FRAP) as a measure of "antioxidant power": The FRAP assay. Analytical Biochemistry, 239(1), 70-76.

Bhatia, S. (2016). Nanoparticles types, classification, characterization, fabrication methods and drug delivery applications. Natural Polymer Drug Delivery Systems: Nanoparticles, Plants, and Algae. Springer International Publishing, 33-93.

Bone K., M. S., Dixon M., Blumenthal M. (2013). Principles of herbal pharmacology, Principles and Practice of Phytotherapy (2nd Edition). Saint Louis: Churchill Livingstone, 17-82.

Bonev, B., Hooper, J., & Parisot, J. (2008). Principles of assessing bacterial susceptibility to antibiotics using the agar diffusion method. Journal of Antimicrobial Chemotherapy, 61(6), 1295-1301.

Bouayad, N., Rharrabe, K., Lamhamdi, M., Nourouti, N. G., & Sayah, F. (2012). Dietary effects of harmine, a *β*-carboline alkaloid, on development, energy reserves and α-amylase activity of *Plodia interpunctella* Hübner (Lepidoptera: Pyralidae). Saudi Journal of Biological Sciences, 19(1), 73-80.

Breytenbach, U., Clark, A., Lamprecht, J., & Bouic, P. (2001). Flow cytometric analysis of the Th1-Th2 balance in healthy individuals and patients infected with the human immunodeficiency virus (HIV) receiving a plant sterol/sterolin mixture. Cell Biology International, 25(1), 43-49.

Bruice, P. Y. (2014). Mass spectrometry, infrared spectroscopy and ultraviolet/ visible spectroscopy. Organic Chemistry (7th Edition). Pearson/Prentice Hall, 595-648.

Calderón, C. B., & Sabundayo, B. P. (2007). Antimicrobial classifications: Drugs for bugs. Antimicrobial Susceptibility Testing Protocols. CRC Press, 7-52.

Cooper, R., & Nicola, G. (2014). Natural Products Chemistry: Sources, Separations and Structures. CRC Press. Taylor & Francis.

Doughari, J. H. (2012). Phytochemicals: extraction methods, basic structures and mode of action as potential chemotherapeutic agents. Dr Venketeshwer Rao (Ed.) In Phytochemicals-A global perspective of their role in nutrition and health. InTech, 1-32.

Dube, A., & Ebrahim, N. (2017). The nanomedicine landscape of South Africa. Nanotechnology Reviews, 6(4), 339-344.

Edison, T. J. I., & Sethuraman, M. G. (2012). Instant green synthesis of silver nanoparticles using *Terminalia chebula* fruit extract and evaluation of their catalytic activity on reduction of methylene blue. Process Biochemistry, 47(9), 1351-1357.

Escárcega-González, C. E., Garza-Cervantes, J. A., Vázquez-Rodríguez, A., Montelongo-Peralta, L. Z., Treviño-González, M. T., Díaz Barriga Castro, E., Morones-Ramírez, J. R. (2018). In vivo antimicrobial activity of silver nanoparticles produced via a green chemistry synthesis using *Acacia rigidula* as a reducing and capping agent. International Journal of Nanomedicine, 13.

Evans, W. C., & Evans, D. (2009). Alkaloids. In Trease and Evans' Pharmacognosy (16th Edition). W.B. Saunders (Ed), E-Book. Elsevier Health Sciences, 353-415.

Fleger, Y., & Rosenbluh, M. (2009). Surface plasmons and surface enhanced raman spectra of aggregated and alloyed gold-silver nanoparticles. Research Letters in Optics, 2009, 5.

Fultz, B., & Howe, J. M. (2012). Transmission electron microscopy and diffractometry of materials (4th Edition). Springer Science & Business Media.

Gnanajobitha, D., Paulkumar, K., Vanaja, M., Shanmugam, R., Chelladurai, M., Gurusamy, A., & Kannan, C. (2013). Fruit-mediated synthesis of silver nanoparticles using *Vitis vinifera* and evaluation of their antimicrobial efficacy. Journal of Nanostructure in Chemistry, 3(1), 67.

Grattan, J. B. (2013). Plant sterols as anticancer nutrients: evidence for their role in breast cancer. Nutrients, 5(2), 359-387.

Halilu, M. E., October, N., Balogun, M., Lall, N., & Abubakar, M. S. (2013). Studies of in-vitro antioxidant and cytotoxic activities of extracts and isolated compounds from *Parinari curatellifolia* (Chrysobalanaceae). Journal of Natural Sciences Research. 3(13), 149-154.

Harborne, J. B. (1984). Triterpenoids and steroids. Phytochemical Methods: A guide to modern techniques of plant analysis (2nd Edition). Chapman and Hall, 120-128.

Ibrahim, J., Ajaegbu, V. C., & Egharevba, H. (2010). Pharmacognostic and phytochemical analysis of *Commelina benghalensis* L. Ethnobotanical Leaflets, 7(5), 610-615.

Hosnedlova, B., Kepinska, M., Skalickova, S., Fernandez, C., Ruttkay-Nedecky, B., Peng, Q. & Bjørklund, G. (2018). Nano-selenium and its nanomedicine applications: A critical review. International journal of nanomedicine, 13, 2107.

Iravani, S. (2011). Green synthesis of metal nanoparticles using plants. Green Chemistry, 13(10), 2638-2650.

IUPAC. (1997). Compendium of Chemical Terminology (the "Gold Book") (2nd Edition). Compiled by A. D. McNaught and A. Wilkinson. Blackwell Scientific Publications, Oxford, 845.

Jyoti, K., Baunthiyal, M., & Singh, A. (2016). Characterization of silver nanoparticles synthesized using *Urtica dioica* Linn. leaves and their synergistic effects with antibiotics. Journal of Radiation Research and Applied Sciences, 9(3), 217-227.

Kannan, S., Mohanraj, K., Prabhu, K., Barathan, S., & Sivakumar, G. (2014). Synthesis of selenium nanorods with assistance of biomolecule. Bulletin of Materials Science, 37(7), 1631-1635.

Kau, A. L., Martin, S. M., Lyon, W., Hayes, E., Caparon, M. G., & Hultgren, S. J. (2005). *Enterococcus faecalis* tropism for the kidneys in the urinary tract of C57BL/6J mice. Infection and Immunity, 73(4), 2461-2468.

Kazempour, Z. B., Yazdi, M. H., Rafii, F., & Shahverdi, A. R. (2013). Sub-inhibitory concentration of biogenic selenium nanoparticles lacks post antifungal effect for *Aspergillus niger* and *Candida albicans* and stimulates the growth of *Aspergillus niger*. Iranian journal of microbiology, 5(1), 81-85.

Khan, M. A., Islam, M. T., Rahman, M. A., & Ahsan, Q. (2011). Antibacterial activity of different fractions of *Commelina benghalensis* L. Der Pharmacia Sinica. 2(2), 320-326.

Khan, M. A. A., Islam, M. T., & Sadhu, S. K. (2011). Evaluation of phytochemical and antimicrobial properties of *Commelina diffusa* Burm. F. Oriental Pharmacy and Experimental Medicine, 11(4), 235-241.

Kiguba, R., Ononge, S., Karamagi, C., & Bird, S. M. (2016). Herbal medicine use and linked suspected adverse drug reactions in a prospective cohort of Ugandan inpatients. BMC Complement Alternative Medicine. 16(1), 145.

Kim, S. W., Park, S. S., Min, T. J., & Yu, K. H. (1999). Antioxidant activity of ergosterol peroxide (5,8-epidioxy-5 alpha,8 alpha-ergosta-6,22E-dien-3 beta-ol) in *Armillariella mellea*. Bulletin-Korean Chemical Society, 20(7), 819-823.

Kokila, K., Elavarasan, N., & Sujatha, V. (2017). *Diospyros montana* leaf extract-mediated synthesis of selenium nanoparticles and their biological applications. New Journal of Chemistry, 41(15), 7481-7490.

Kora, A. J., Beedu, S. R., & Jayaraman, A. (2012). Size-controlled green synthesis of silver nanoparticles mediated by gum ghatti (*Anogeissus latifolia*) and its biological activity. Organic and Medicinal Chemistry Letters, 2(1), 17-17.

Kritchevsky, D., & Chen, S. (2005). Phytosterols-health benefits and potential concerns: A review (Vol. 25). Nutrition Research, 25(5), 413-428.

Kumar, S. (2006). Spectroscopy of organic compounds. In Organic Chemistry; National Science Digital Library at NISCAIR: India, E-book, 1-36.

Lin, P. C., Lin, S., Wang, P. C., & Sridhar, R. (2014). Techniques for physicochemical characterization of nanomaterials. Biotechnology Advance, 32(4), 711-726.

Lin, X., Racette, S. B., Lefevre, M., Spearie, C. A., Most, M., Ma, L., & Ostlund, R. E., Jr. (2010). The effects of phytosterols present in natural food matrices on cholesterol metabolism and LDL-cholesterol: a controlled feeding trial. European Journal Clinical Nutrition, 64(12), 1481-1487.

Mahlangeni, N. T. (2012). Phytochemical and elemental analysis of *Cyrtanthus obliquus* and *Lippia javanica*. (Masters of Science in Chemistry), University of KwaZulu-Natal, Durban.

Malhotra, S., Jha, N., & Desai, K. (2014). A superficial synthesis of selenium nanospheres using wet chemical approach. International Journal of Nanotechnology and Applications, (3), 7-14.

Mander, M., Ntuli, L., Diederichs Mander, N., & Mavundla, K. (2007). Economics of the traditional medicine trade in South Africa: health care delivery. South African health review, (1), 189-196.

Mehta, B. K., Chhajlani, M., & Shrivastava, B. D. (2017). Green synthesis of silver nanoparticles and their characterization by XRD. Journal of Physics: Conference Series, 836.

Milgate, J., & Roberts, D. C. K. (1995). The nutritional & biological significance of saponins. *Nutrition Research*, 15(8), 1223-1249.

Mills, E., Cooper, C., Seely, D., & Kanfer, I. (2005). African herbal medicines in the treatment of HIV: *Hypoxis* and *Sutherlandia*. An overview of evidence and pharmacology. Nutrition Journal, 4, 19.

Mishra, K., Ojha, H., & Chaudhury, N. K. (2012). Estimation of antiradical properties of antioxidants using DPPH assay: A critical review and results. Food Chemistry, 130(4), 1036-1043.

Mittal, A. K., Chisti, Y., & Banerjee, U. C. (2013). Synthesis of metallic nanoparticles using plant extracts. Biotechnology Advances, 31(2), 346-356.

Muthupandian, S., Ramachandran, B., Barabadi, H., & Giardiello, M. (2018). Barriers for the development, translation, and implementation of nanomedicine: an African perspective. Journal of Interdisciplinary Nanomedicine, 3(3), 106-110.

Ndhlala, A. R. (2009). Pharmacological, phytochemical and safety evaluation of commercial herbal Preparations common in South Africa. (Doctor of Philosophy), University of KwaZulu-Natal, Pietermaritzburg.

Negri, G., & Tabach, R. (2013). Saponins, tannins and flavonols found in hydroethanolic extract from *Periandra dulcis* roots. Revista Brasileira de Farmacognosia, 23(6), 851-860.

Nikolajsen, T., Nielsen, F., Rasch, V., Sorensen, P. H., Ismail, F., Kristiansen, U., & Jager, A. K. (2011). Uterine contraction induced by Tanzanian plants used to induce abortion. Journal of Ethnopharmacology, 137(1), 921-925.

Ogbe, R. J., Ochalefu, D. O., Mafulul, S. G., & Olaniru, B. O. (2015). A review on dietary phytosterols: Their occurrence, metabolism and health benefits. Asian Journal of Plant Science Research, 5(4), 10-21.

Ory, E. M., & Yow, E. M. (1963). The use and abuse of the broad spectrum antibiotics. The Journal of the American Medical Association, 185(4), 273-279.

Oyebode, O., Kandala, N.-B., Chilton, P. J., & Lilford, R. J. (2016). Use of traditional medicine in middle-income countries: a WHO-SAGE study. Health Policy and Planning, 31(8), 984-991.

Panpipat, W., Keskin, H., & Guo, Z. (2015). Mapping the structure-activity relationship of *β*-sitosteryl fatty acid esters in condensing phospholipid monolayers. Frontiers of Chemical Science and Engineering, 9(1), 105-113.

Ponarulselvam, S., Panneerselvam, C., Murugan, K., Aarthi, N., Kalimuthu, K., & Thangamani, S. (2012). Synthesis of silver nanoparticles using leaves of *Catharanthus roseus* Linn. G. Don and their antiplasmodial activities. Asian Pacific Journal of Tropical Biomedicine, 2(7), 574-580.

Radzig, M. A., Nadtochenko, V. A., Koksharova, O. A., Kiwi, J., Lipasova, V. A., & Khmel, I. A. (2013). Antibacterial effects of silver nanoparticles on gram-negative bacteria: Influence on the growth and biofilms formation, mechanisms of action. Colloids and Surfaces B: Biointerfaces, 102, 300-306.

Rai, M., Yadav, A., & Gade, A. (2009). Silver nanoparticles as a new generation of antimicrobials. Biotechnology Advances, 27(1), 76-83.

Rocha, M., Banuls, C., Bellod, L., Jover, A., Victor, V. M., & Hernandez-Mijares, A. (2011). A review on the role of phytosterols: new insights into cardiovascular risk. Current Pharmaceutical Design, 17(36), 4061-4075.

Ruffo, C. K., Birnie, A., & Tegnas, B. (2002). The species. Edible Wild Plants of Tanzania, Regional Land Management Unit (27), 206-207.

Rukangira, E. (2001). Medicinal plants and traditional medicine in Africa: constraints and challenges. Sustainable Development International, 4, 179-184.

Sahoo, S. K. (2005). Applications of nanomedicine. Asia-Pacific Biotech News, 09 (20), 1048-1050.

Saidi, T., Fortuin, J., & Douglas, T. (2018). Nanomedicine for drug delivery in South Africa: a protocol for systematic review. Systematic reviews, *7*(1), 154.

Sarkar, B., Bhattacharjee, S., Daware, A., Tribedi, P., Krishnani, K. K., & Minhas, P. S. (2015). Selenium nanoparticles for stress-resilient fish and livestock. Nanoscale Research Letters, 10(1), 371.

Sarkar, J., Dey, P., Saha, S., & Acharya, K. (2011). Mycosynthesis of selenium nanoparticles. IET Micro and Nano Letters, *6*(8), 599-602.

Sasidharan, S., Chen, Y., Saravanan, D., Sundram, K. M., & Yoga Latha, L. (2011). Extraction, isolation and characterization of bioactive compounds from plants' extracts. African Journal of Traditional, Complementary, and Alternative Medicines, 8(1), 1-10.

Serra, A., Rossi, M., Buccolieri, A., & Manno, D. (2014). Solid-to-solid phase transformations of nanostructured selenium-tin thin films induced by thermal annealing in oxygen atmosphere. AIP Conference Proceedings, 1603(1), 31-39.

Sethiya, N. K., Trivedi, A., & Mishra, S. (2014). The total antioxidant content and radical scavenging investigation on 17 phytochemical from dietary plant sources used globally as functional food. Biomedicine & Preventive Nutrition, 4(3), 439-444.

Shahzad, N., Khan, W., Md, S., Ali, A., Saluja, S. S., Sharma, S., Al-Ghamdi, S. S. (2017). Phytosterols as a natural anticancer agent: Current status and future perspective. Biomedicine & Pharmacotherapy, 88, 786-794.

Sharma, R. K. (1993). Phytosterols: Wide-spectrum antibacterial agents. Bioorganic Chemistry, 21(1), 49-60.

Shelembe, B. G. (2014). Phytochemical and elemental studies of two indigenous medicinal plants of South Africa, *Bridelia micrantha* and *Sideroxylon inerme*. (Masters of Science in Chemistry), University of KwaZulu-Natal, Durban.

Song, J. Y., & Kim, B. S. (2009). Rapid biological synthesis of silver nanoparticles using plant leaf extracts. Bioprocess and Biosystems Engineering, 32(1), 79-84.

Srivastava, N., & Mukhopadhyay, M. (2013). Biosynthesis and structural characterization of selenium nanoparticles mediated by *Zooglea ramigera*. Powder Technology, 244, 26-29.

Street, R. A., Ngcobo, M., Mbatha, M., & Gqaleni, N. (2012). Potential occupational health challenges in the traditional medicine practice: back to basics. Occupational Health Southern Africa, 18(6), 13-17.

Suganya, R. A., & Jothi, J. (2014). Preliminary phytochemical screening, antibacterial and antioxidant activities of *Commelina nudiflora* (Commelinaceae). International Research Journal of Pharmacy, 5(11), 581-855.

Sumithra, D., & Purushothaman, S. (2017). Phytochemical profiling of ethanolic leaves extract of *Commelina benghalensis* L. World Journal of Pharmaceutical Research, 6(2), 1101-1107.

Tamura, Y., Miyakoshi, M., & Yamamoto, M. (2012). Application of saponin-containing plants in foods and cosmetics (Ed.), Alternative Medicine, 85-101.

Ullah, H., & Ali, S. (2017). Classification of anti-bacterial agents and their functions. Antibacterial agents, 1-16.

van den Wildernberg, W. (2005). Roadmap report on nanoparticles. W&W Espana sl, Barcelona, Spain, 157.

Walock, M. (2012). Nanocomposite coatings based on quaternary metal-nitrogen and nanocarbon systems. (PhD in Physics), University of Alabama at Birmingham.

Weekley, C. M., & Harris, H. H. (2013). Which form is that? The importance of selenium speciation and metabolism in the prevention and treatment of disease. Chemical Society Reviews, 42(23), 8870-8894.

Williams, D. B., & Carter, C. B. (1996). The transmission electron microscope. In Transmission Electron Microscopy. Springer, 3-17.

Wilson, A. K. (1981). Commelinaceae- A review of the distribution, biology and control of the important weeds belonging to this family. International Journal of Pest Management, 27(3), 405-418.

World Health Organization. (2000). General guidelines for methodologies on research and evaluation of traditional medicine (No.WHO/EDM/TRM/2000.1). Geneva: World Health Organization.

World Health Organization. (2005). National policy on traditional medicine and regulation of herbal medicines: Report of a WHO global survey.

Yang, F., Tang, Q., Zhong, X., Bai, Y., Chen, T., Zhang, Y., Zheng, W. (2012). Surface decoration by *Spirulina* polysaccharide enhances the cellular uptake and anticancer efficacy of selenium nanoparticles. International Journal of Nanomedicine, 7, 835-844.

APPENDICES

Antibacterial testing - Sample identity

1- β-sitosterol
2- Lauric acid (REMOVED FROM STUDY)
3- Ergosterol peroxide
4- Campestanol
5- Stigmasterol
6- Water extract
7- Hexane extract
8- Methanol extract
9- AgNPs (1 mL)
10- AgNPs (2 mL)
11- AgNPs (3 mL)
12- AgNPs (4 mL)
13- AgNPs (5 mL)
14- SeNPs (1 mL)
15- SeNPs (2 mL)
16- SeNPs (3 mL)
17- SeNPs (4 mL)
18- SeNPs (5 mL)
19- M-AgNPs (1 mL)
20- M-AgNPs (2 mL)
21- M-AgNPs (3 mL)
22- M-AgNPs (4 mL)
23- M-AgNPs (5 mL)
24- M-SeNPs (1 mL)
25- M-SeNPs (2 mL)
26- M-SeNPs (3 mL)
27- M-SeNPs (4 mL)
28- M-SeNPs (5 mL)
29- Se-AA NPs
30- Se-AA-$NaBH_4$ NPs
31- Ag-$NaBH_4$ NPs

Gram positive bacterial strains - *E. faecalis* (EF) ATCC 51299

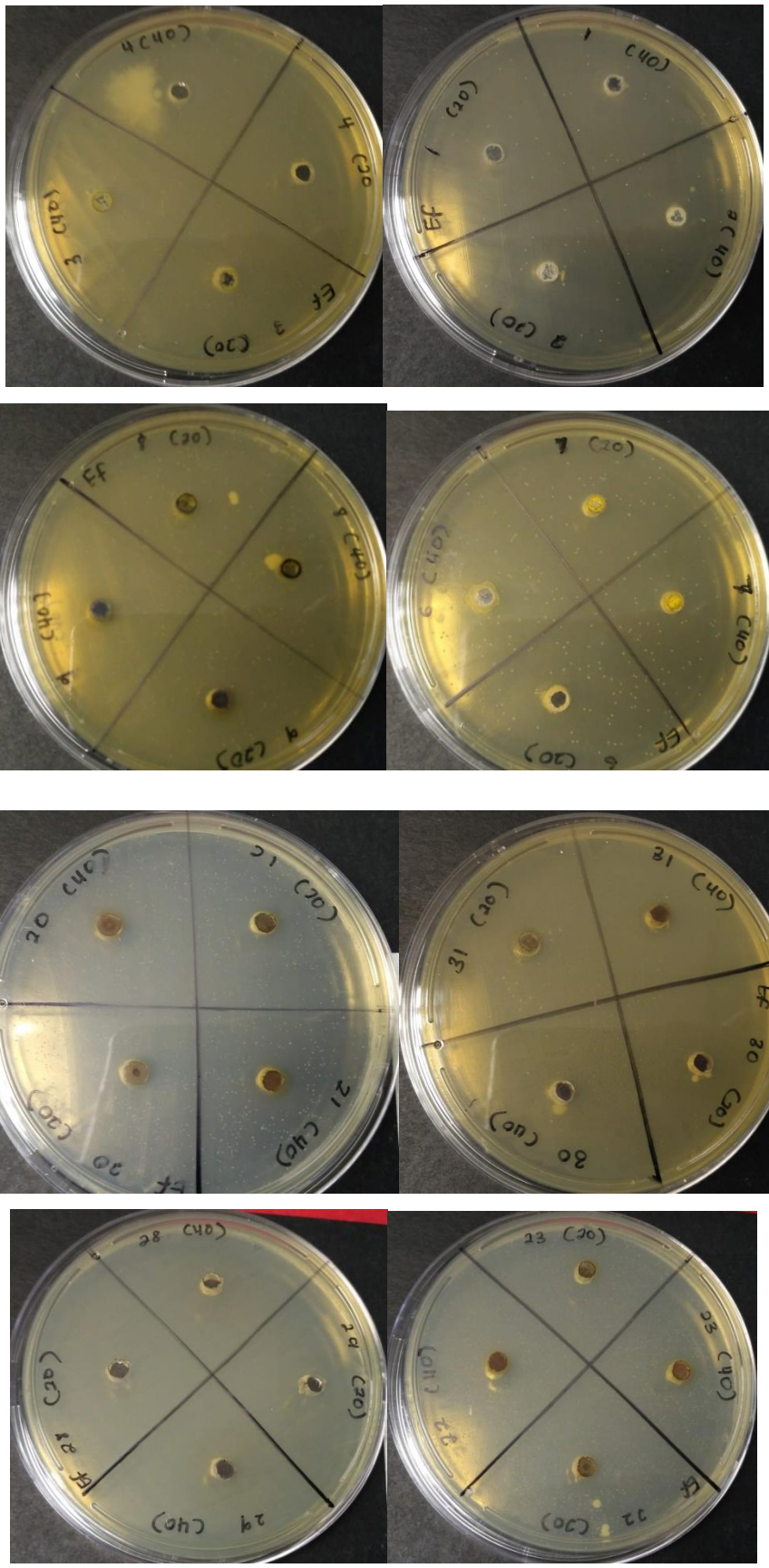

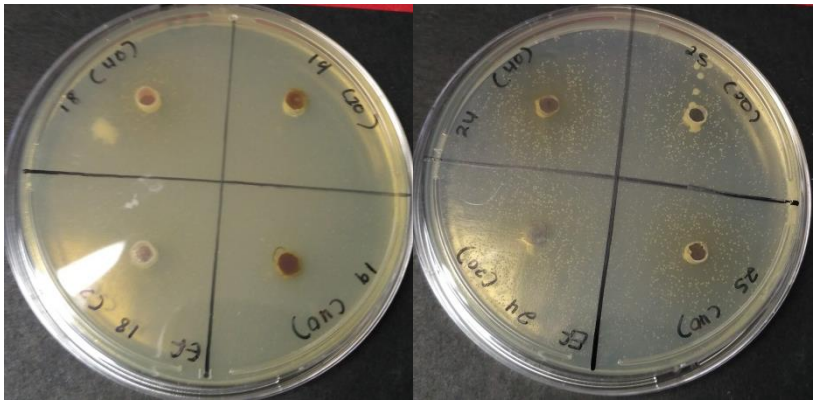
18 (40)
19 (20)
Ef
18 (20)
19 (40)
24 (40)
25 (20)
Ef
24 (20)
25 (40)

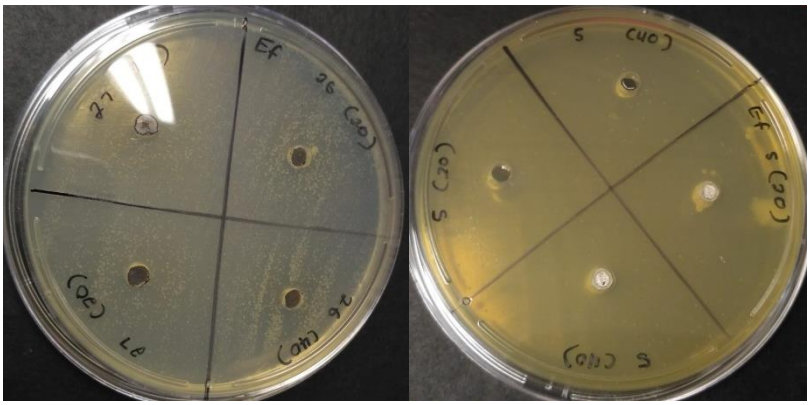
27
Ef
26 (20)
27 (20)
26 (40)
5 (40)
Ef 5 (20)
5 (20)
5 (40)

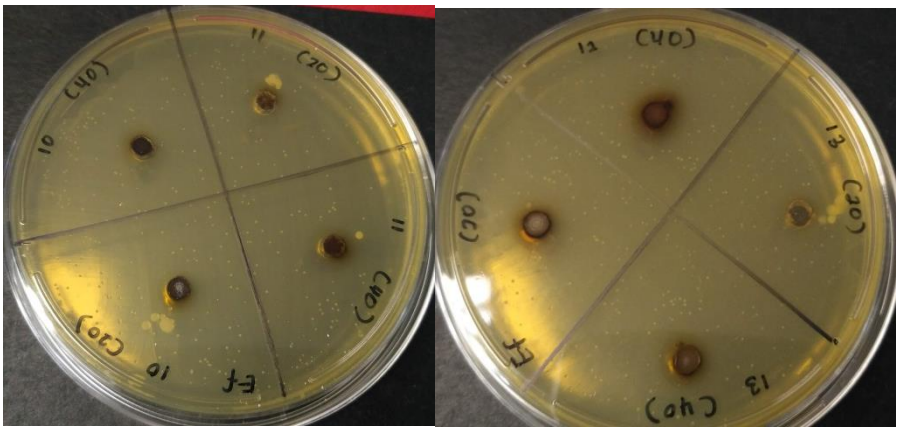
10 (40)
11 (20)
Ef
10 (20)
11 (40)
12 (40)
13 (20)
Ef
13 (40)

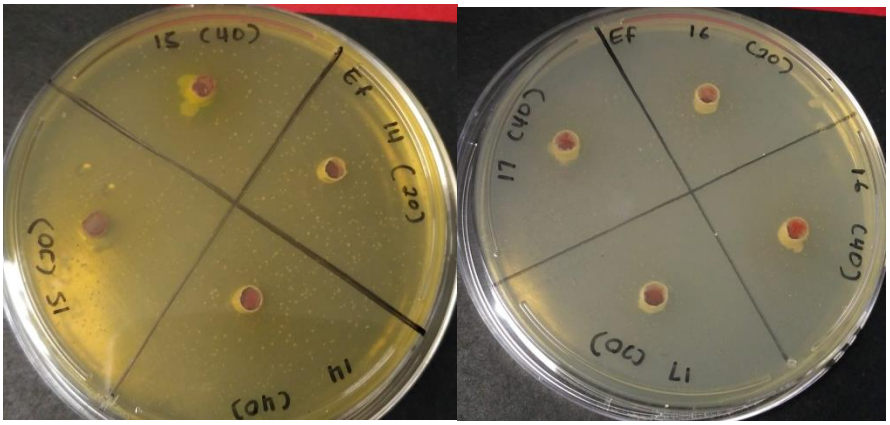
15 (40)
Ef
14 (20)
15 (20)
14 (40)
Ef
16 (20)
17 (40)
17 (20)
16 (40)

S. aureus (SA) ATCC 43300

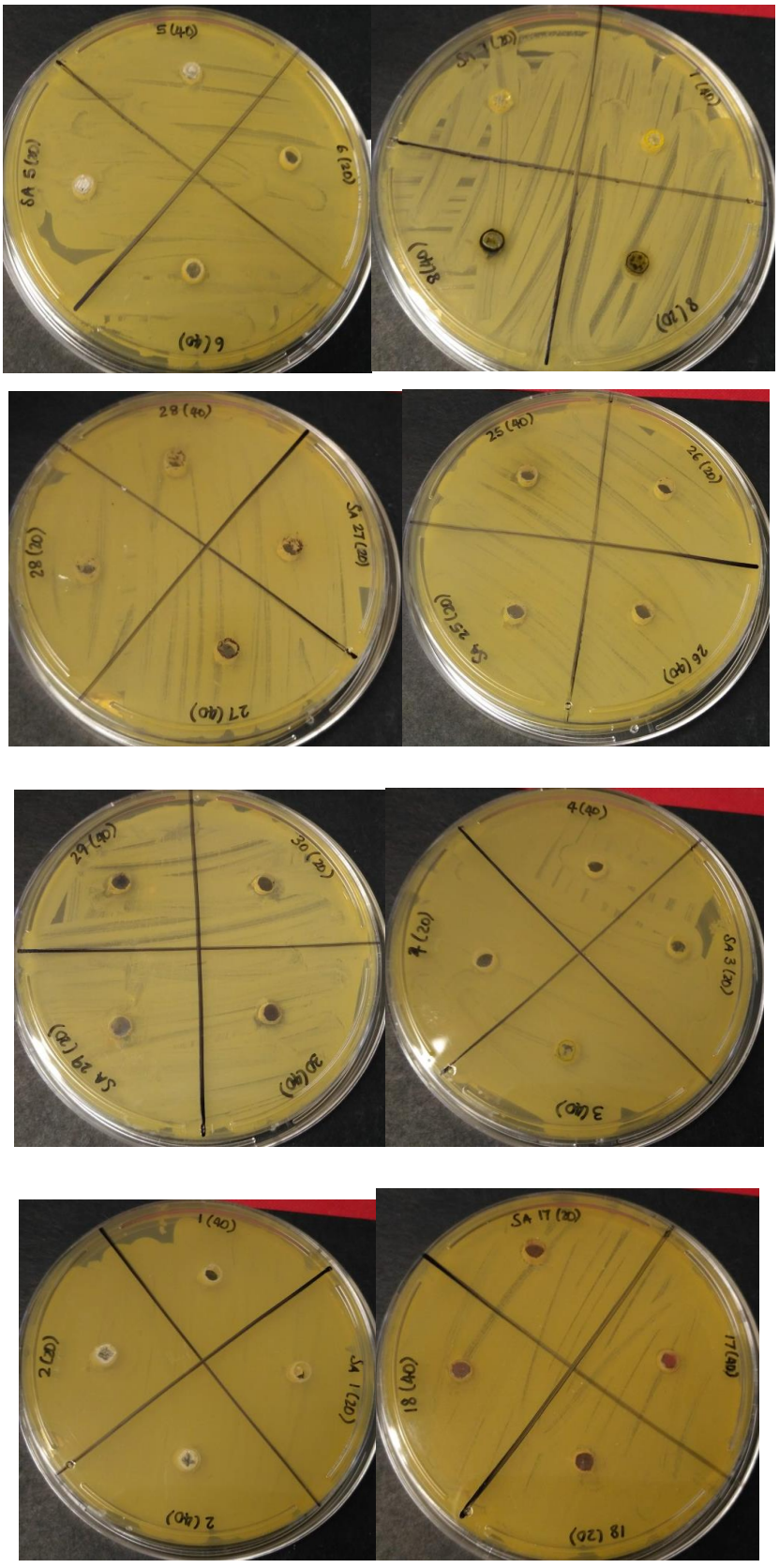

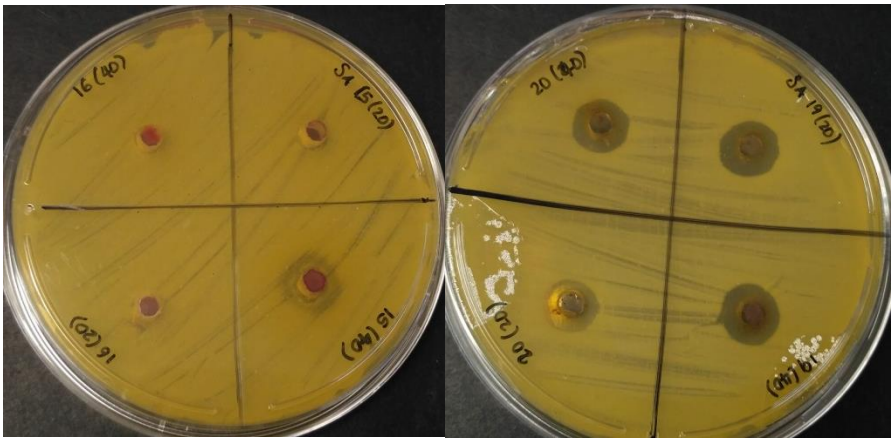
16 (40)
SA 15 (20)
16 (20)
15 (40)
20 (40)
SA 19 (20)
20 (20)
19 (40)

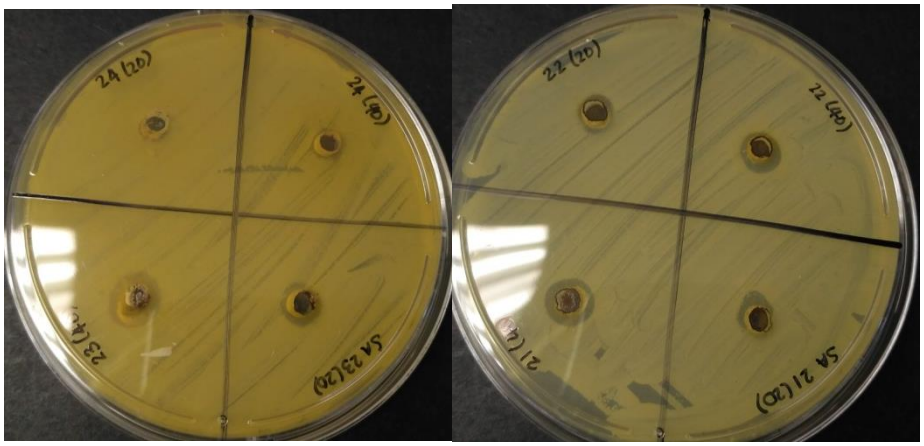
24 (20)
24 (40)
SA 23 (20)
22 (20)
22 (40)
SA 21 (20)

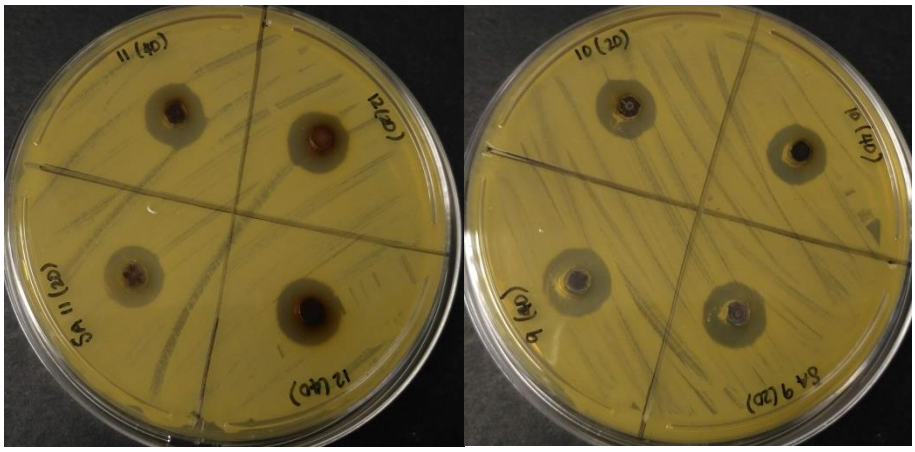
11 (40)
12 (40)
SA 11 (20)
12 (40)
10 (20)
10 (40)
9 (40)
SA 9 (20)

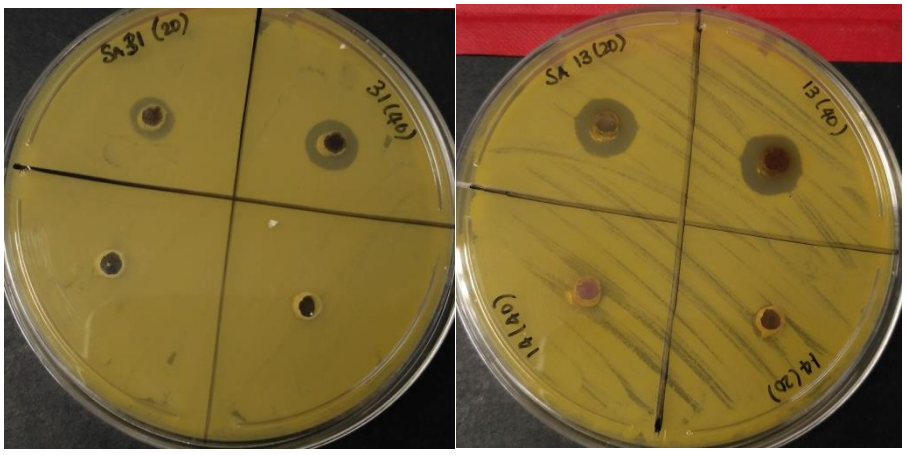
SA 31 (20)
31 (40)
SA 13 (20)
13 (40)
14 (40)
14 (20)

Gram negative bacterial stains

P. aeruginosa (PA) ATCC 27853

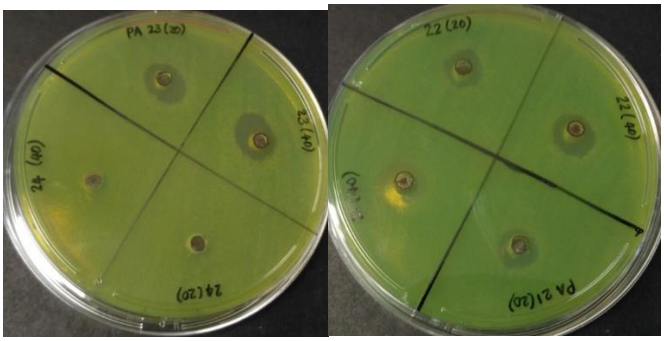

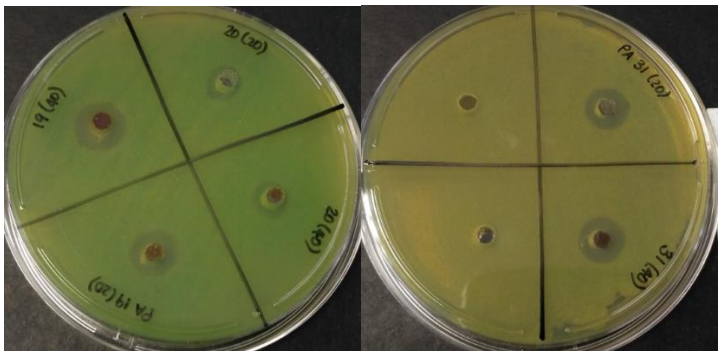

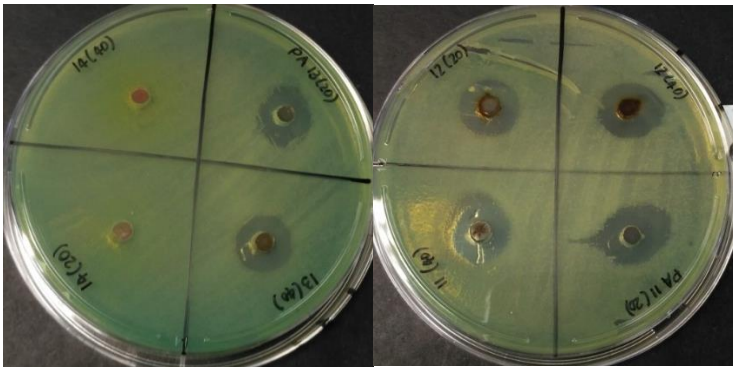

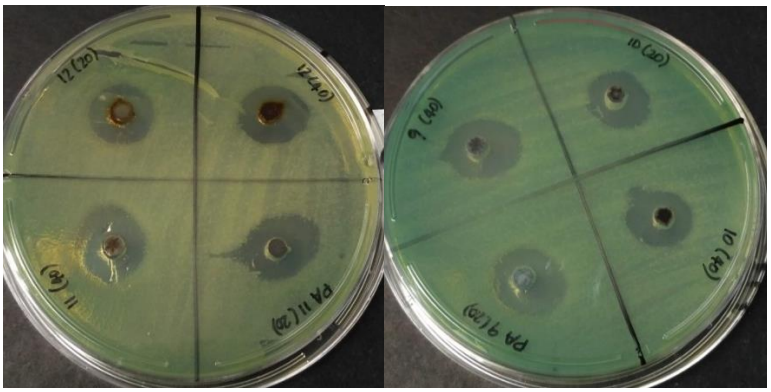

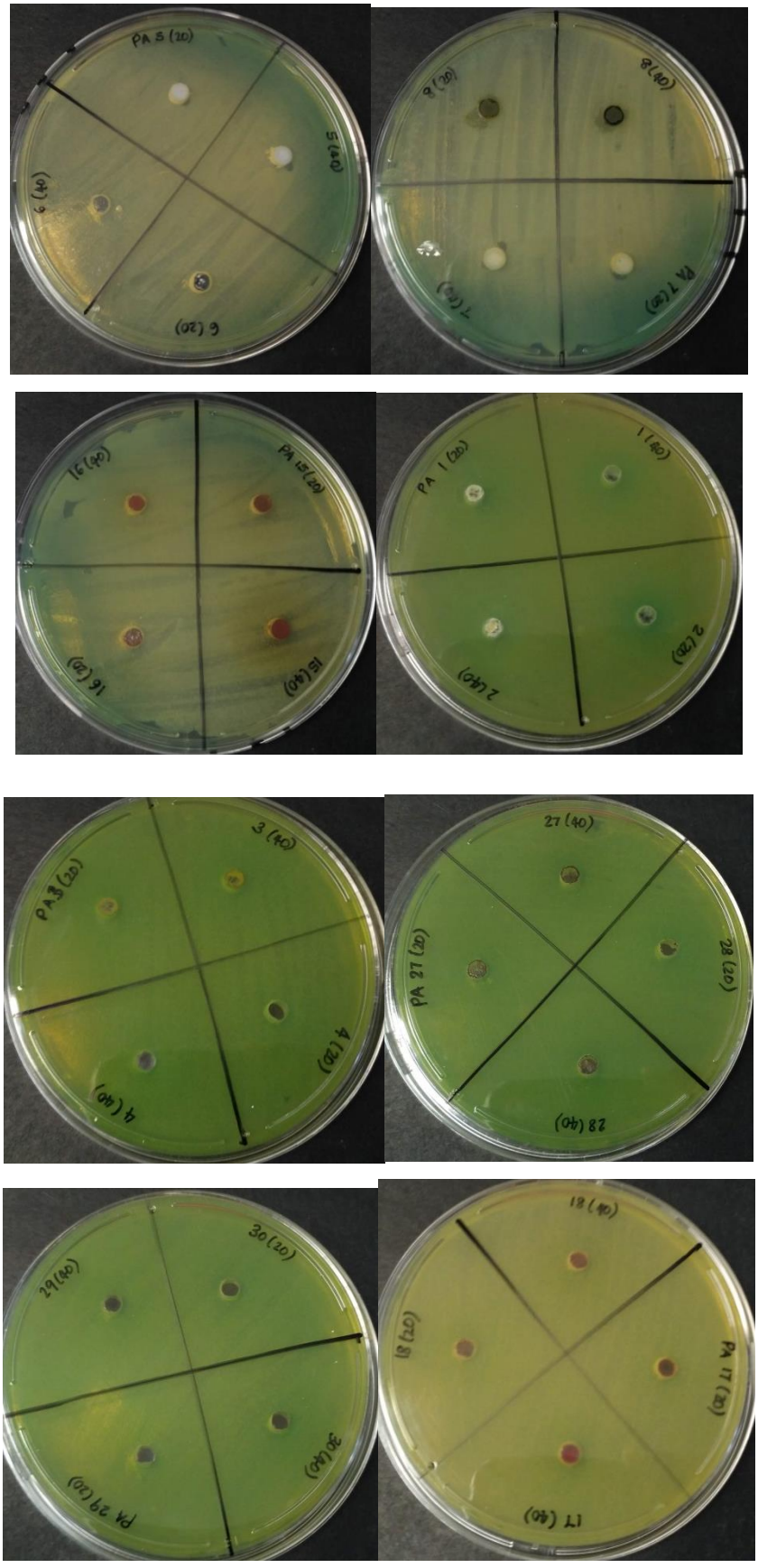
PA 5 (20)
5 (40)
6 (40)
6 (20)
8 (20)
8 (40)
7 (20)
PA 7 (20)
15 (40)
PA 15 (20)
16 (20)
16 (40)
PA 1 (20)
1 (40)
2 (40)
2 (20)
3 (40)
PA 3 (20)
4 (20)
4 (40)
27 (40)
PA 27 (20)
28 (20)
28 (40)
30 (20)
29 (40)
30 (40)
PA 29 (20)
18 (40)
18 (20)
PA 17 (20)
17 (40)

E. coli (EC) ATCC 35128

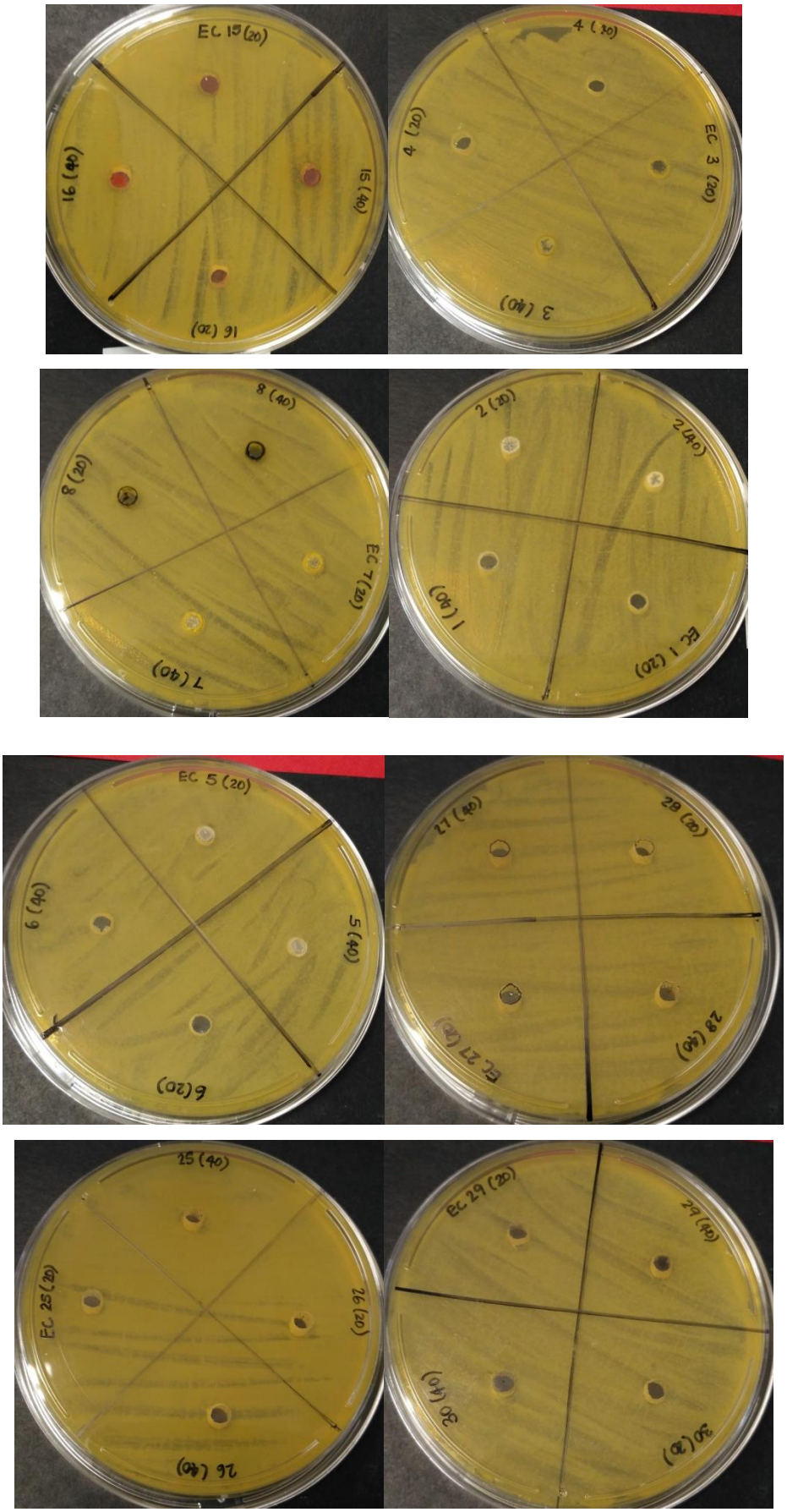

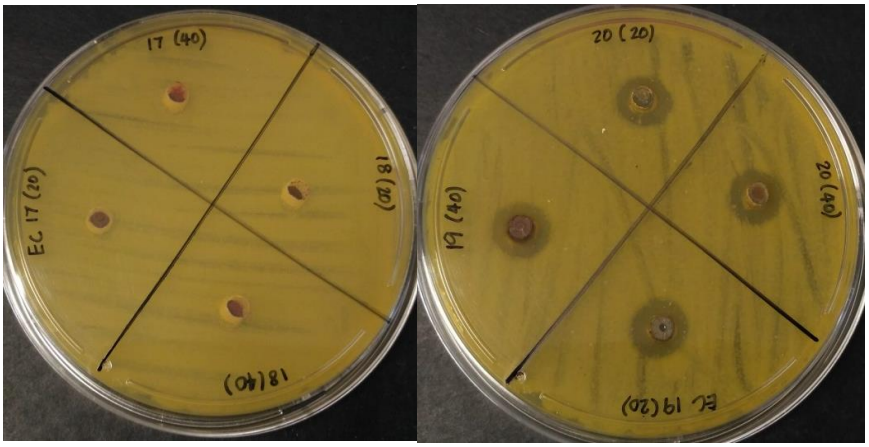
17 (40)
18 (20)
EC 17 (20)
18 (40)
20 (20)
19 (40)
20 (40)
EC 19 (20)

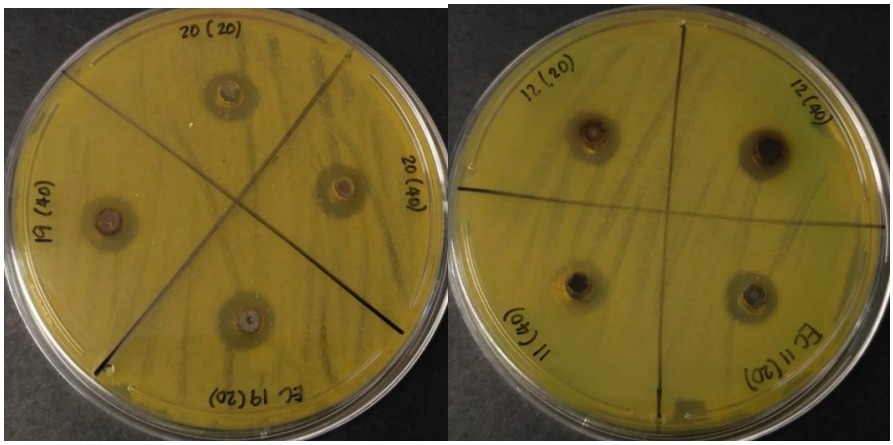
20 (20)
19 (40)
20 (40)
EC 19 (20)
12 (20)
12 (40)
11 (40)
EC 11 (20)

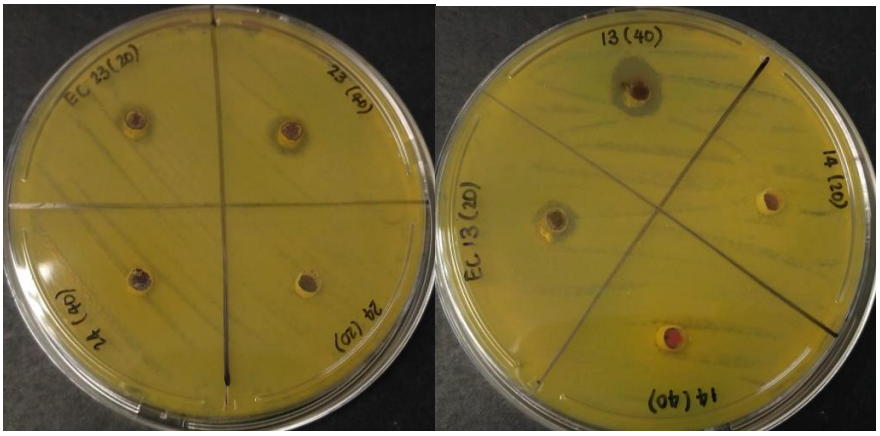
EC 23 (20)
23 (40)
24 (40)
24 (20)
13 (40)
14 (20)
EC 13 (20)
14 (40)

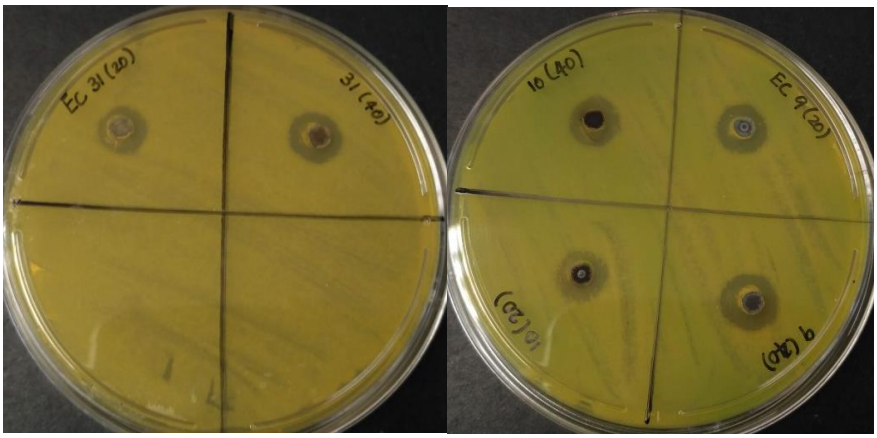
EC 31 (20)
31 (40)
10 (40)
EC 9 (20)
10 (20)
9 (40)

K. pneumonia (KP) ATCC 700 603

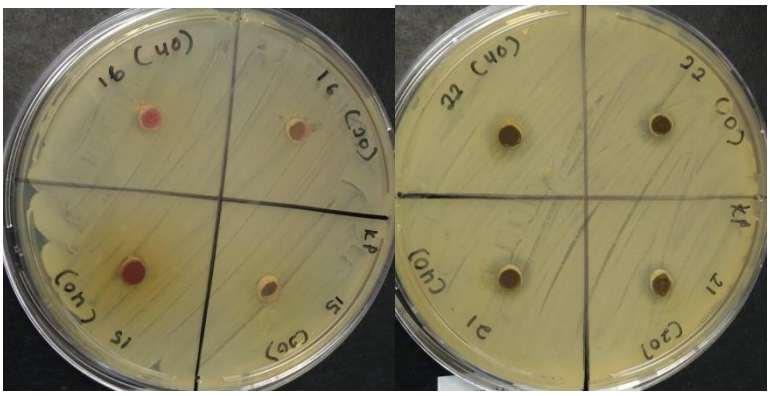

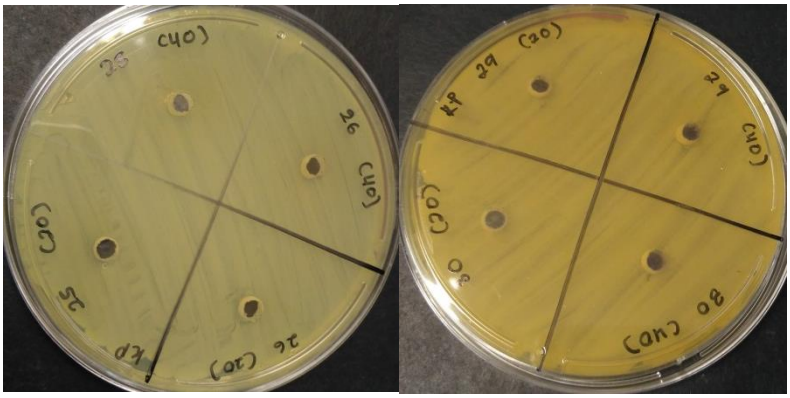

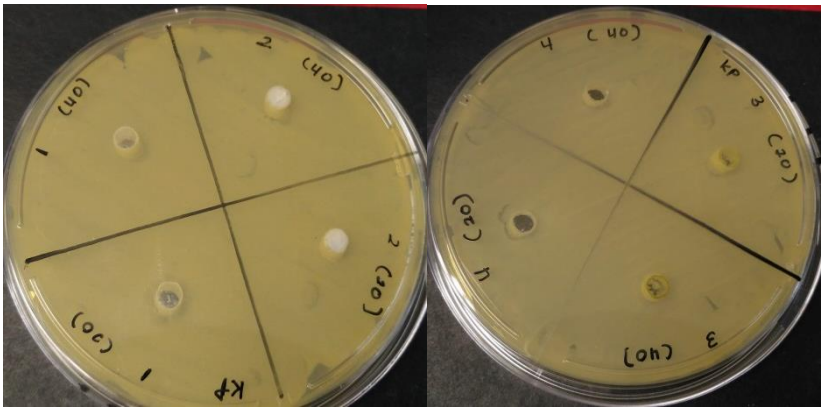

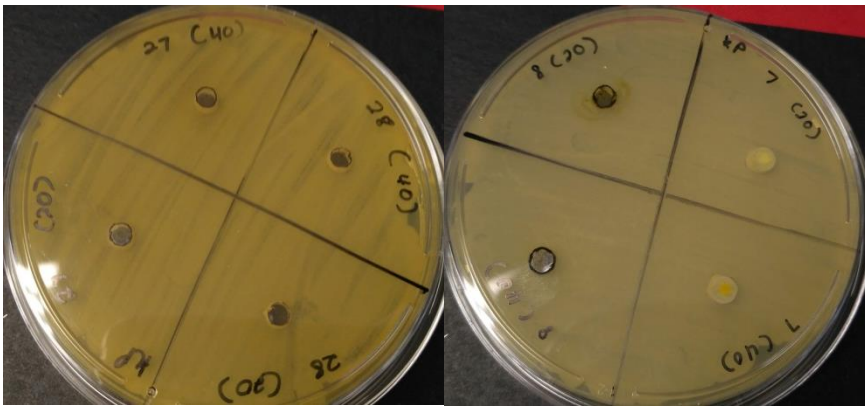

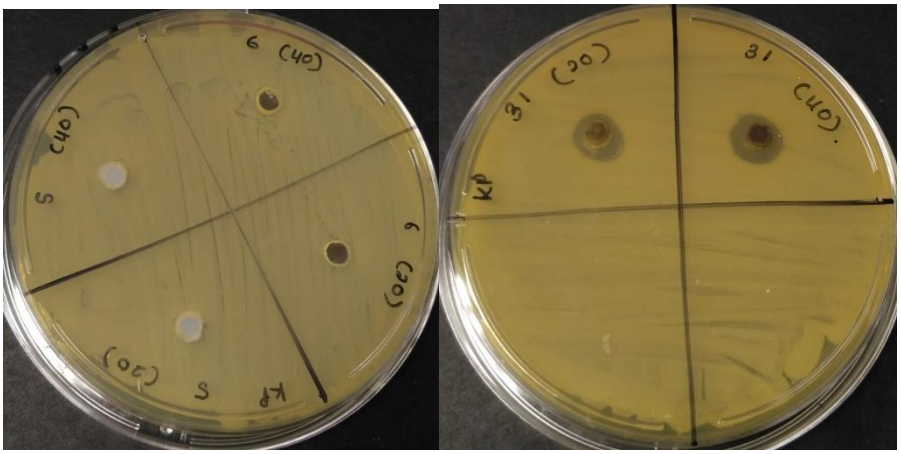
6 (40)
5 (40)
6 (20)
KP 5 (20)
31 (20)
31 (40).
KP

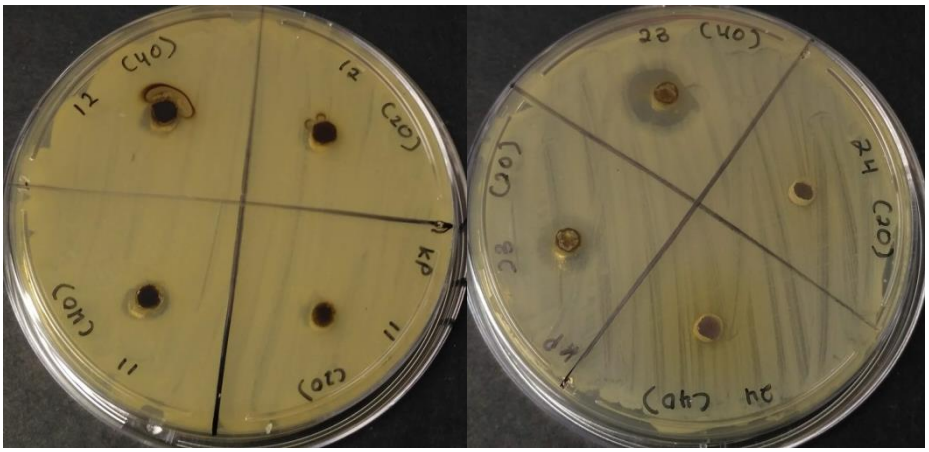
12 (40)
12 (20)
KP
11 (40)
11 (20)
28 (40)
24 (20)
28 (20)
KP
24 (40)

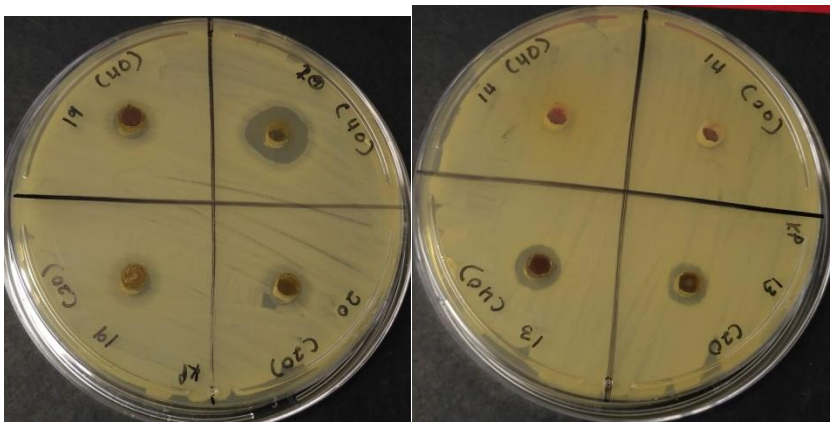
14 (40)
20 (40)
14 (20)
KP
19 (20)
20 (20)
13 (40)
13 (20)

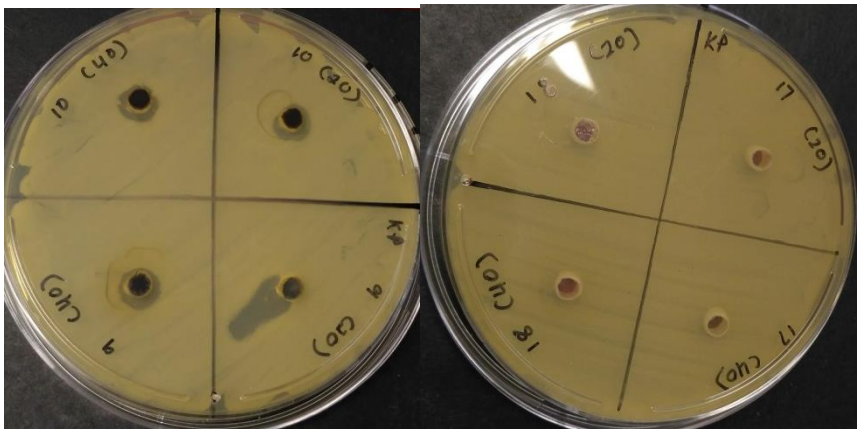
10 (40)
01 (20)
KP
9 (40)
6 (20)
KP
17 (20)
18 (40)
17 (40)

C. violaceum (CV) ATCC 12472

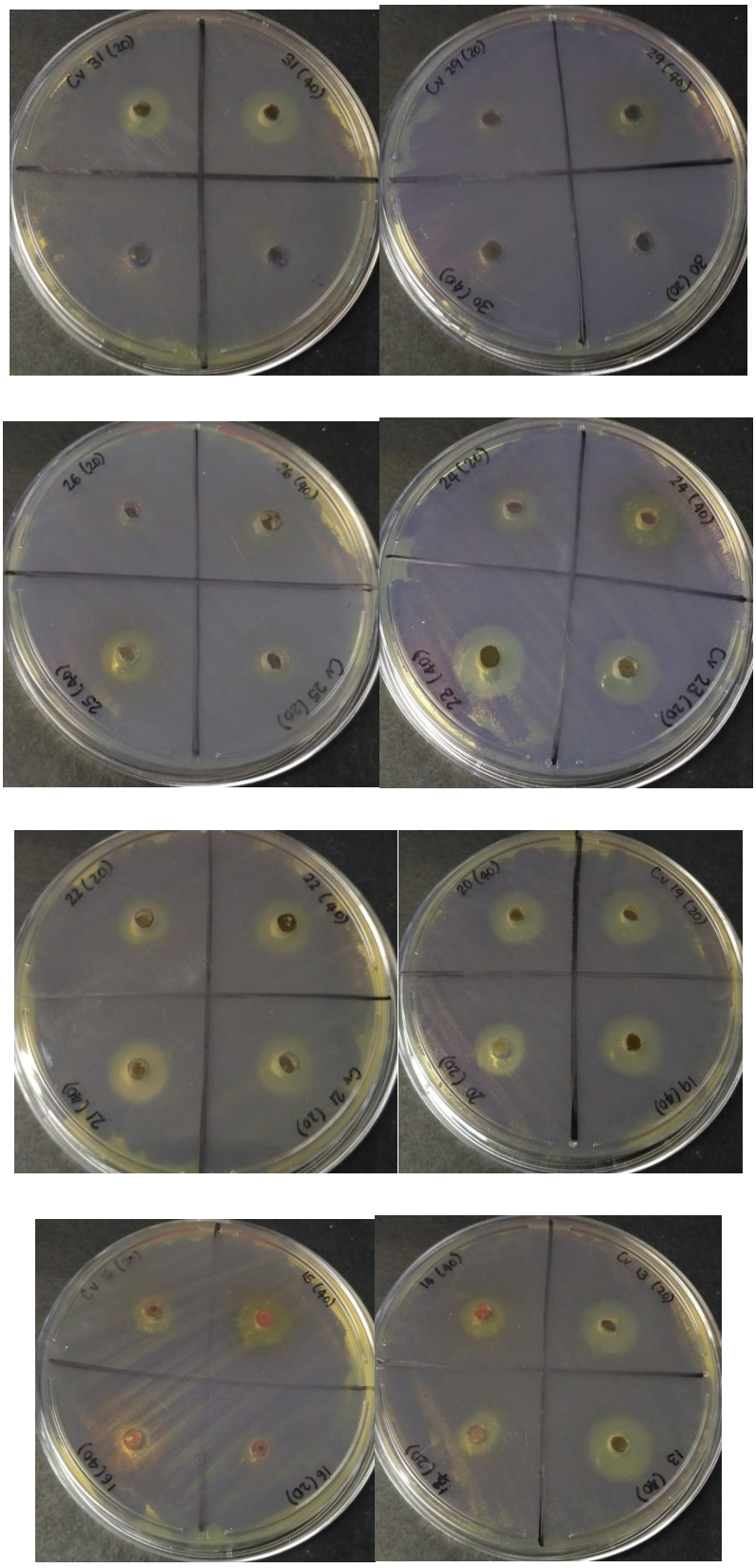

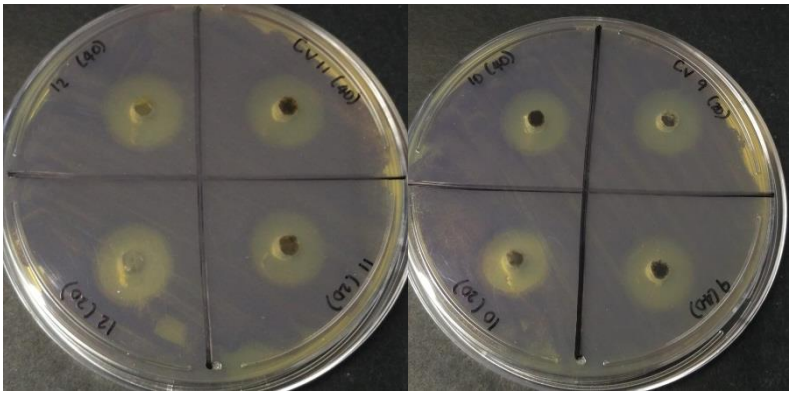

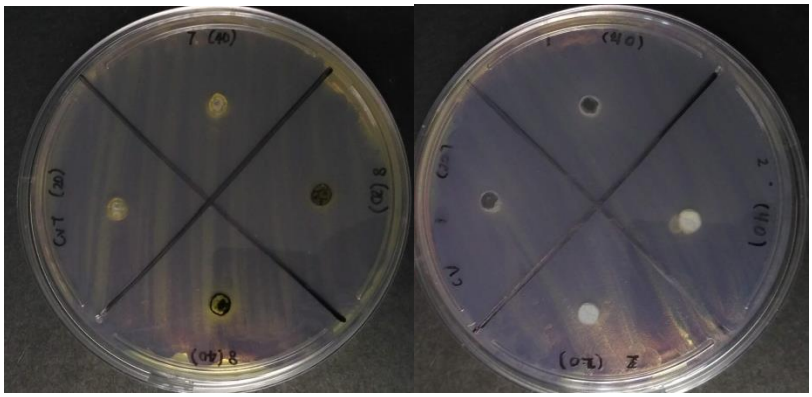

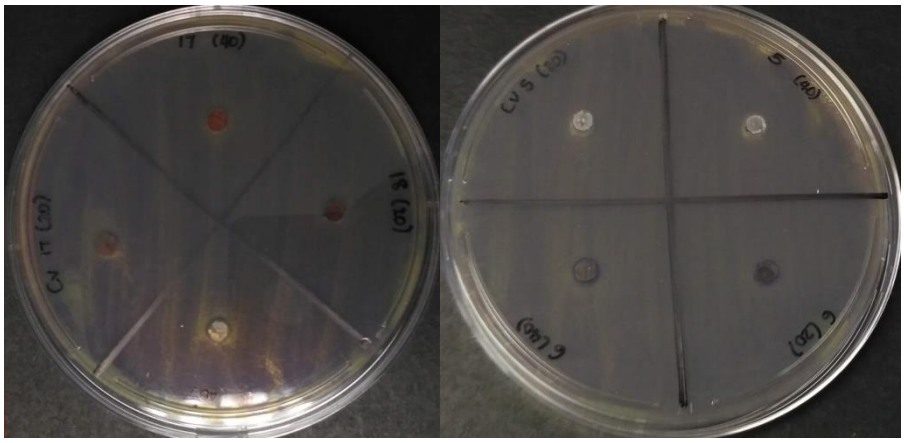

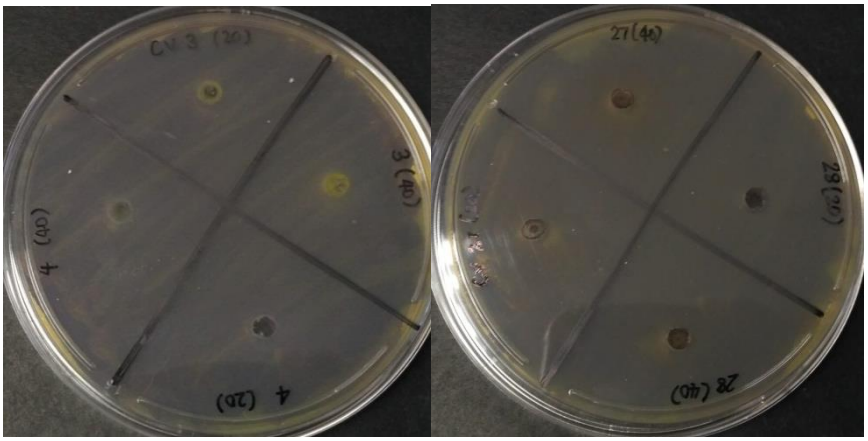

Anti-quorum sensing (CV overlays)

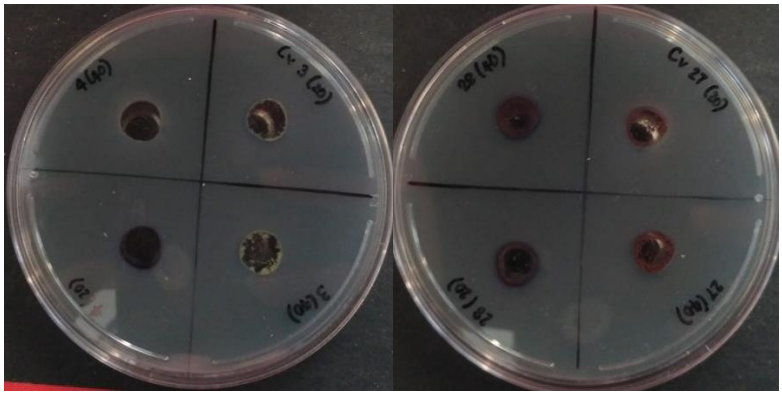

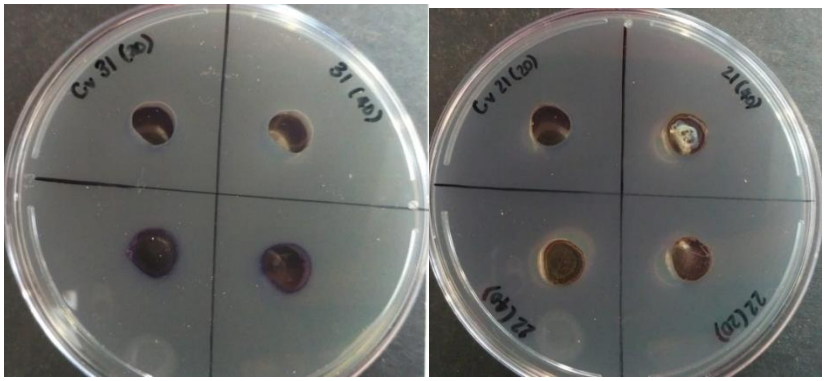

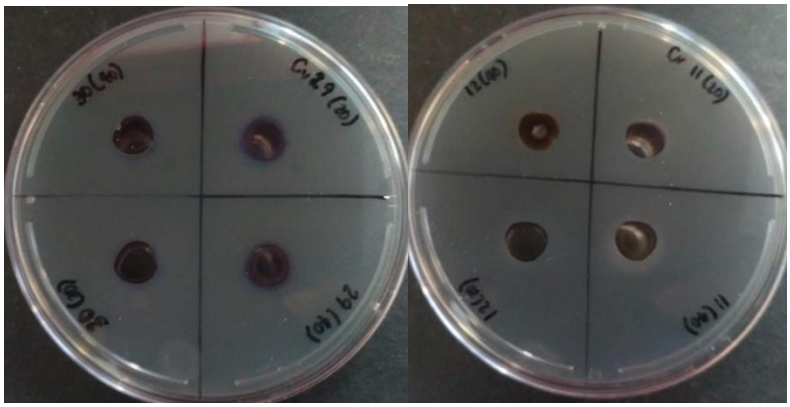

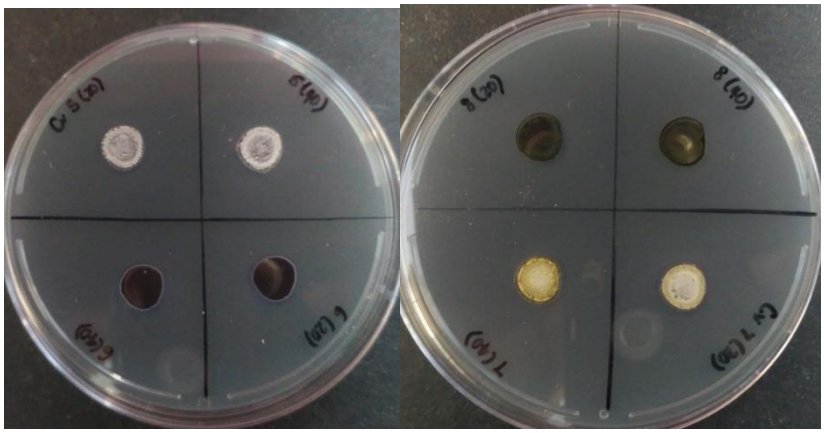

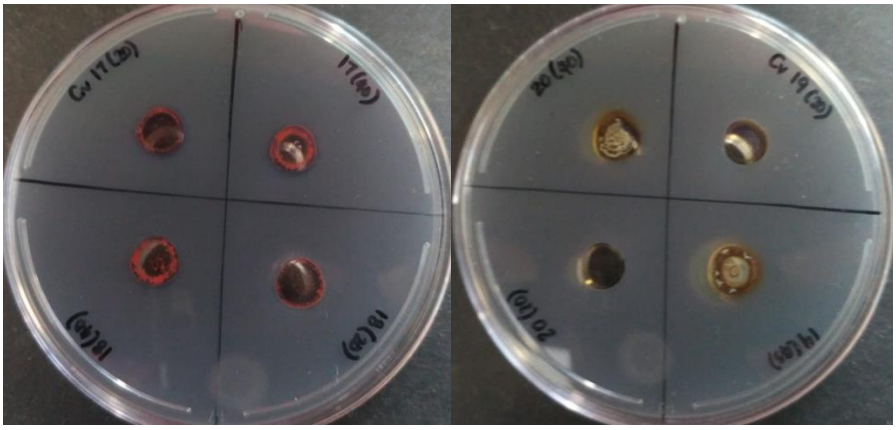

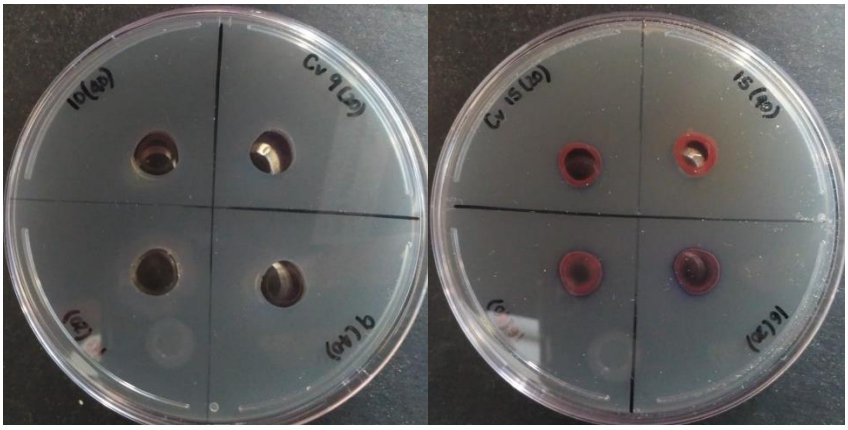

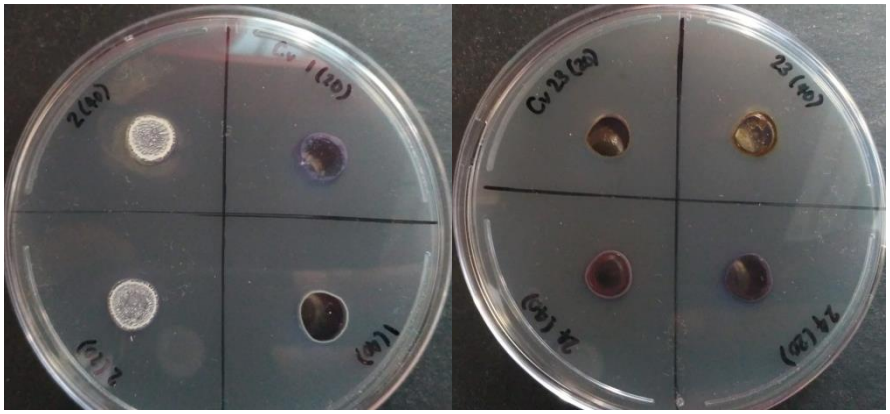

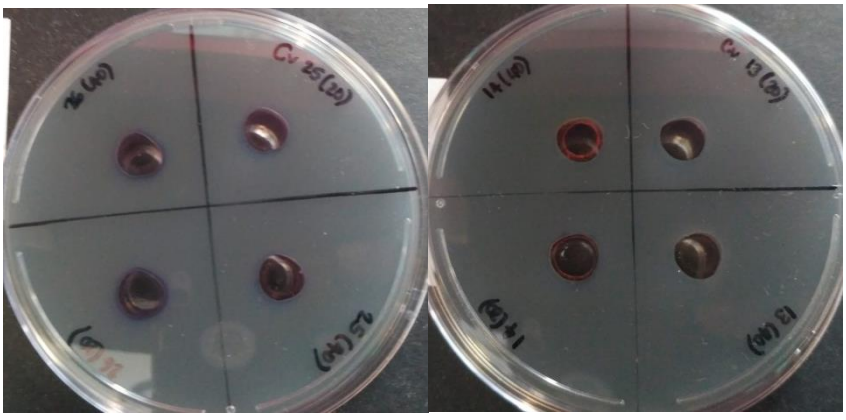

Supporting spectral information containing NMR, UV-Vis, LR-ESI-MS and GC-MS for:

- Stigmasterol (Compound **1**)
- Ergosterol peroxide (Compound **2**)
- β-sitosterol (Compound **3**)
- Campestanol (Compound **4**)

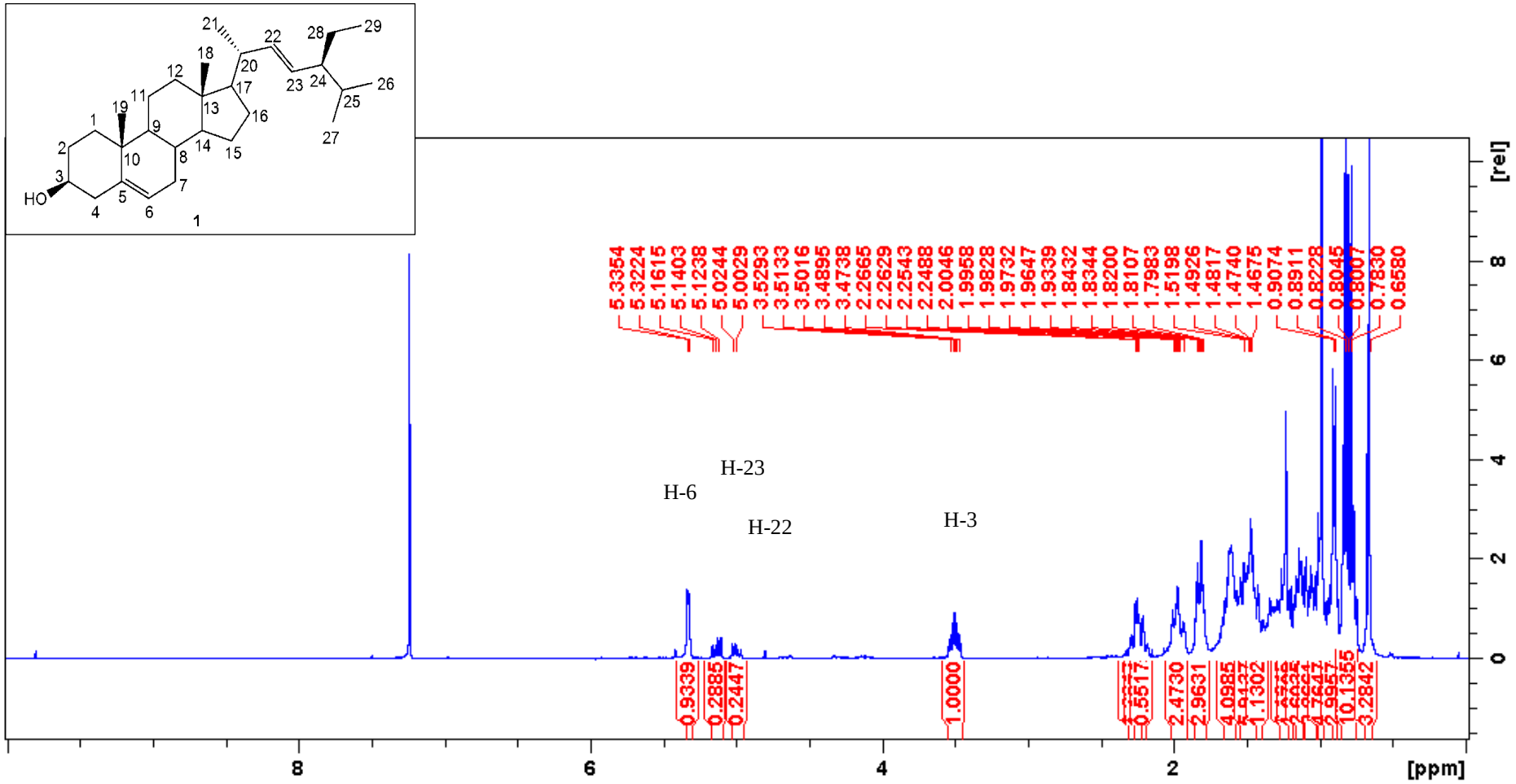

^{1}H NMR spectrum for Stigmasterol

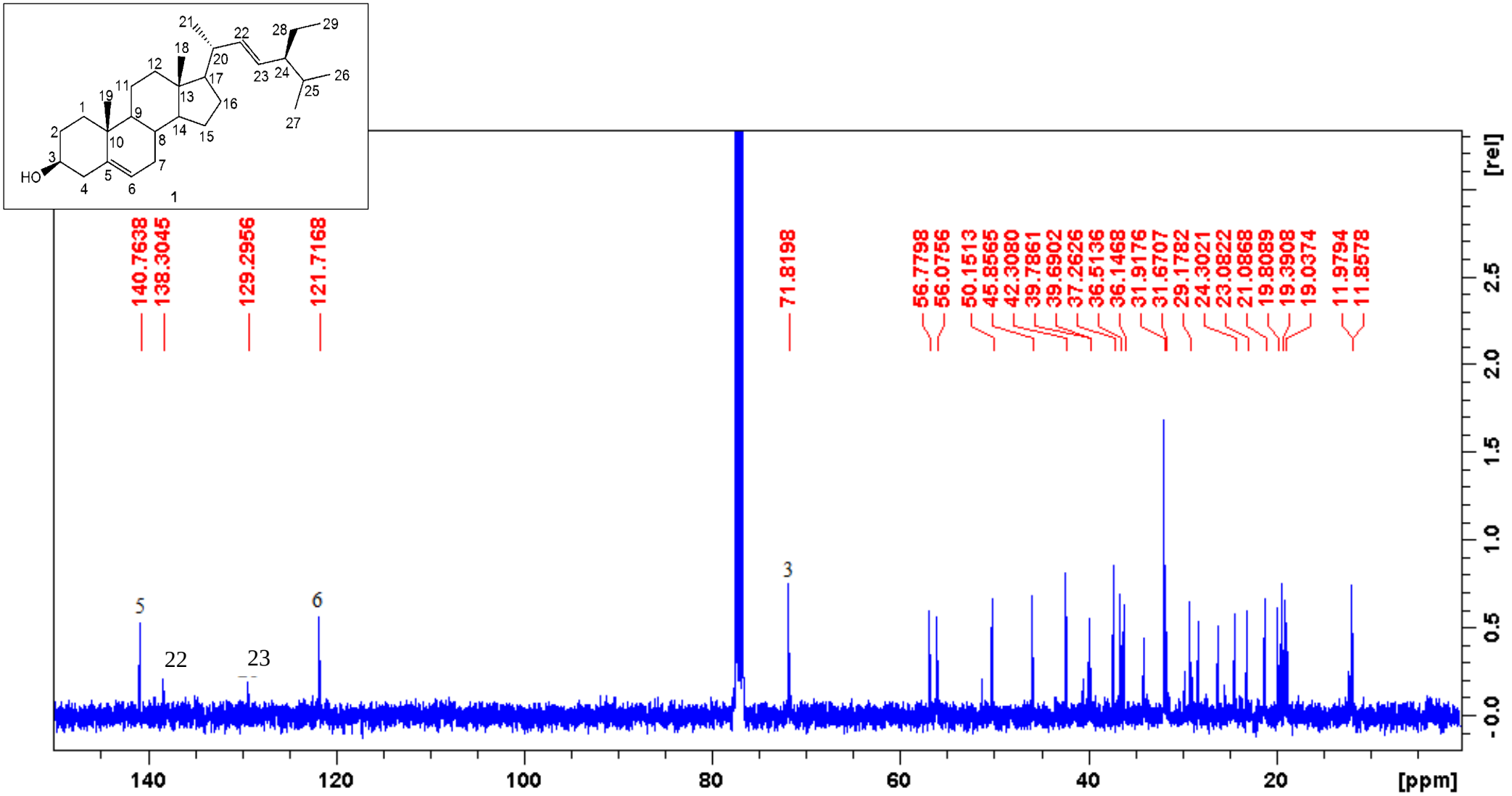

^{13}C NMR spectrum for Stigmasterol

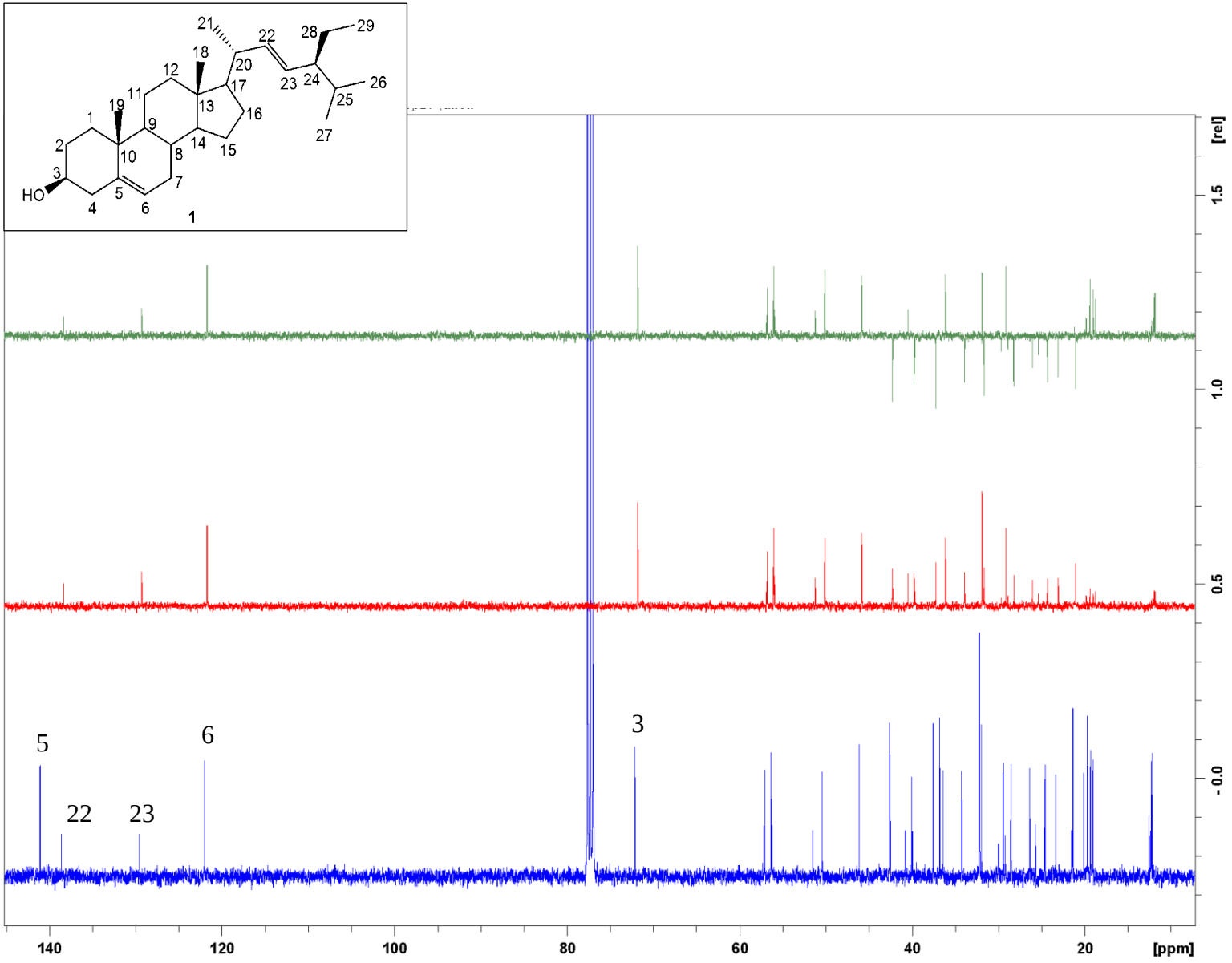

DEPT spectrum for Stigmasterol

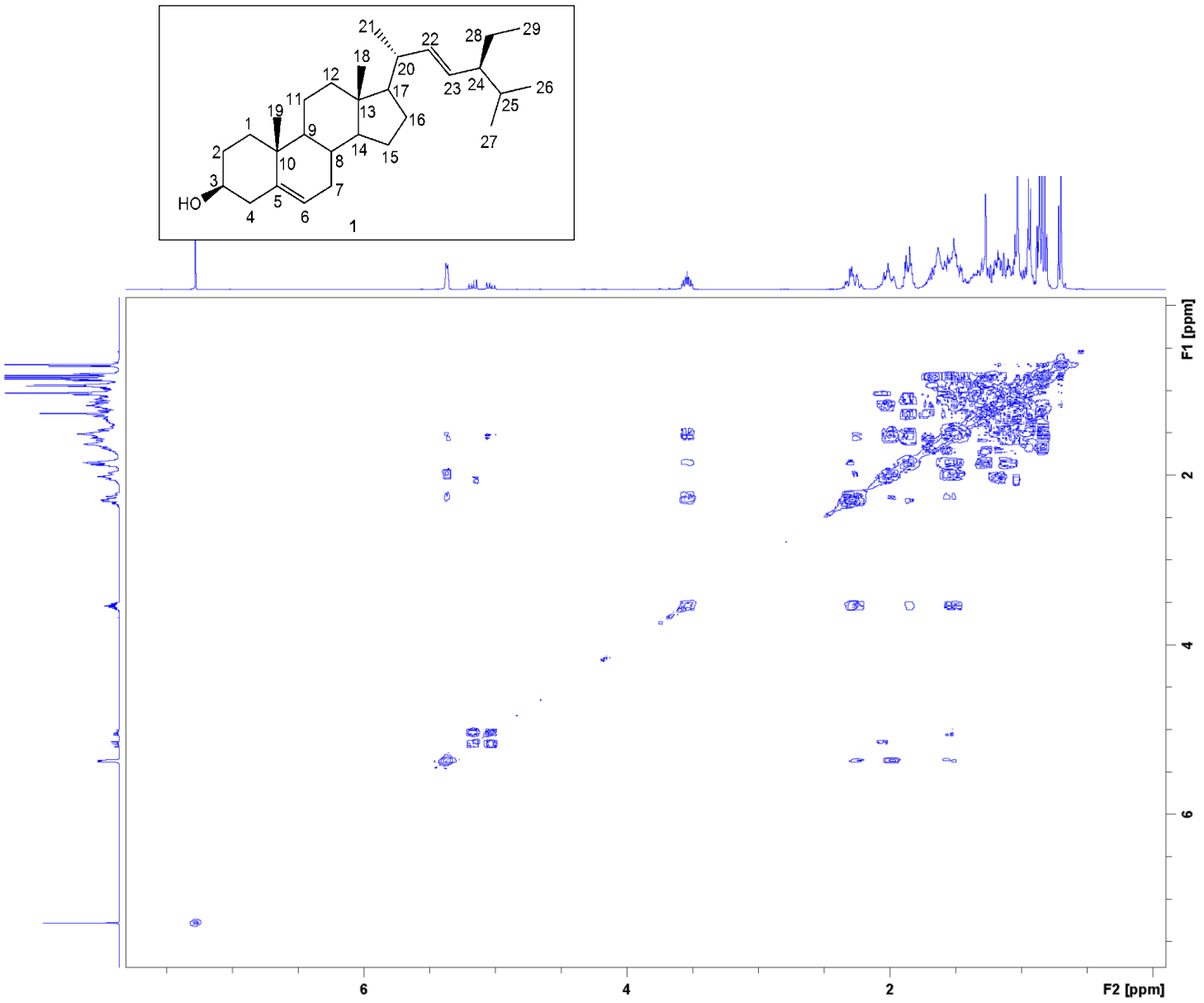

COSY spectrum for Stigmasterol

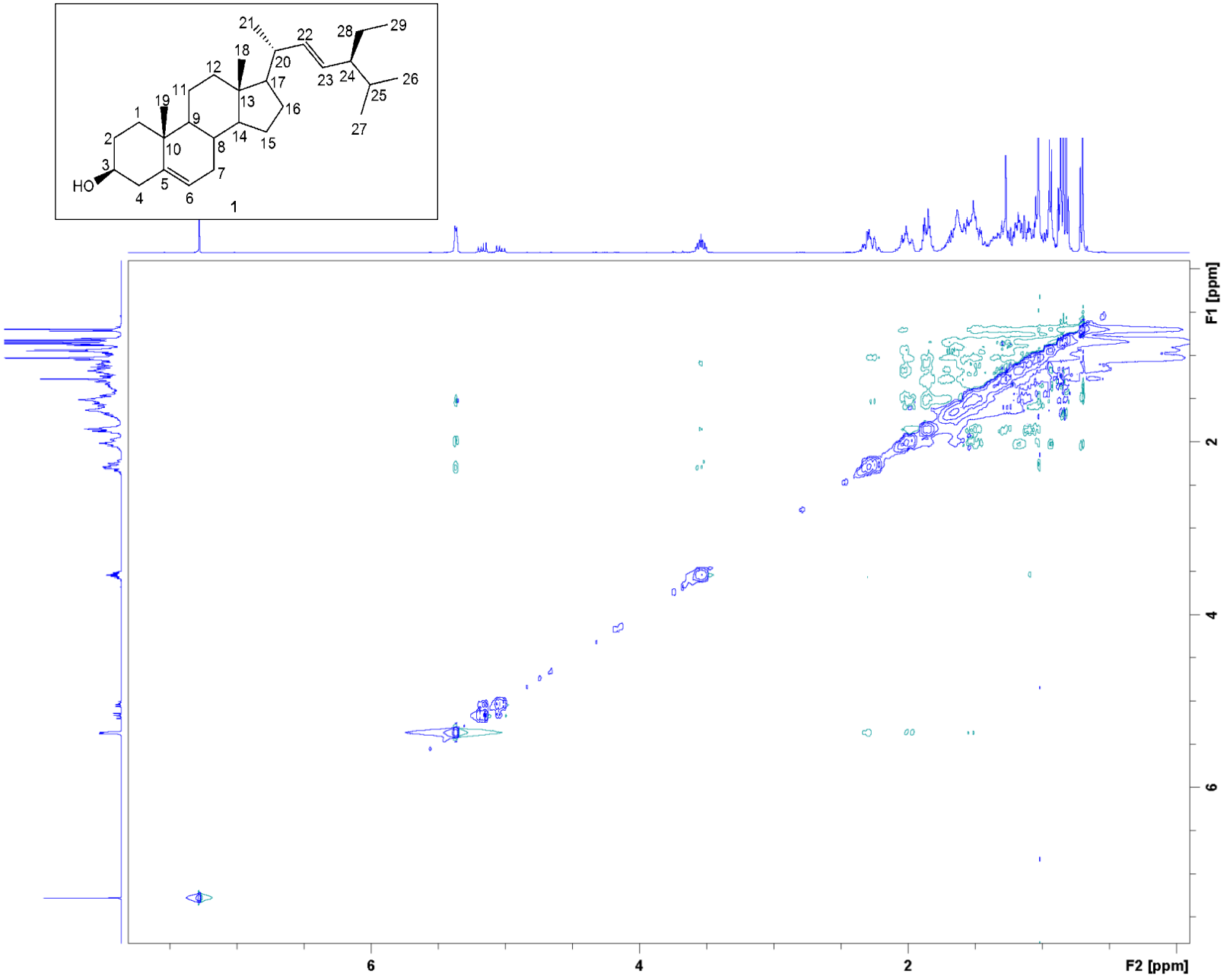

NOESY spectrum for Stigmasterol

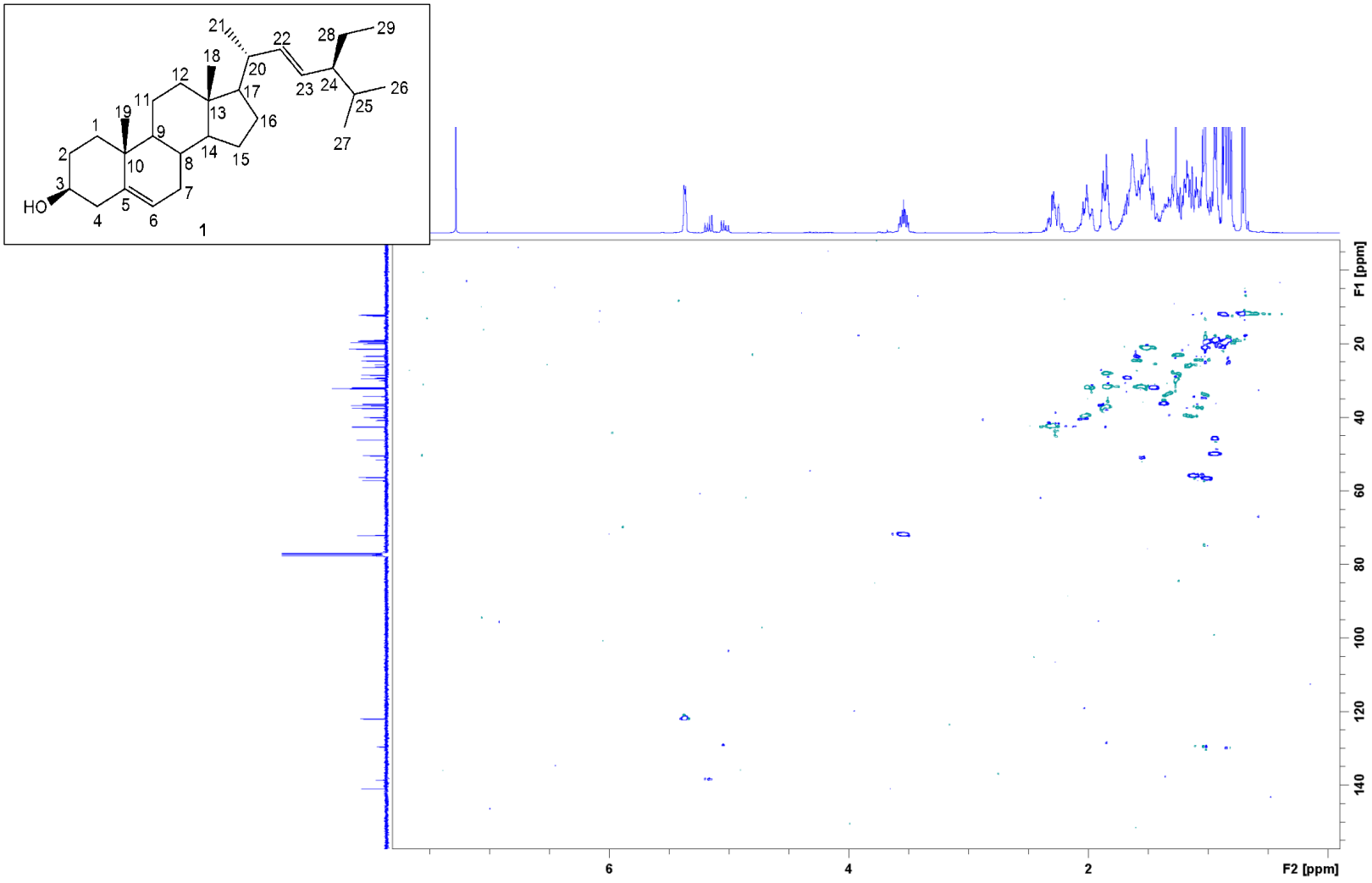

HSQC for Stigmasterol

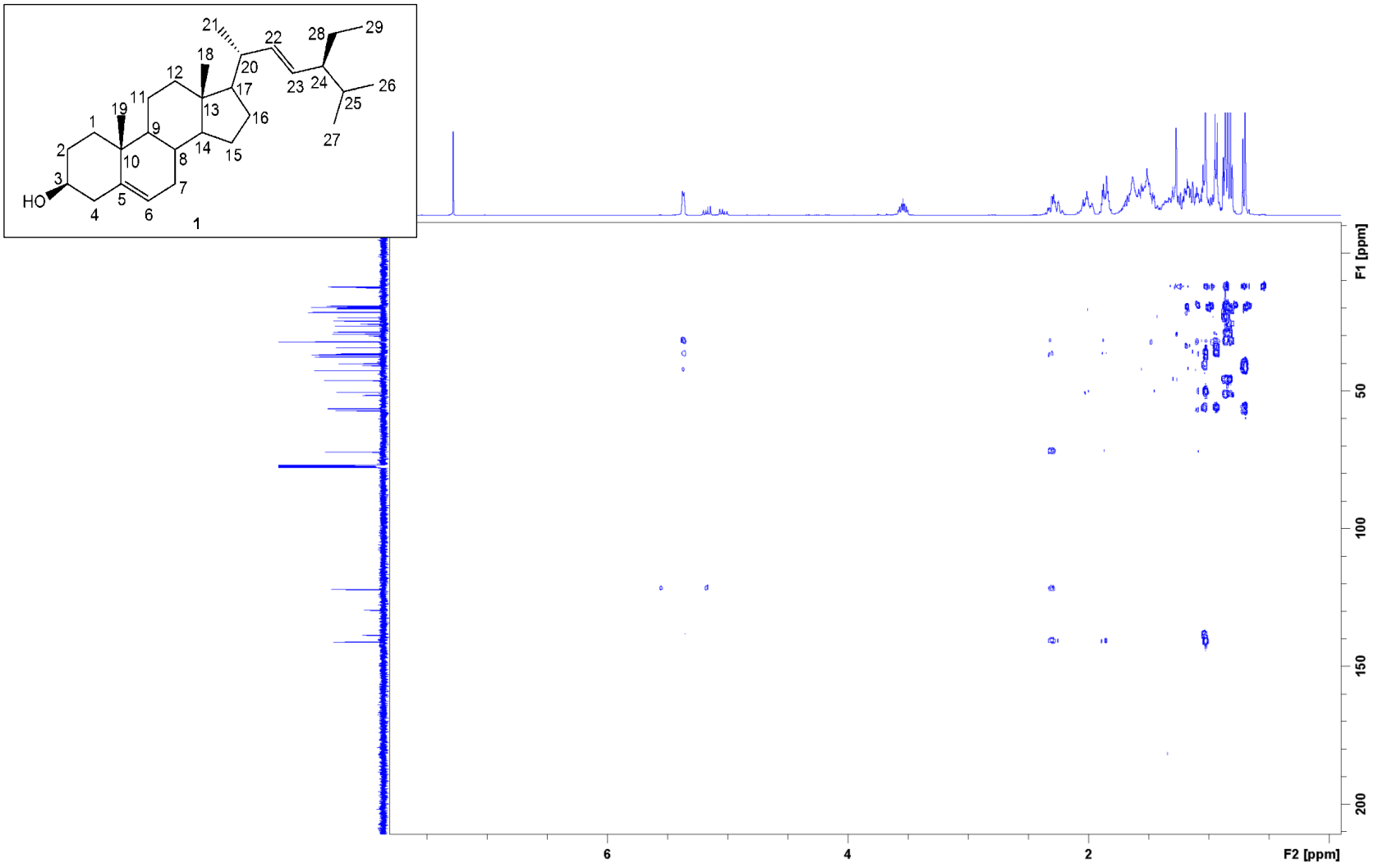

HMBC spectrum for Stigmasterol

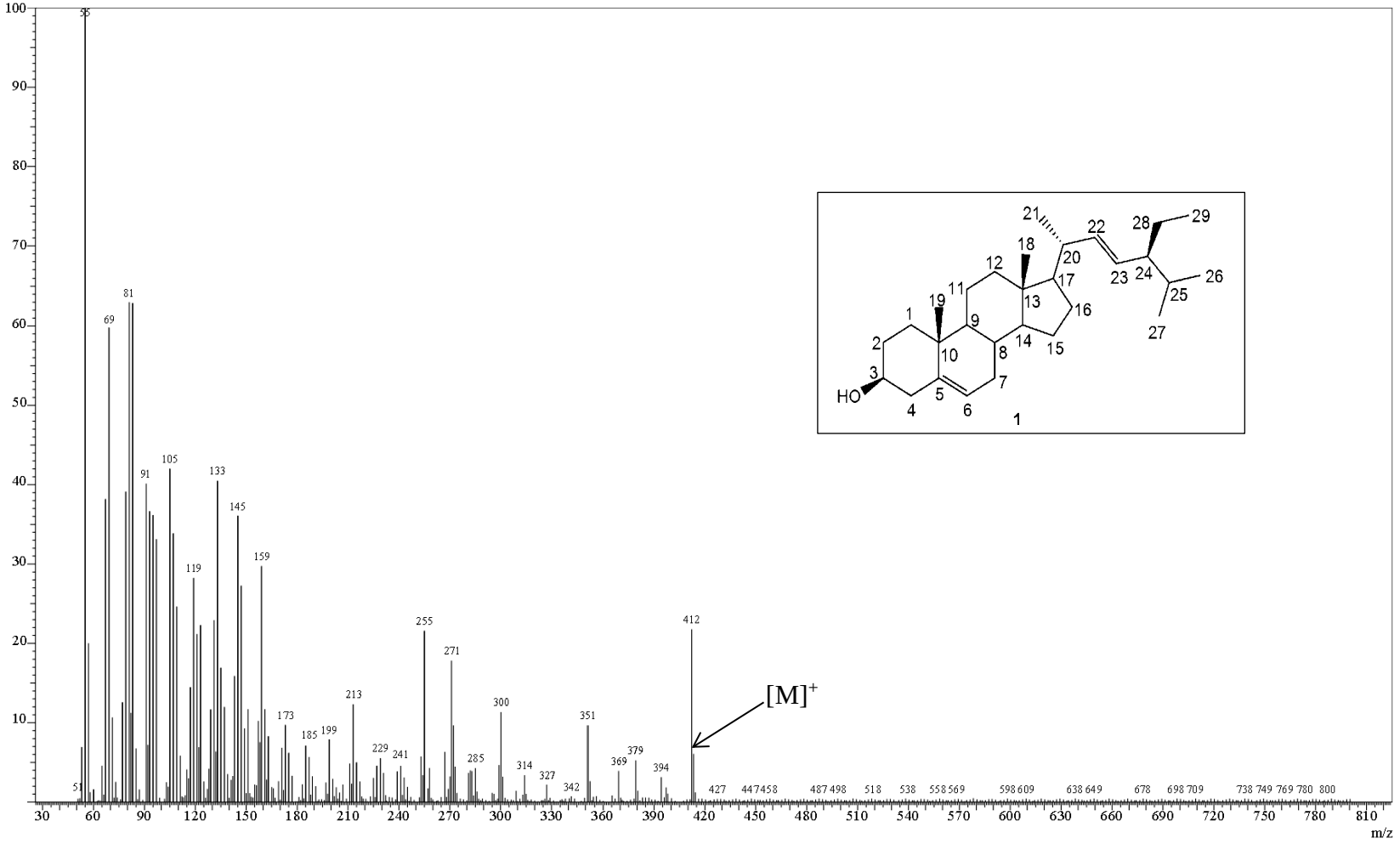

GC-MS spectrum for Stigmasterol

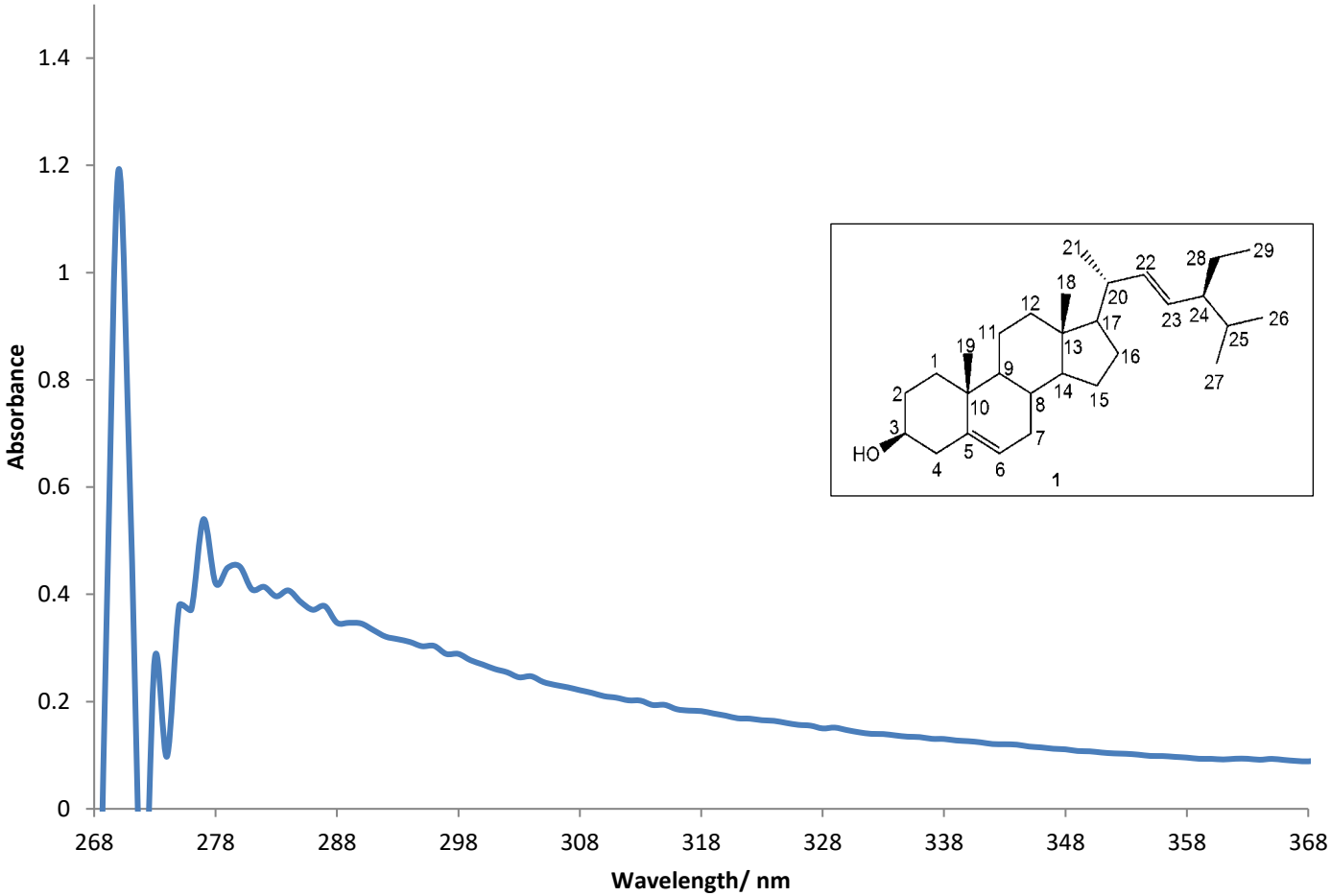

UV-Vis spectrum for Stigmasterol

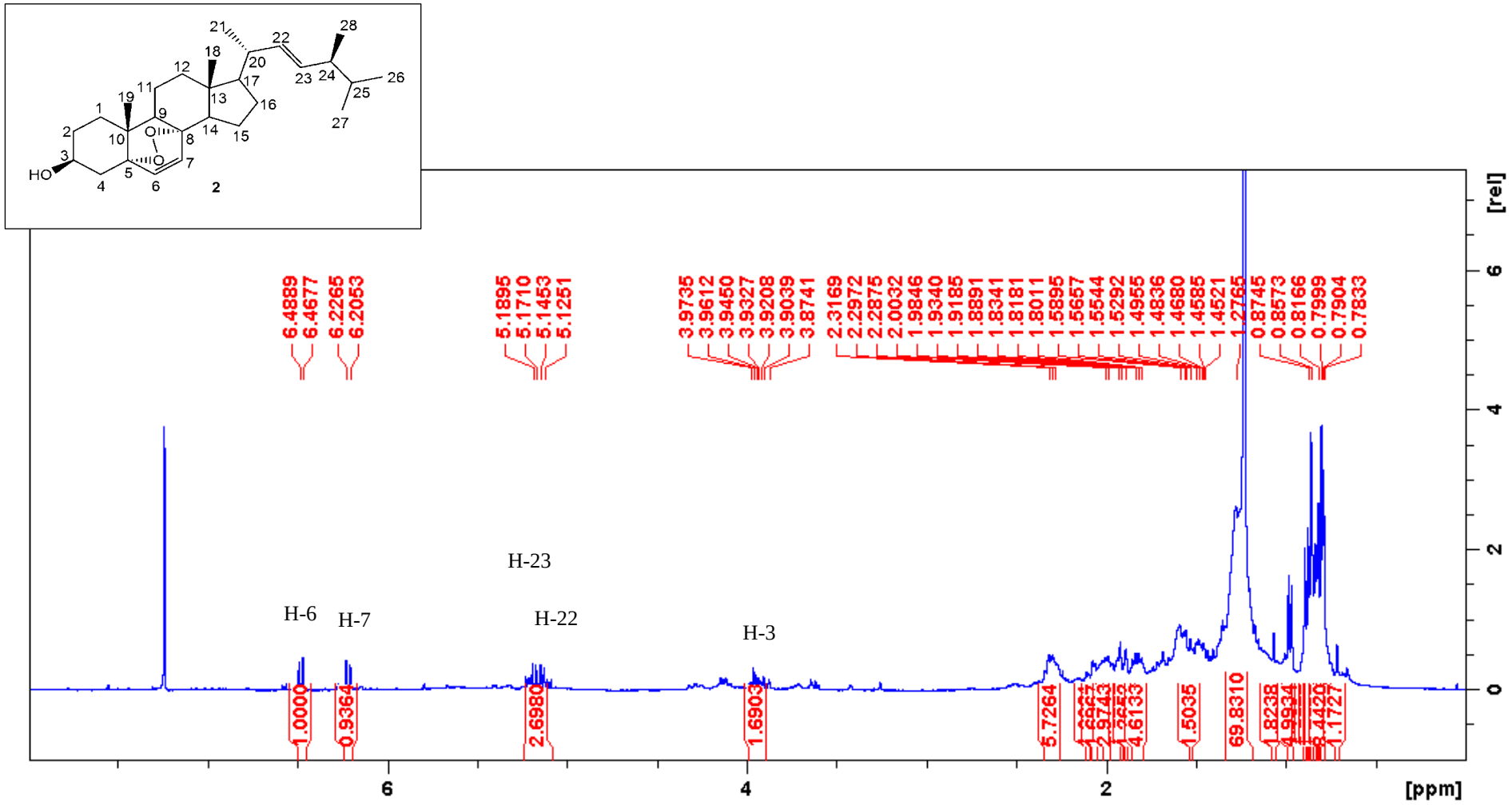

^{1}H NMR spectrum for Ergosterol peroxide

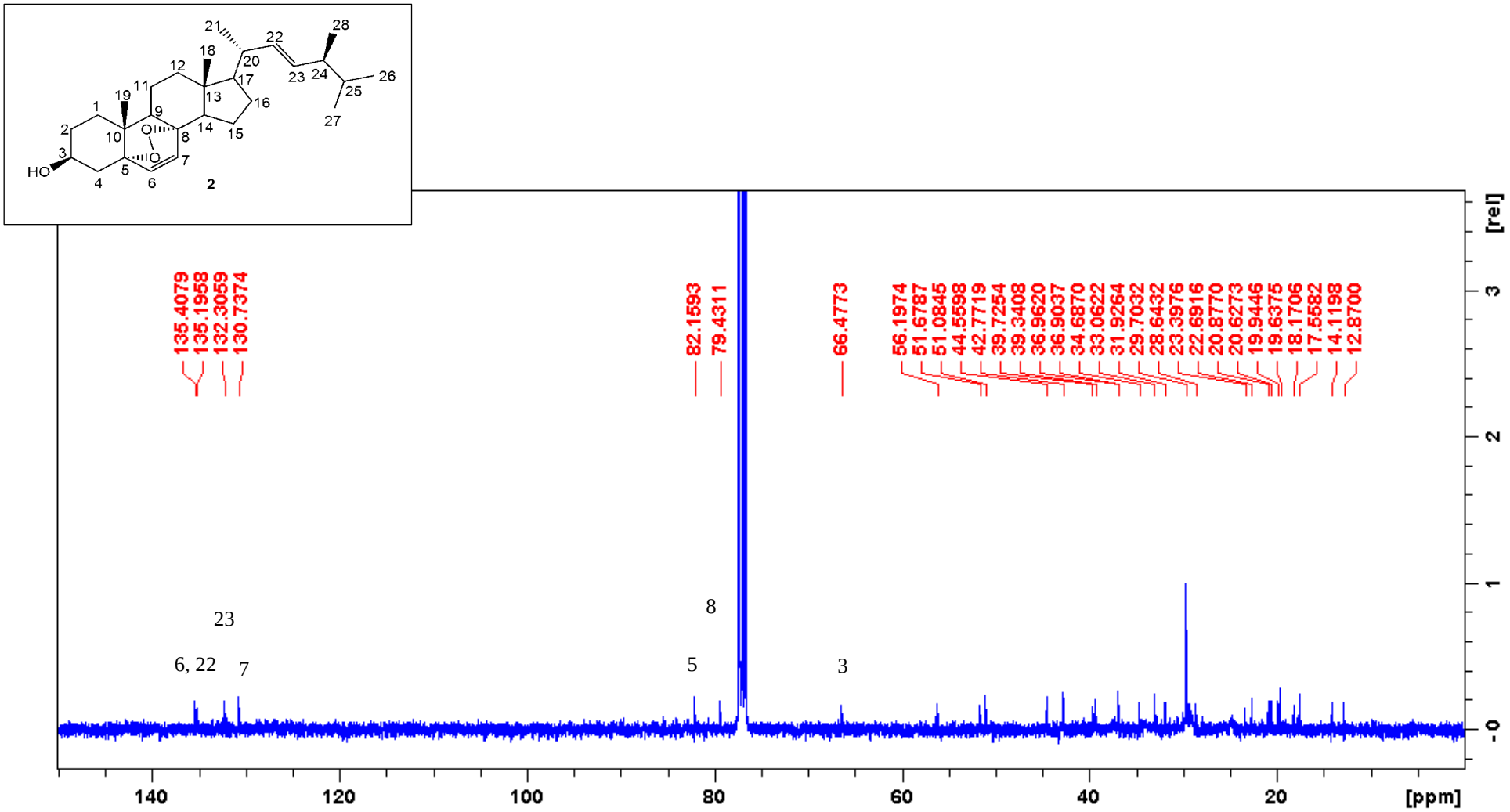

^{13}C NMR spectrum for Ergosterol peroxide

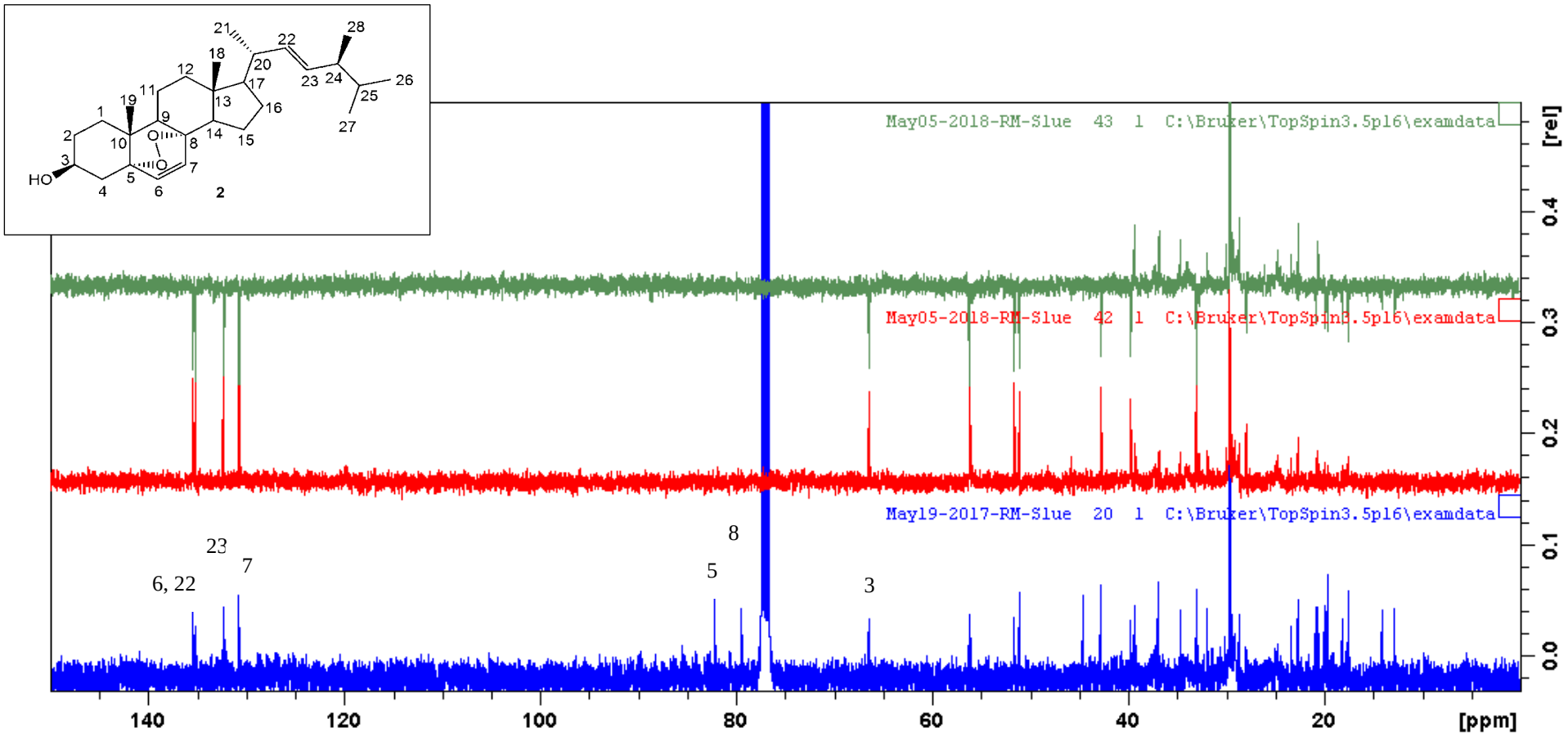

DEPT spectrum for Ergosterol peroxide

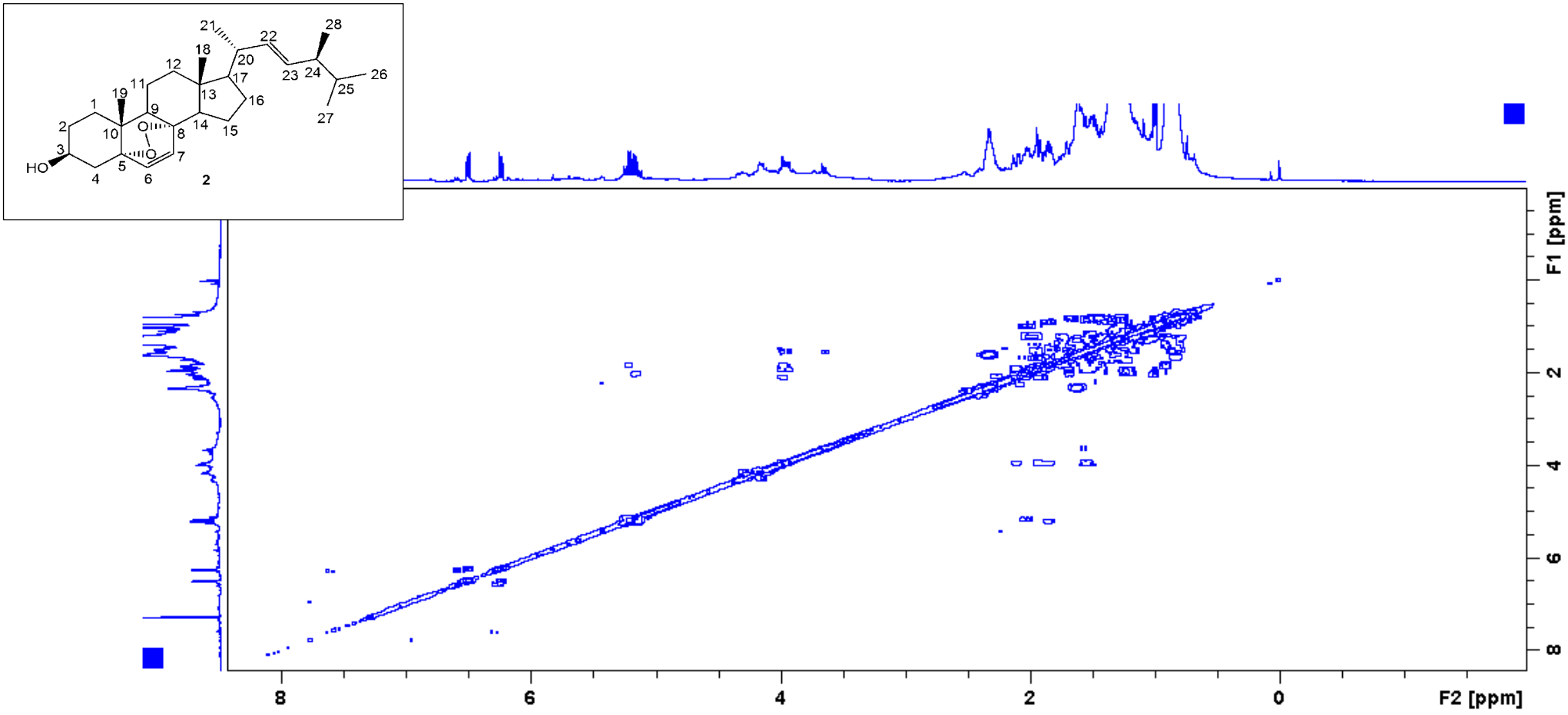

COSY spectrum for Ergosterol peroxide

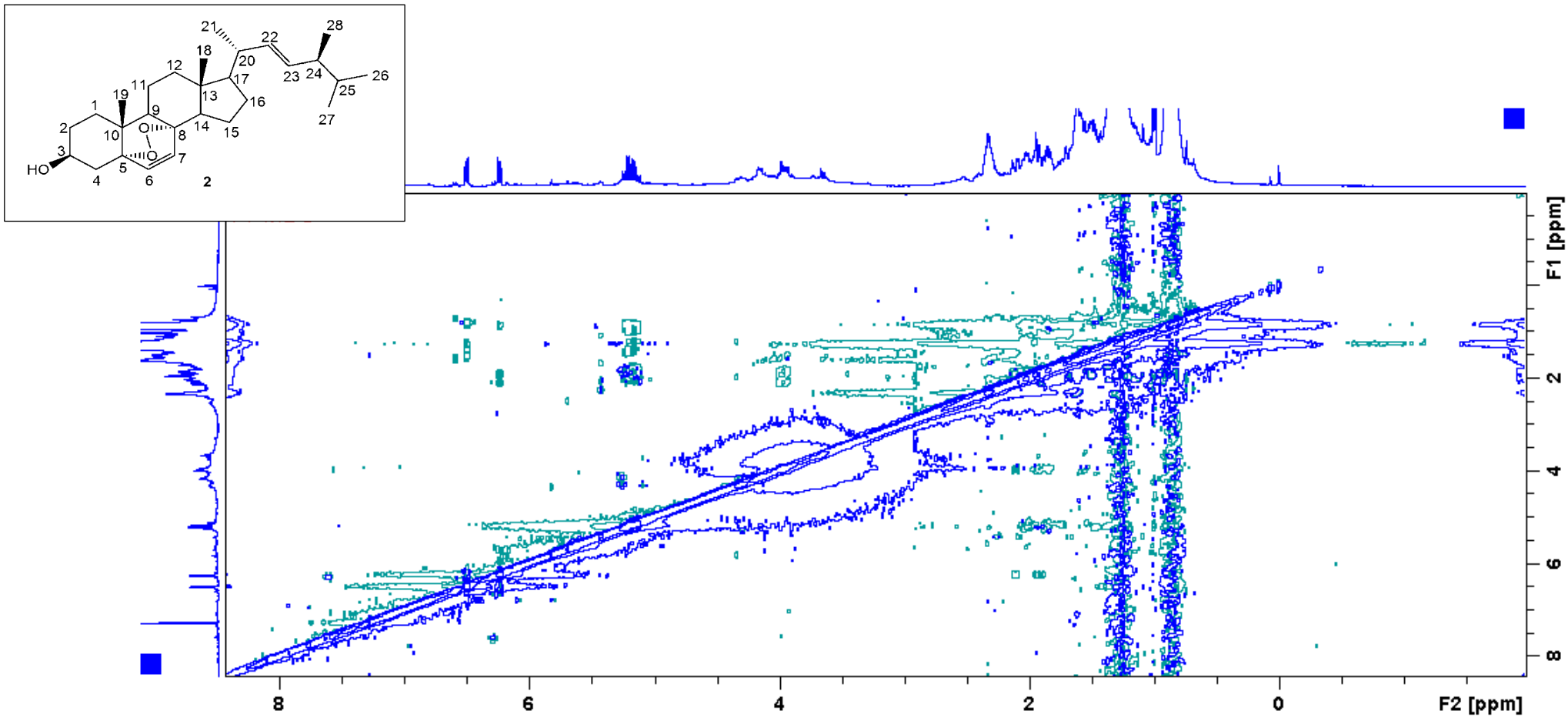

NOESY spectrum for Ergosterol peroxide

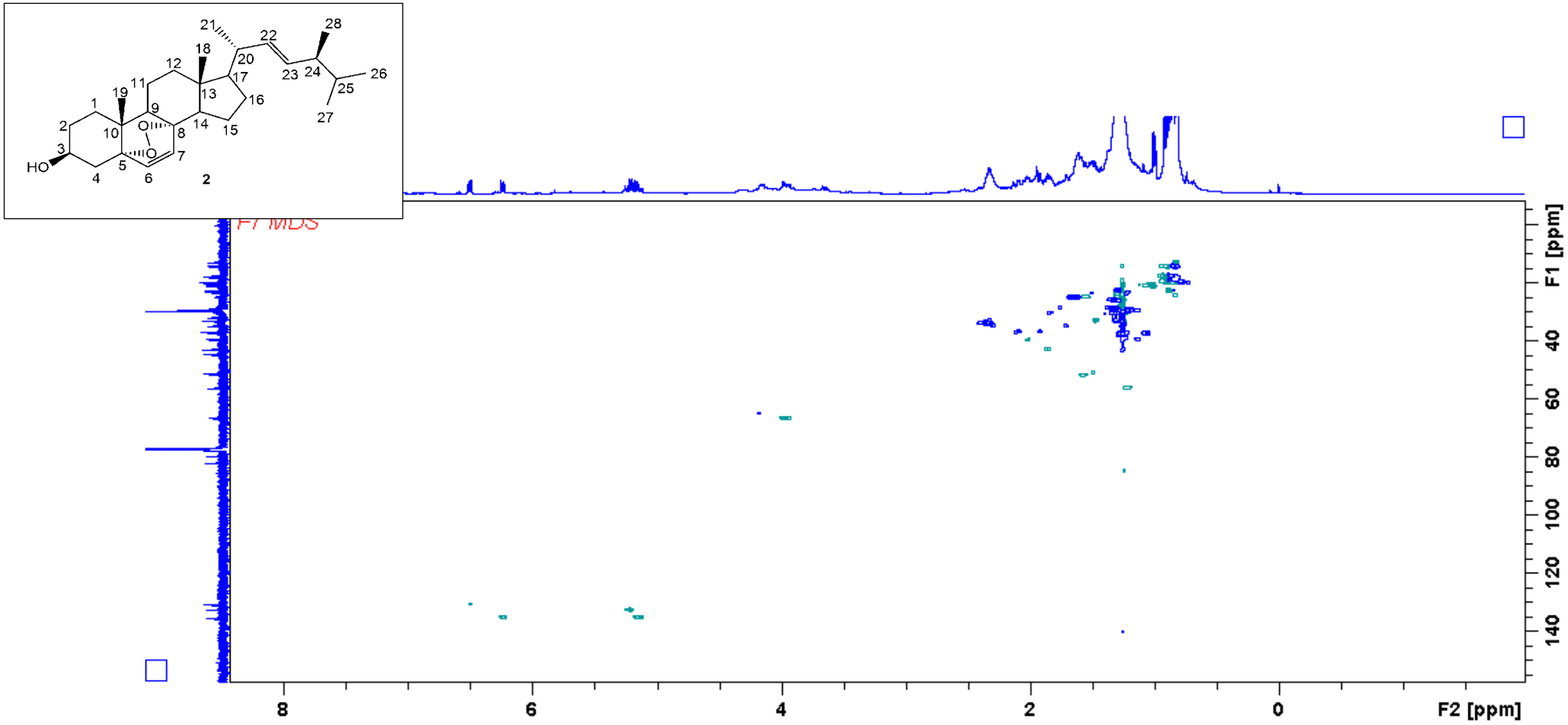

HSQC spectrum for Ergosterol peroxide

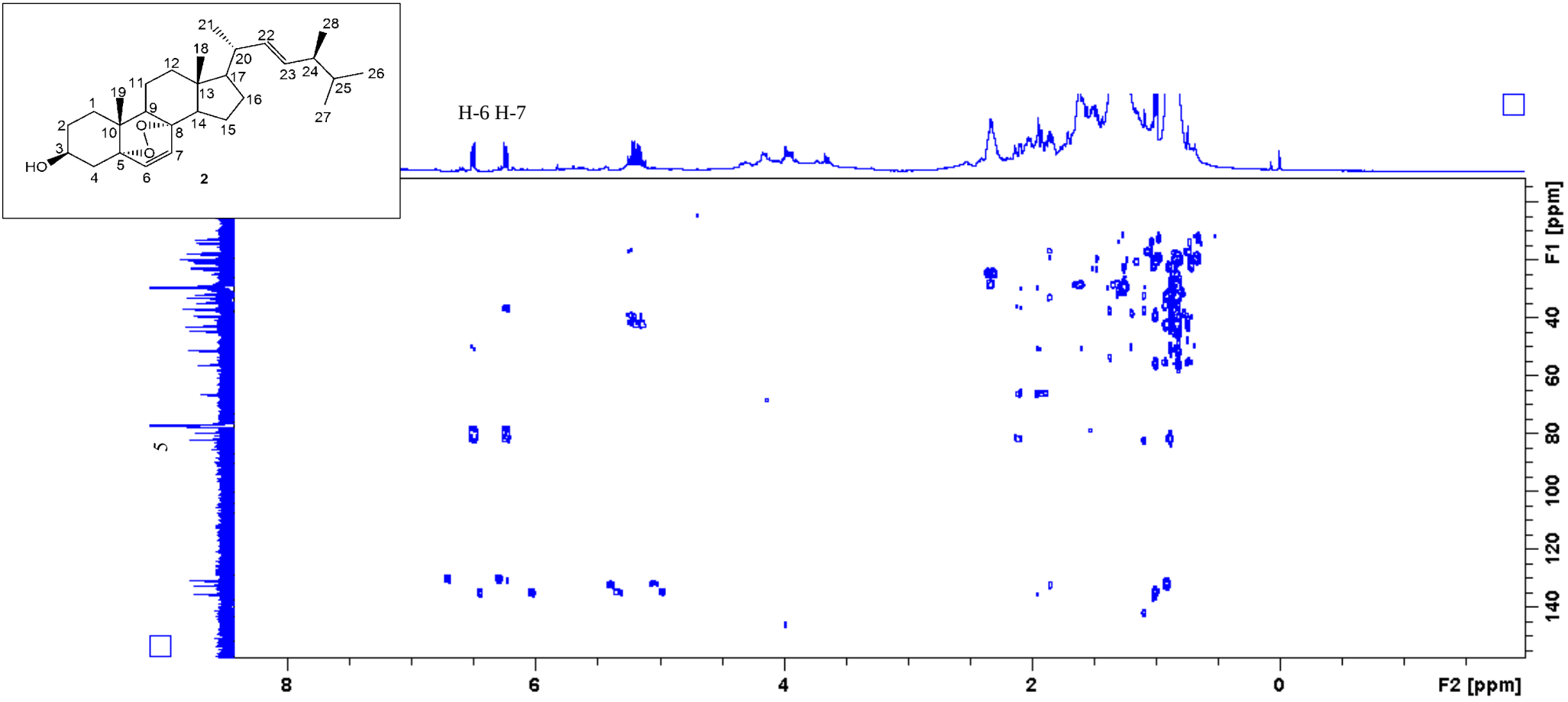

HMBC spectrum for Ergosterol peroxide

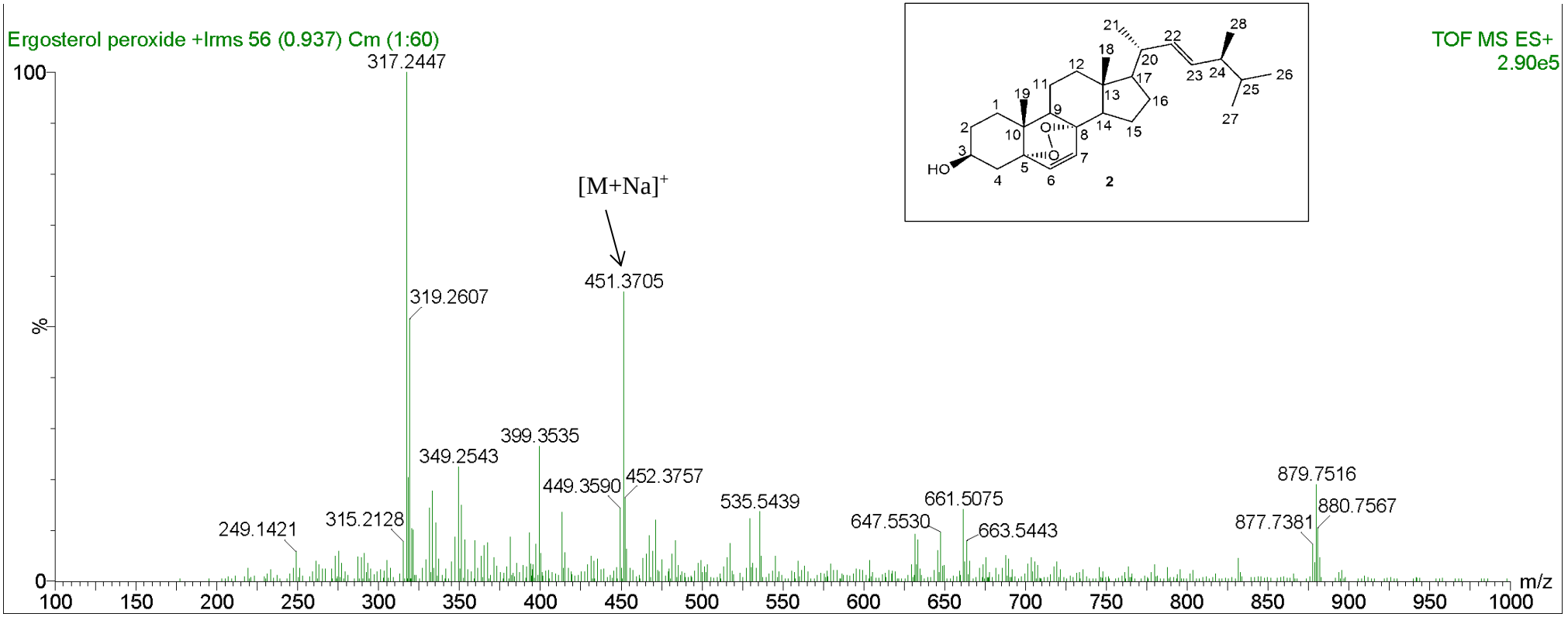

LR-ESI-MS spectrum of Ergosterol peroxide

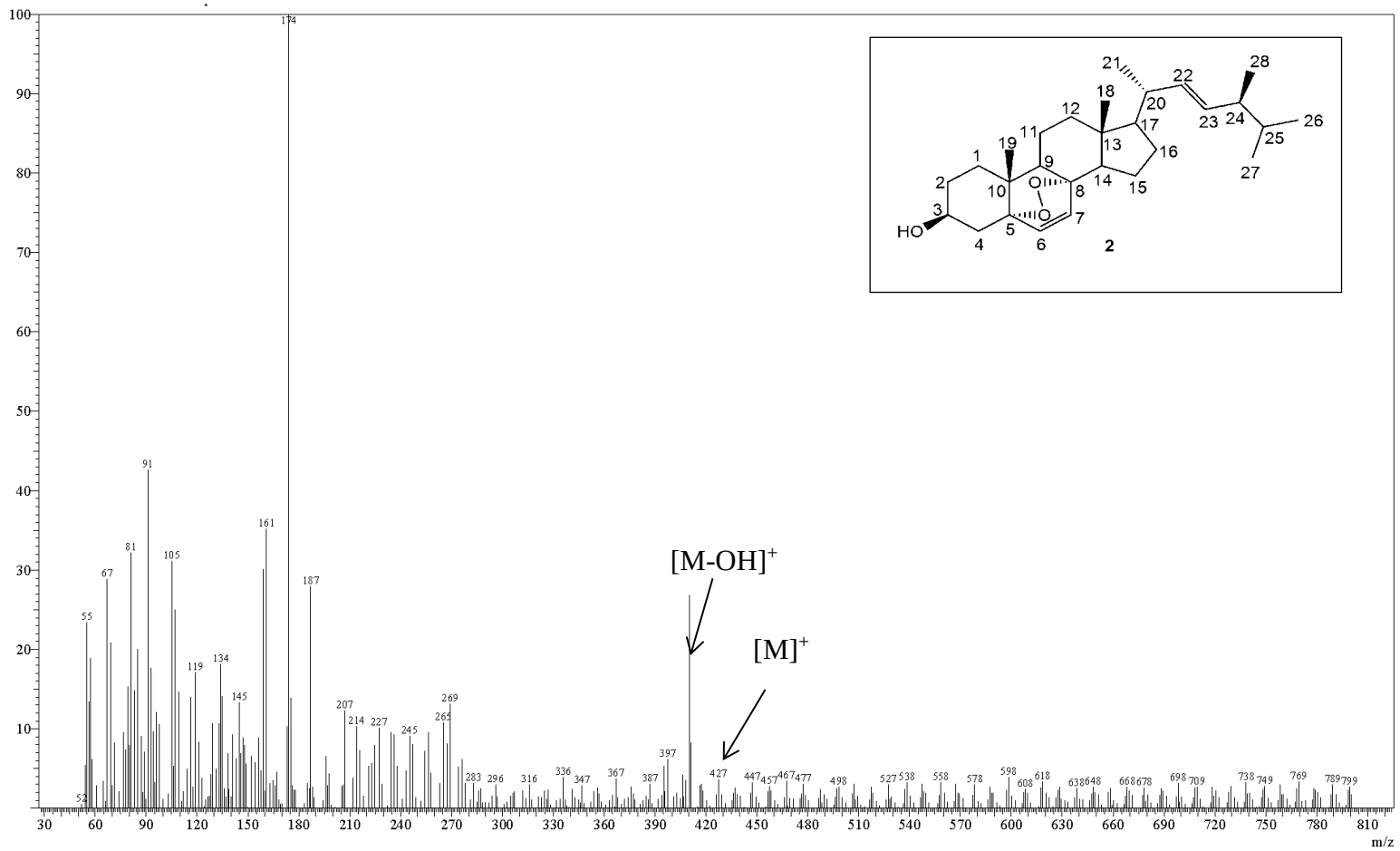

GC-MS spectrum for Ergosterol peroxide

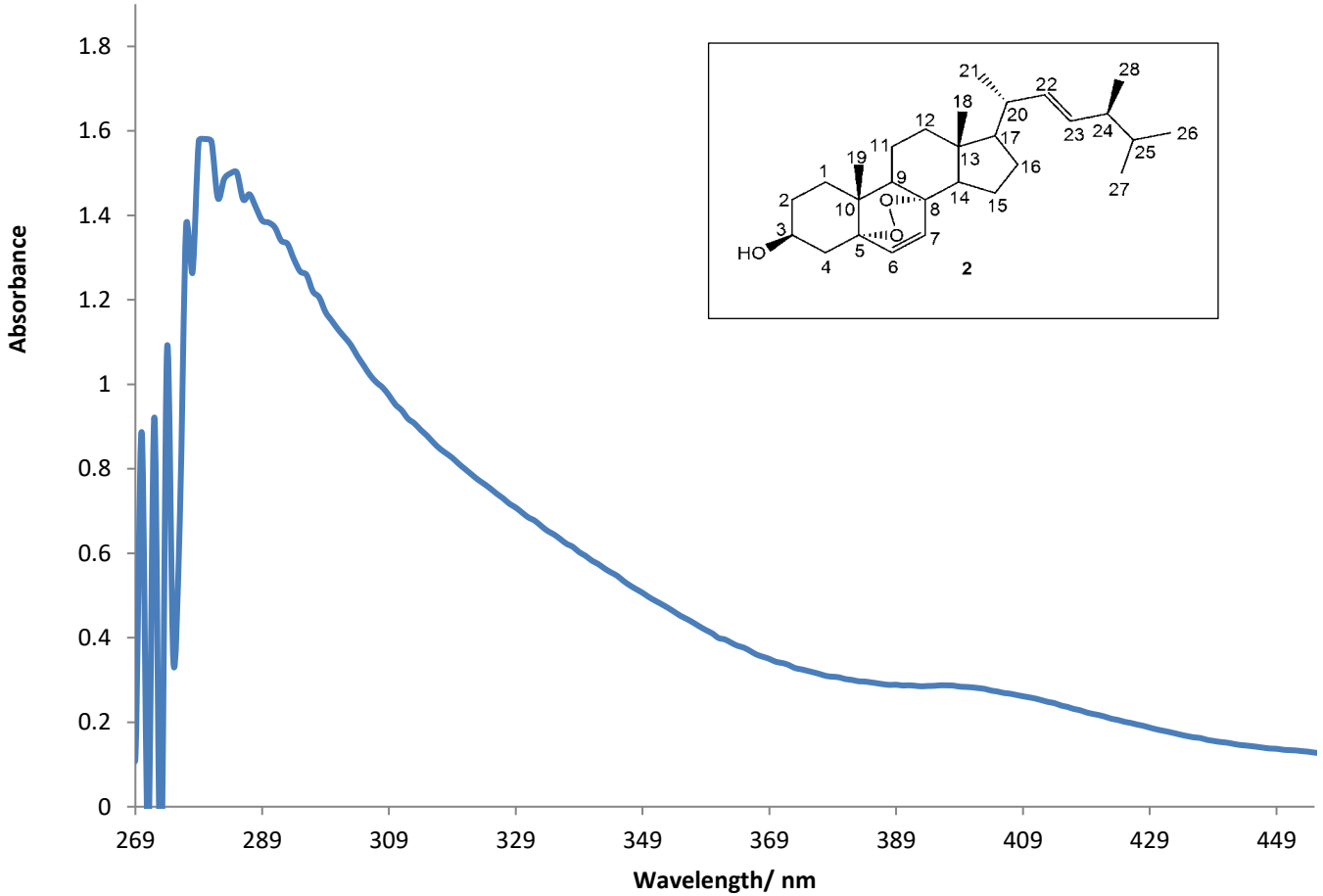

UV-Vis spectrum for Ergosterol peroxide

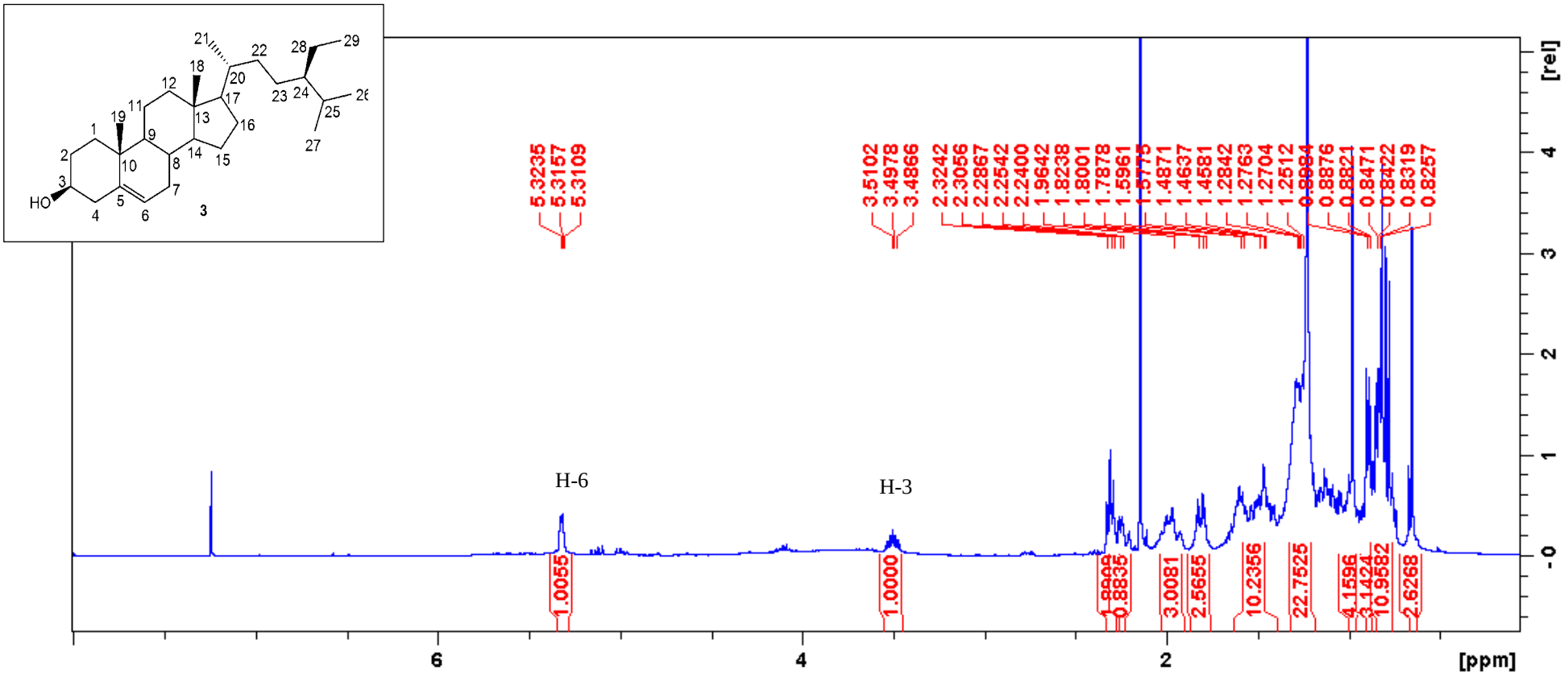

^{1}H NMR spectrum for *β*-sitosterol

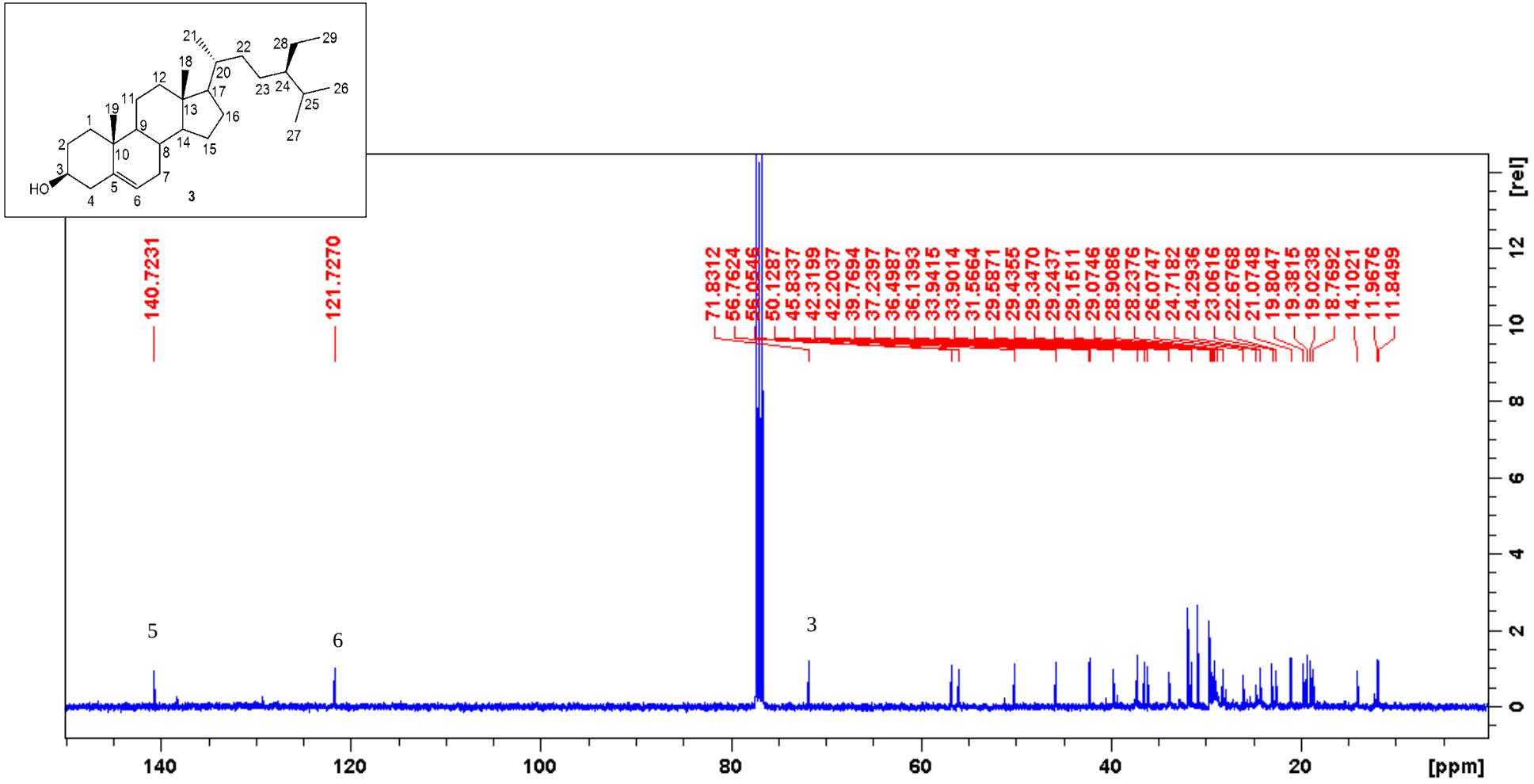

^{13}C NMR spectrum for β-sitosterol

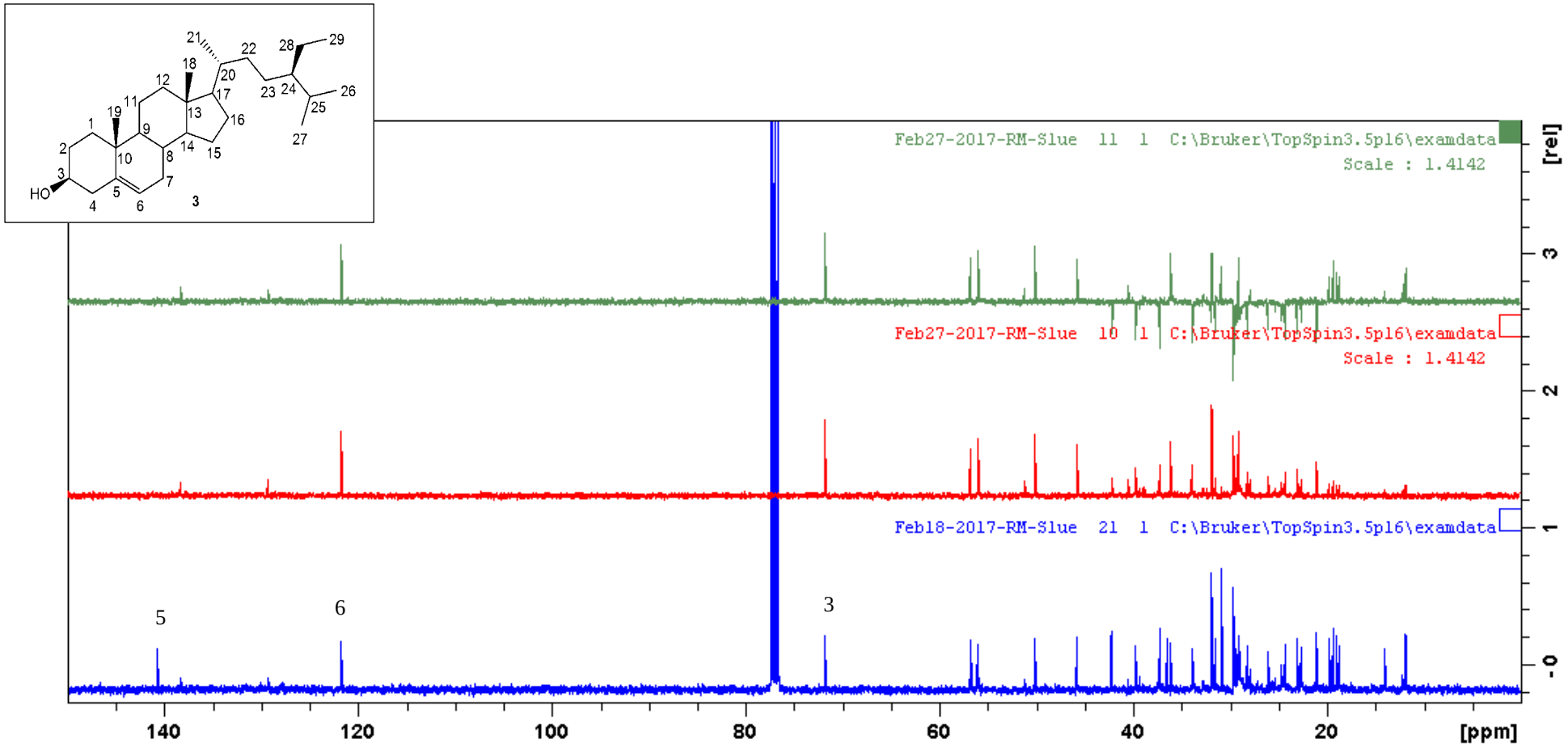

DEPT spectrum for *β*-sitosterol

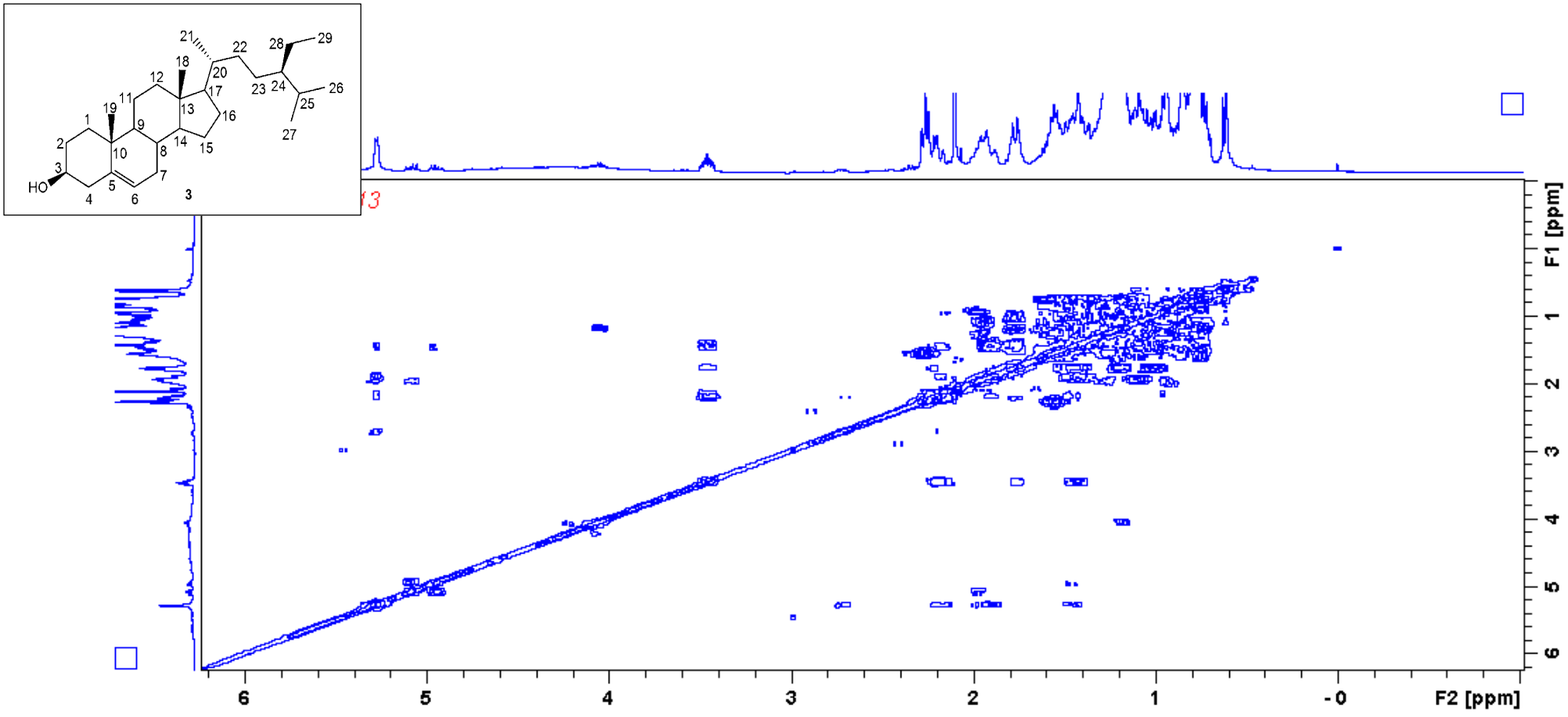

COSY spectrum for *β*-sitosterol

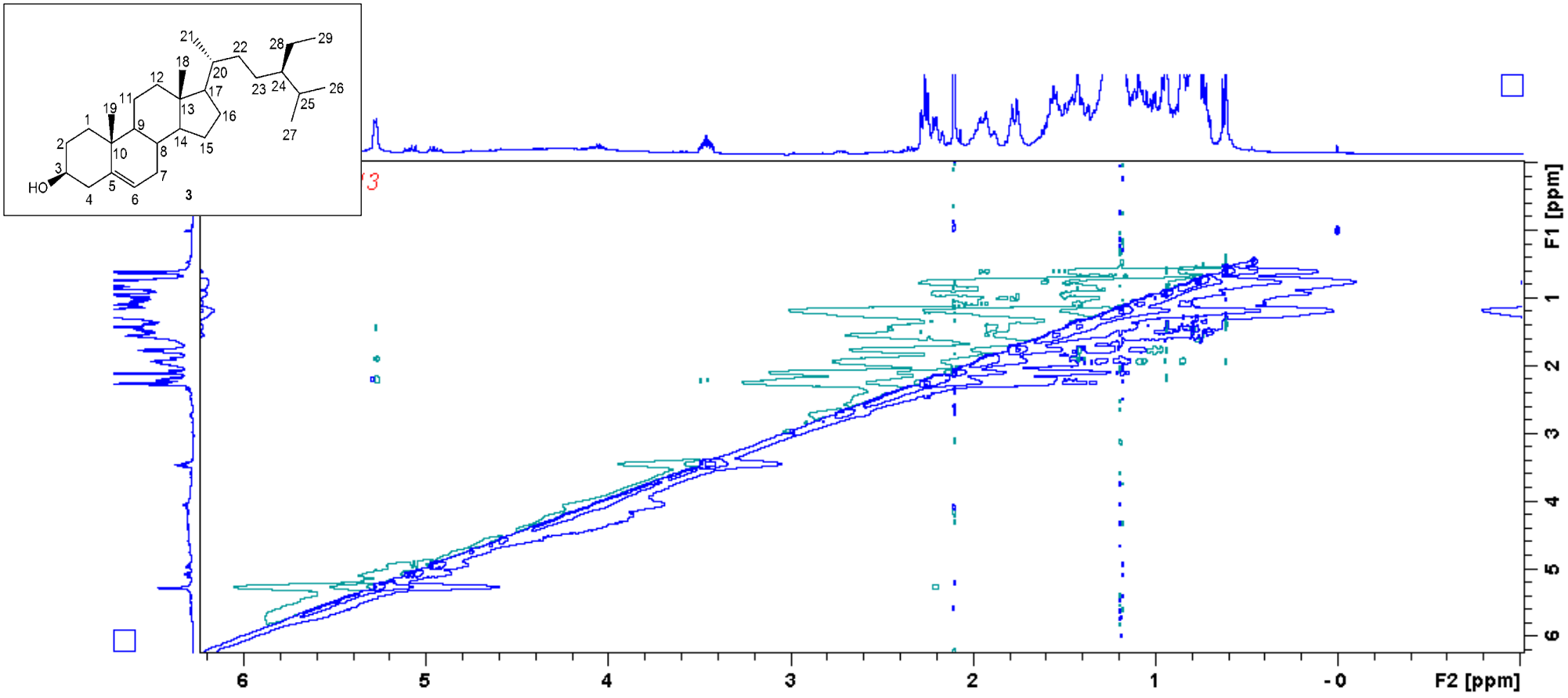

NOESY spectrum for *β*-sitosterol

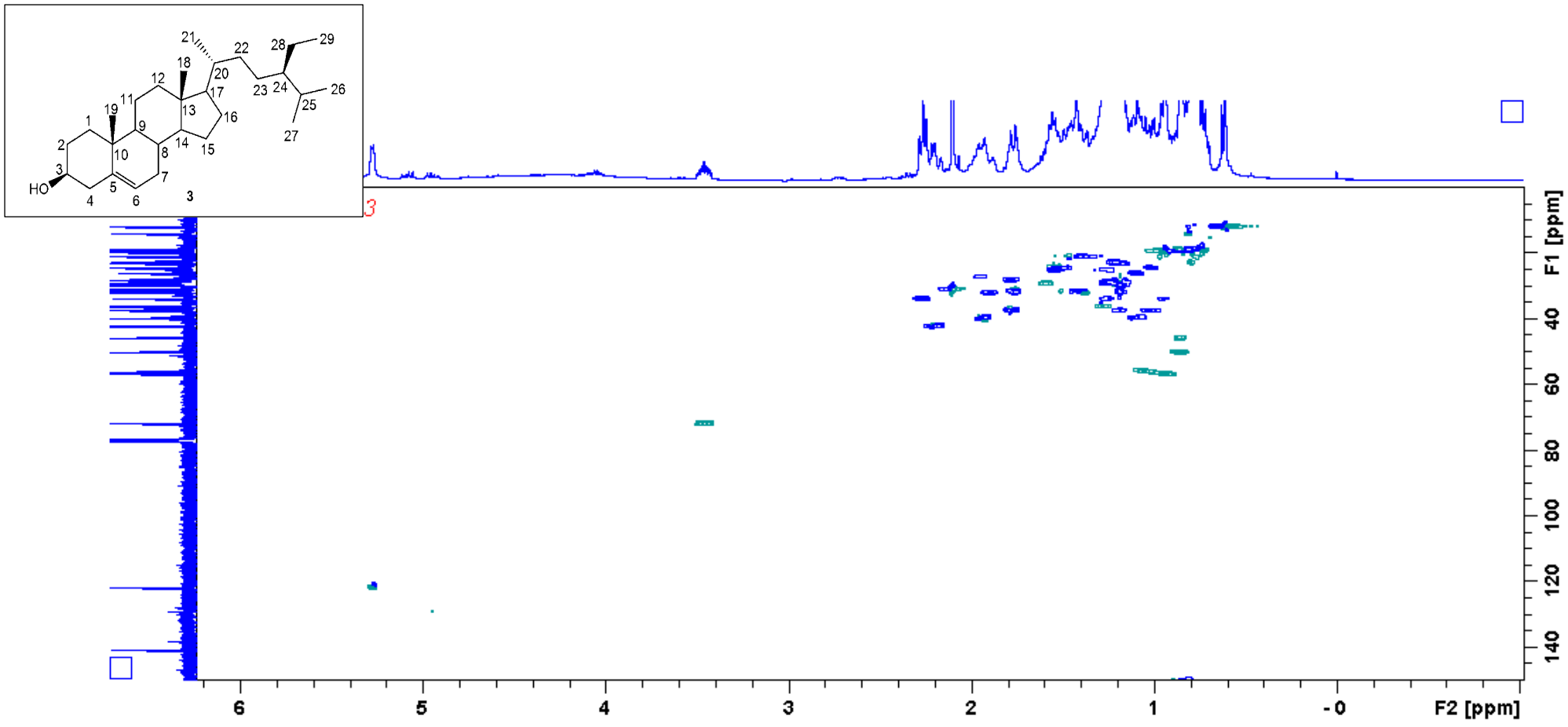

HSQC spectrum for *β*-sitosterol

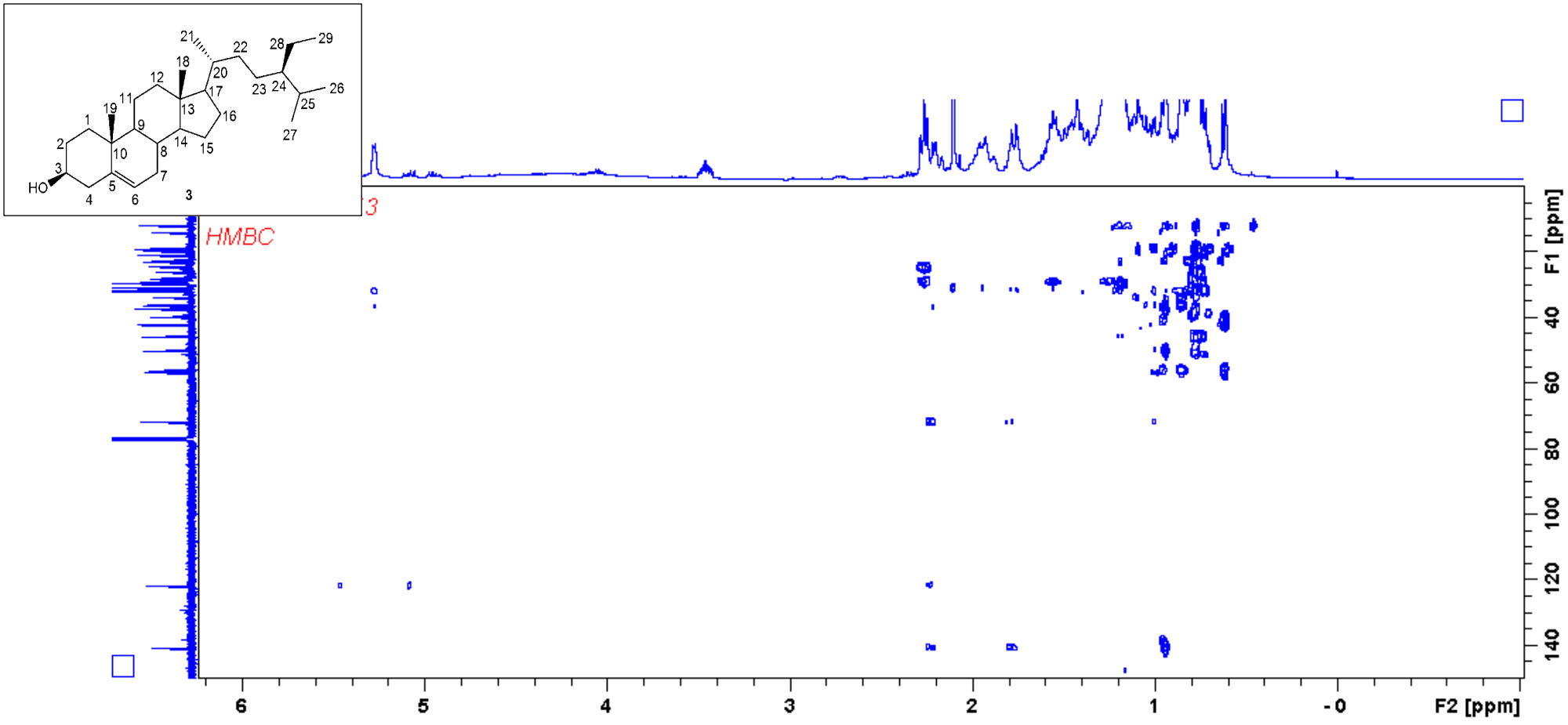

HMBC spectrum for β-sitosterol

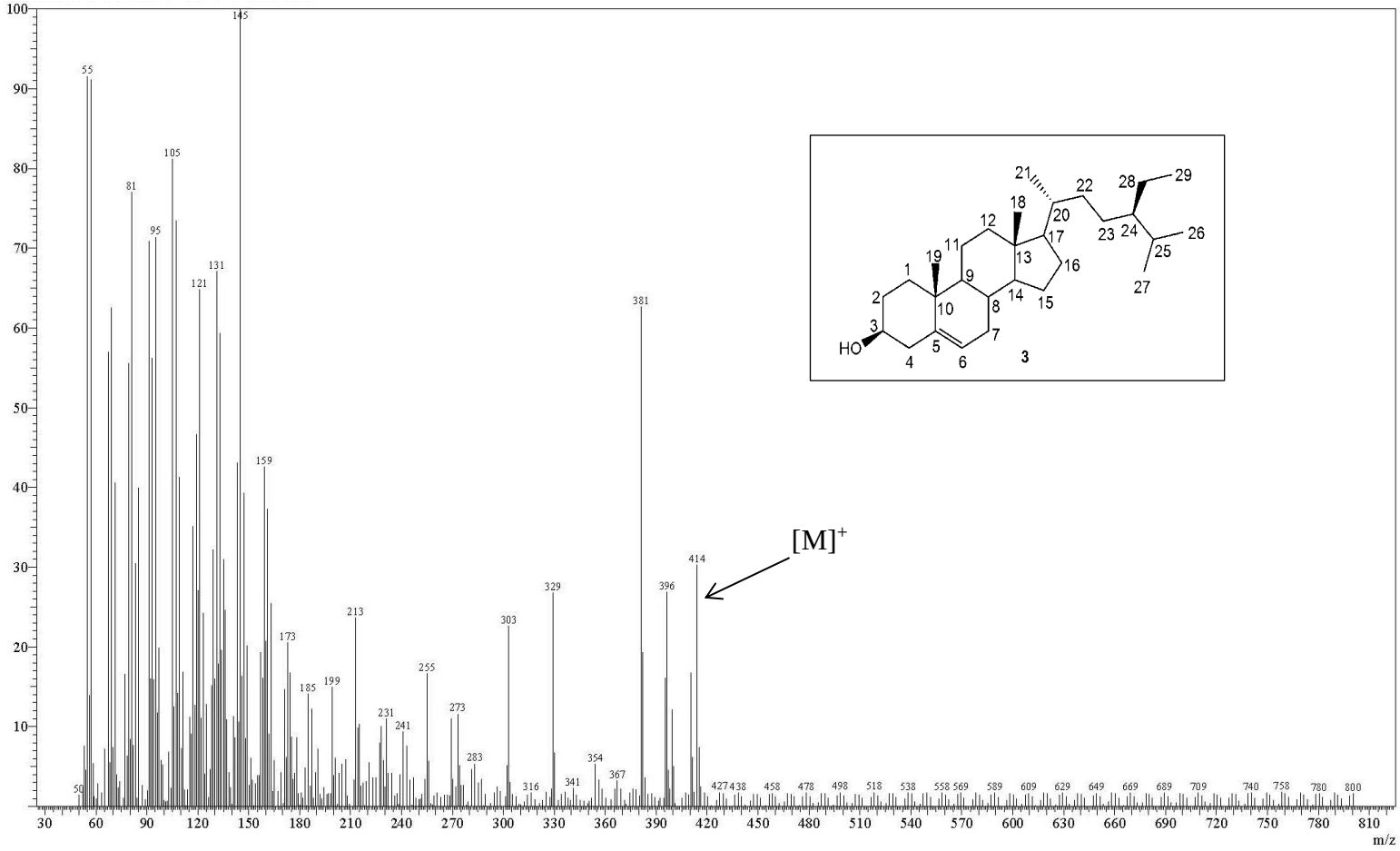

GC-MS spectrum for β-sitosterol

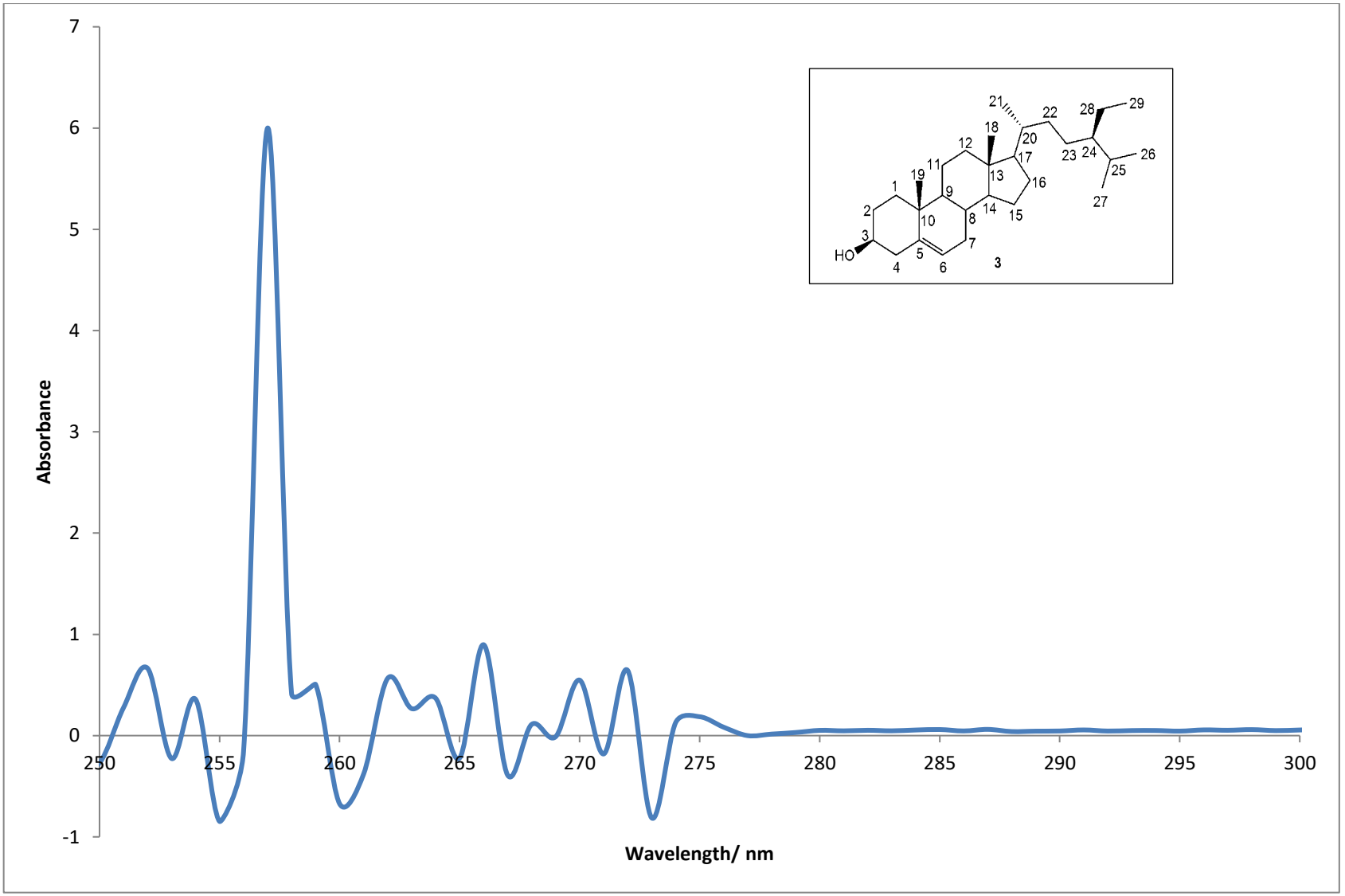

UV-Vis spectrum for β-sitosterol

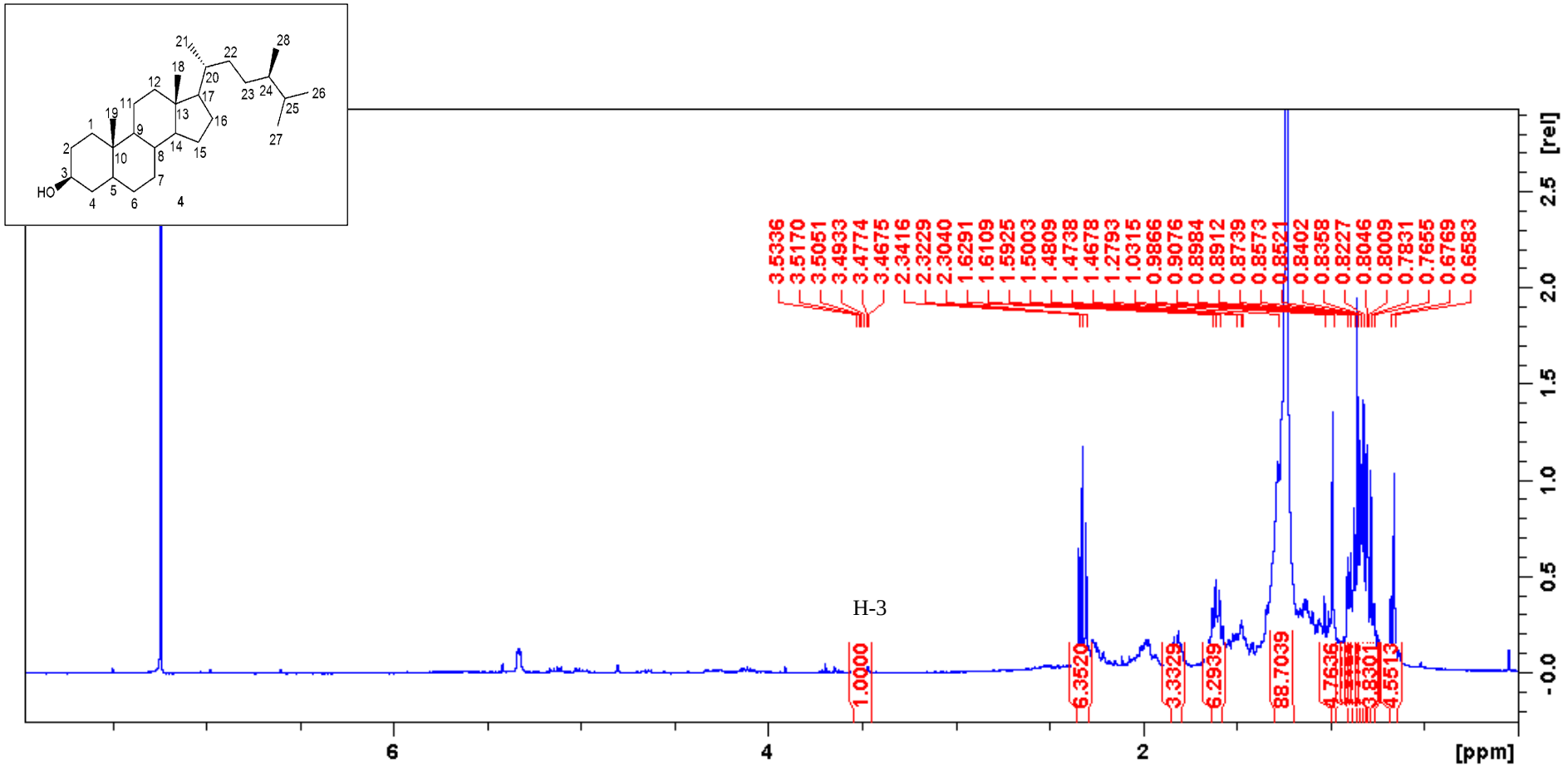

^{1}H spectrum for Campestanol

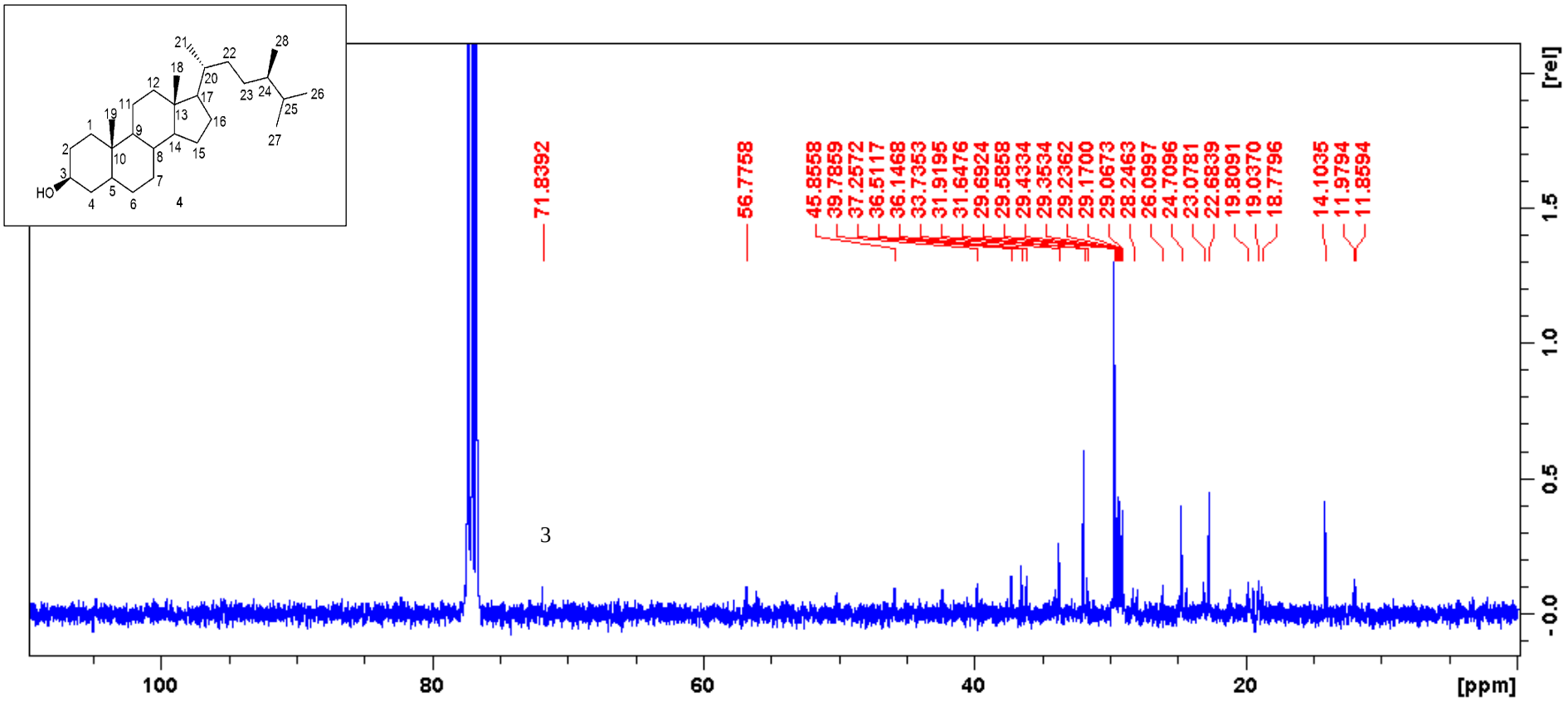

^{13}C spectrum for Campestanol

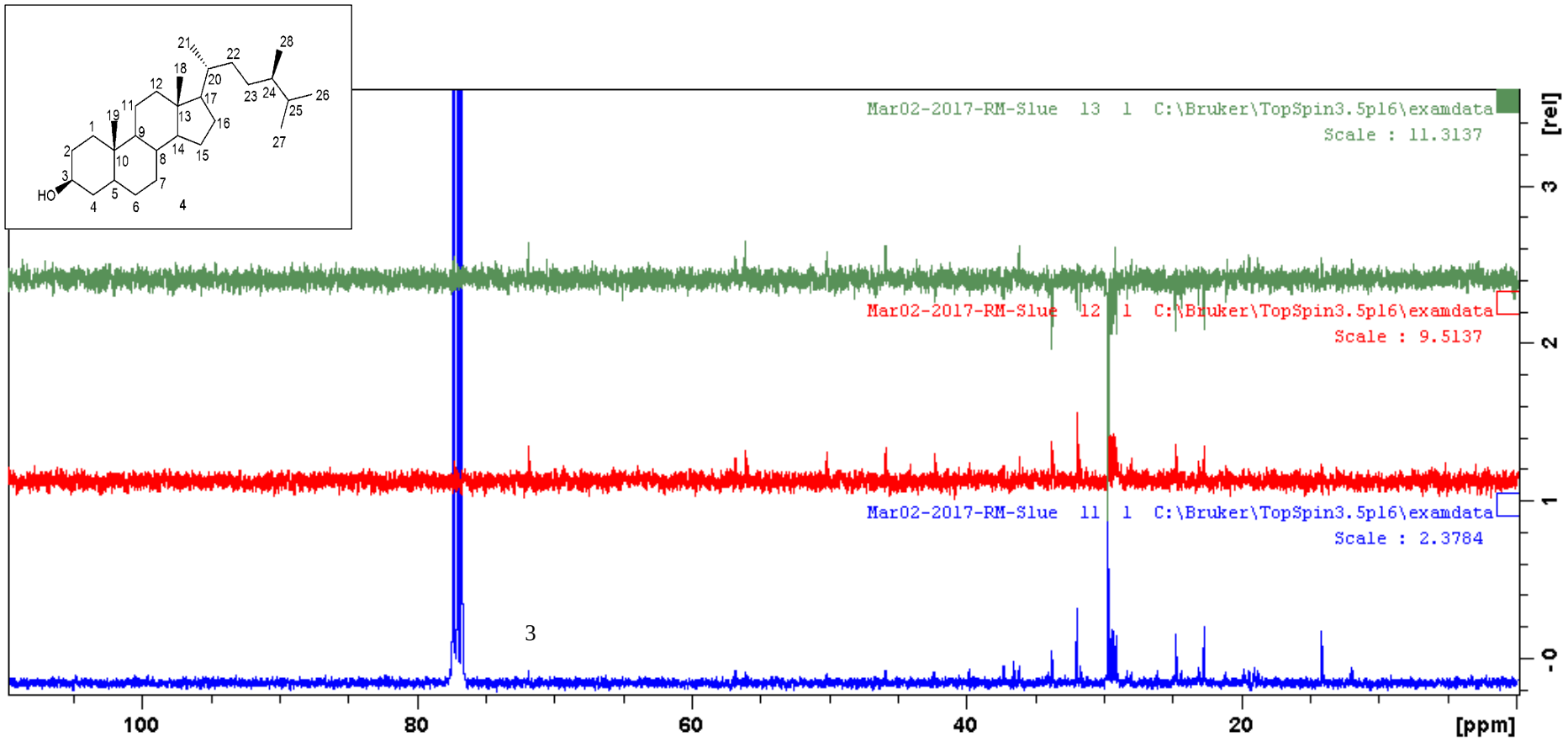

DEPT spectrum for Campestanol

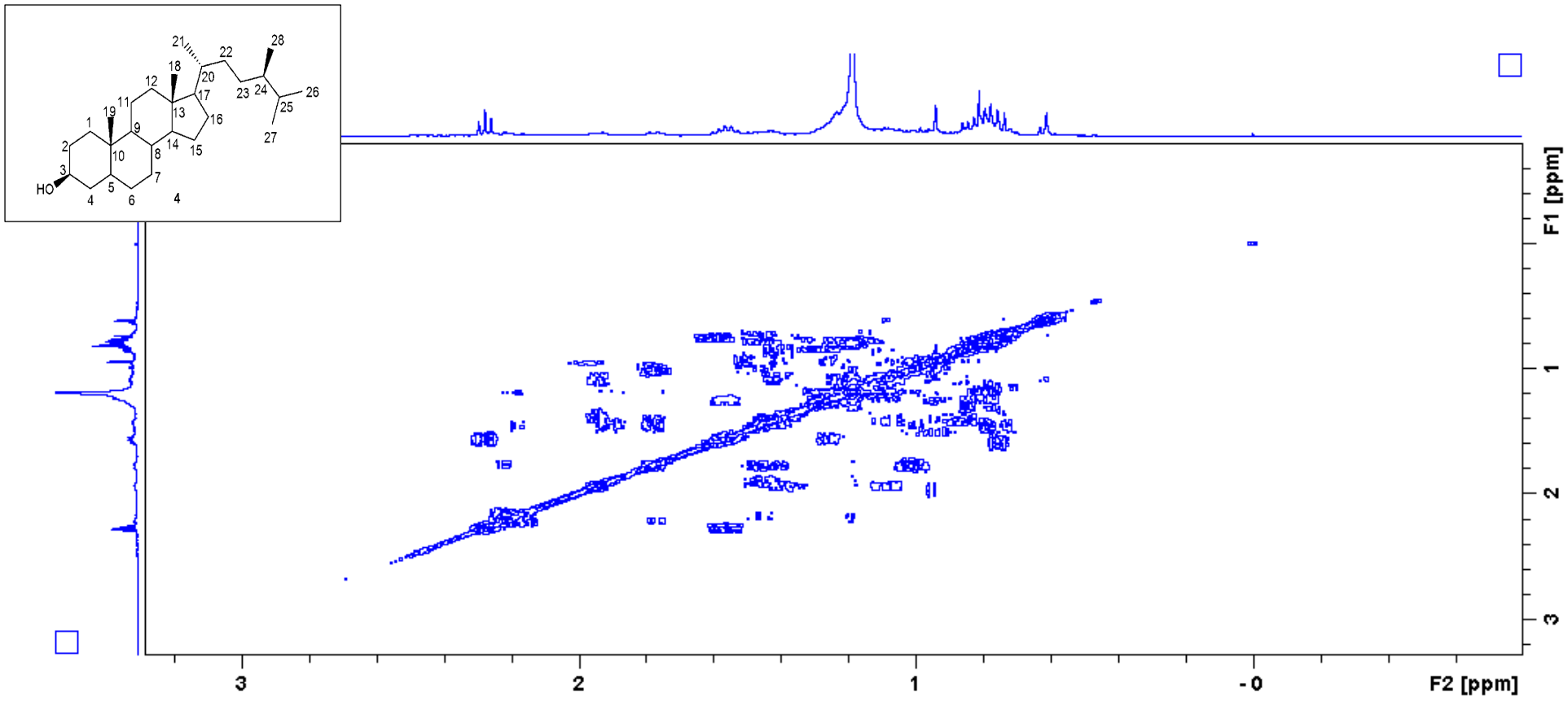

COSY spectrum for Campestanol

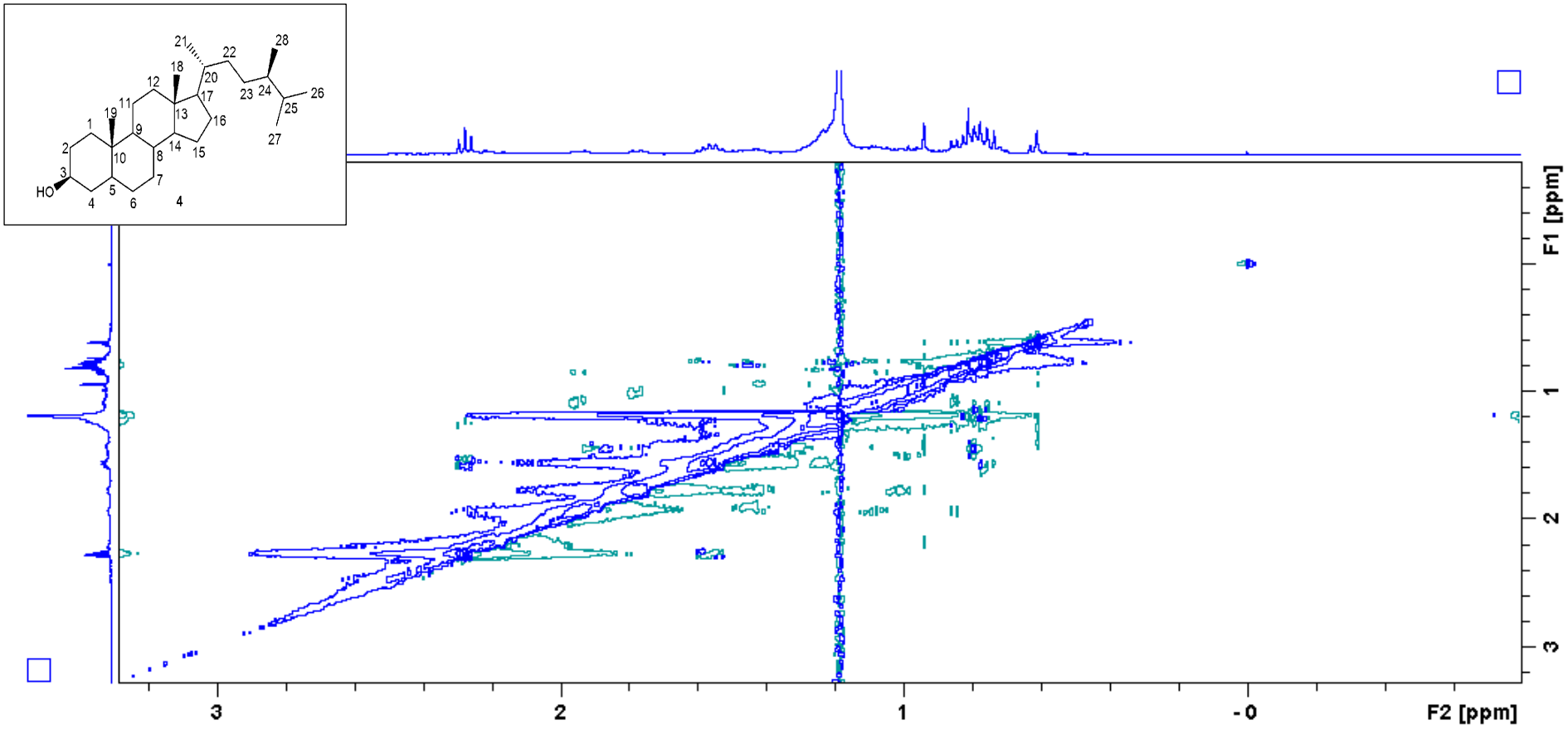

NOESY spectrum for Campestanol

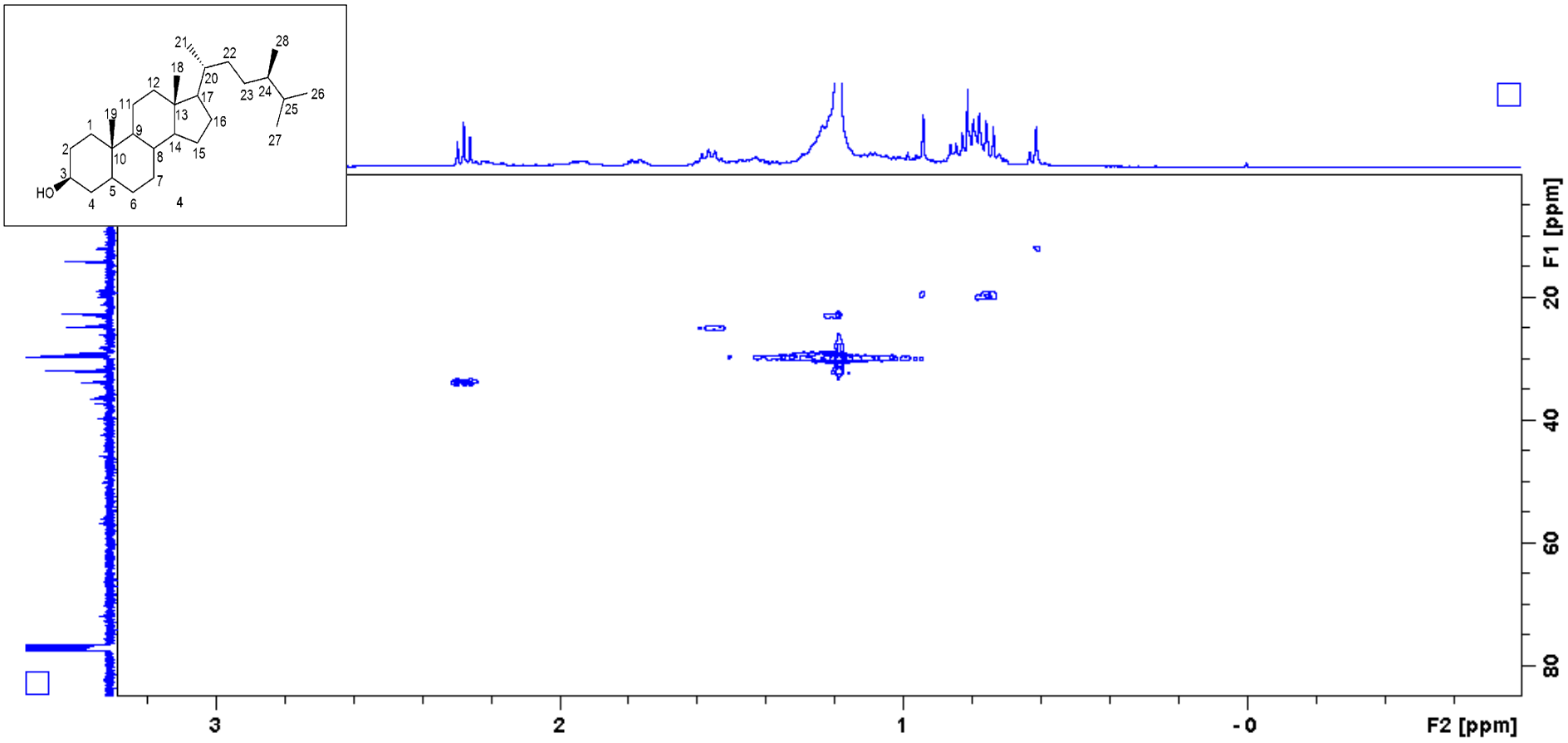

HSQC spectrum for Campestanol

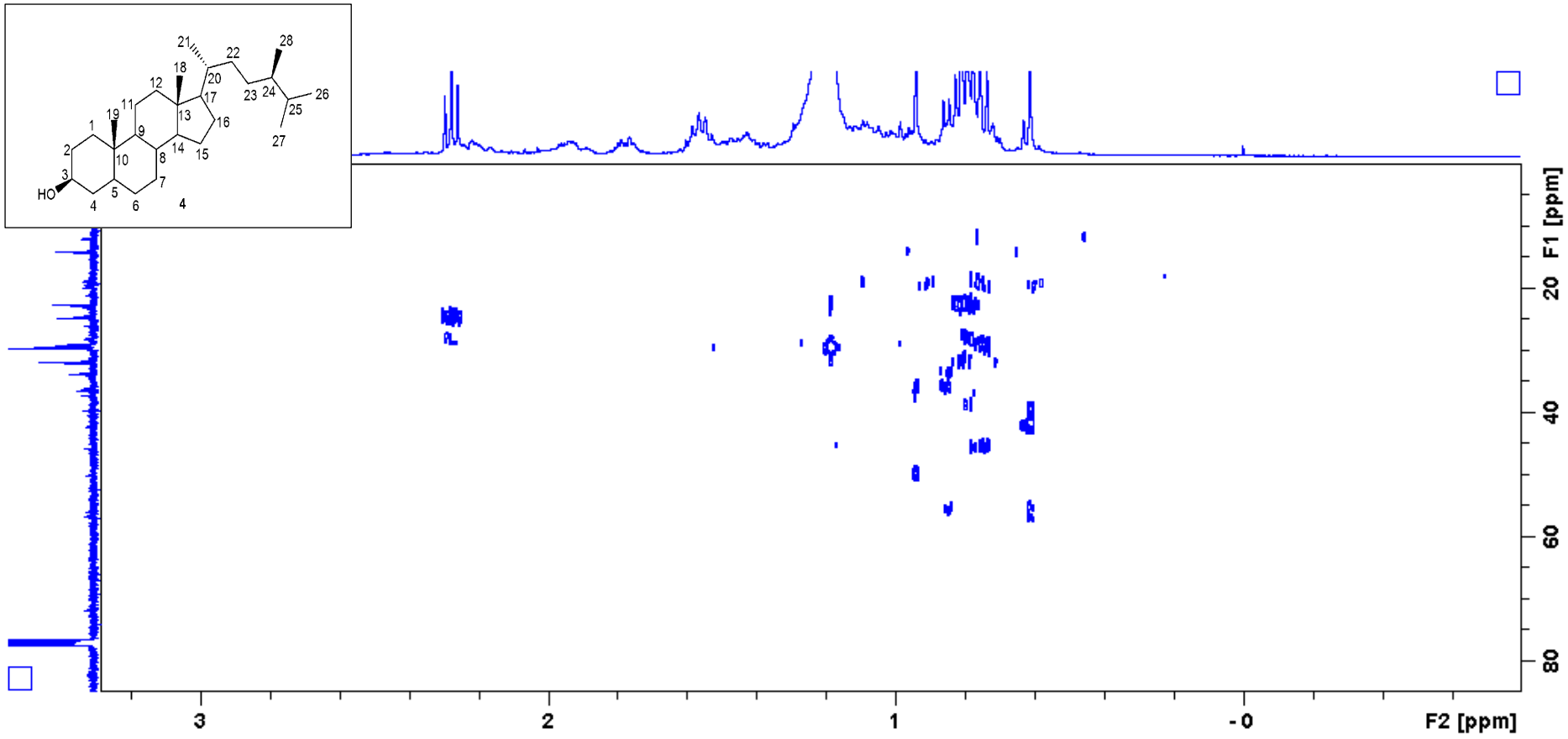

HMBC spectrum for Campestanol

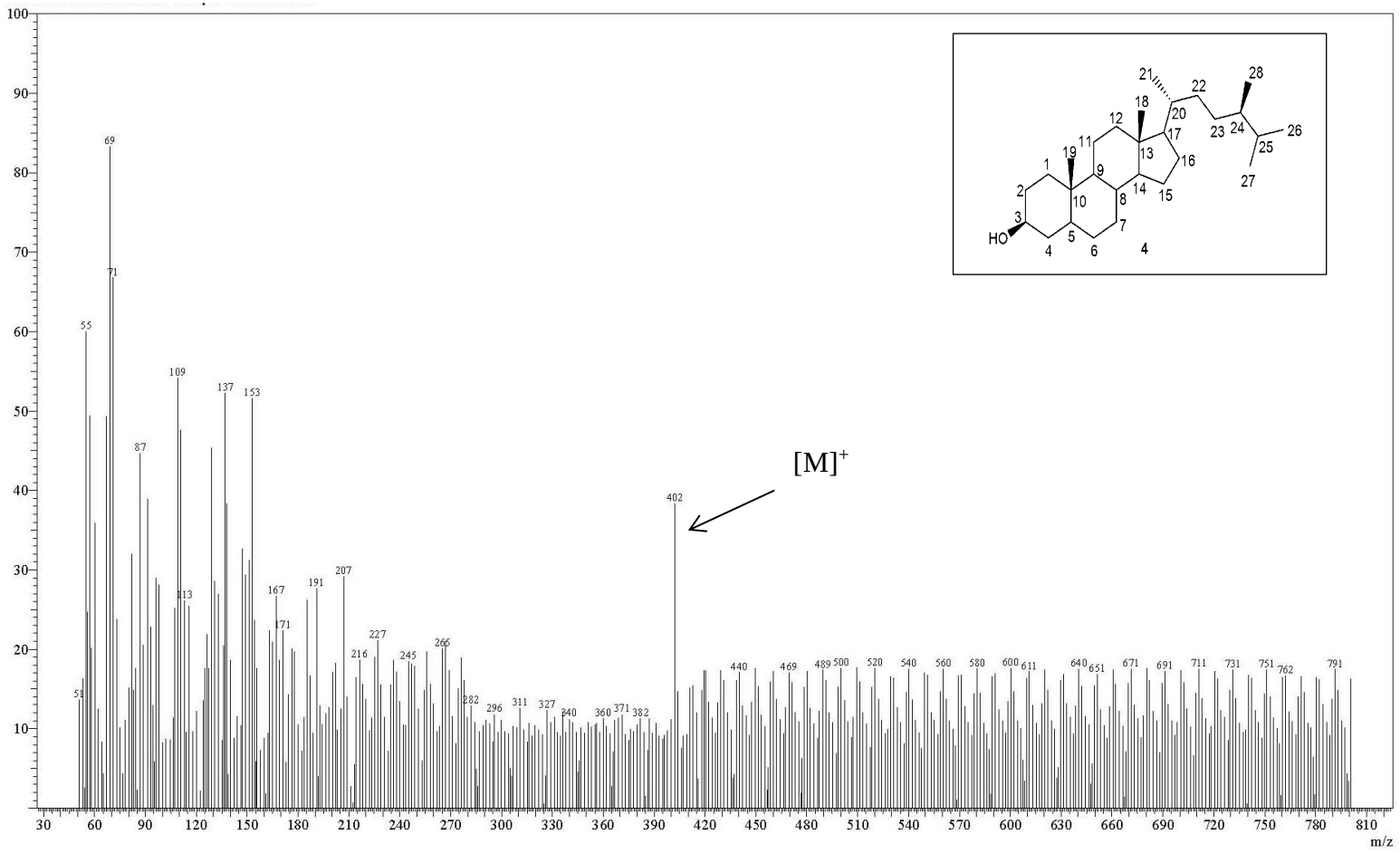

GC-MS spectrum for Campestanol

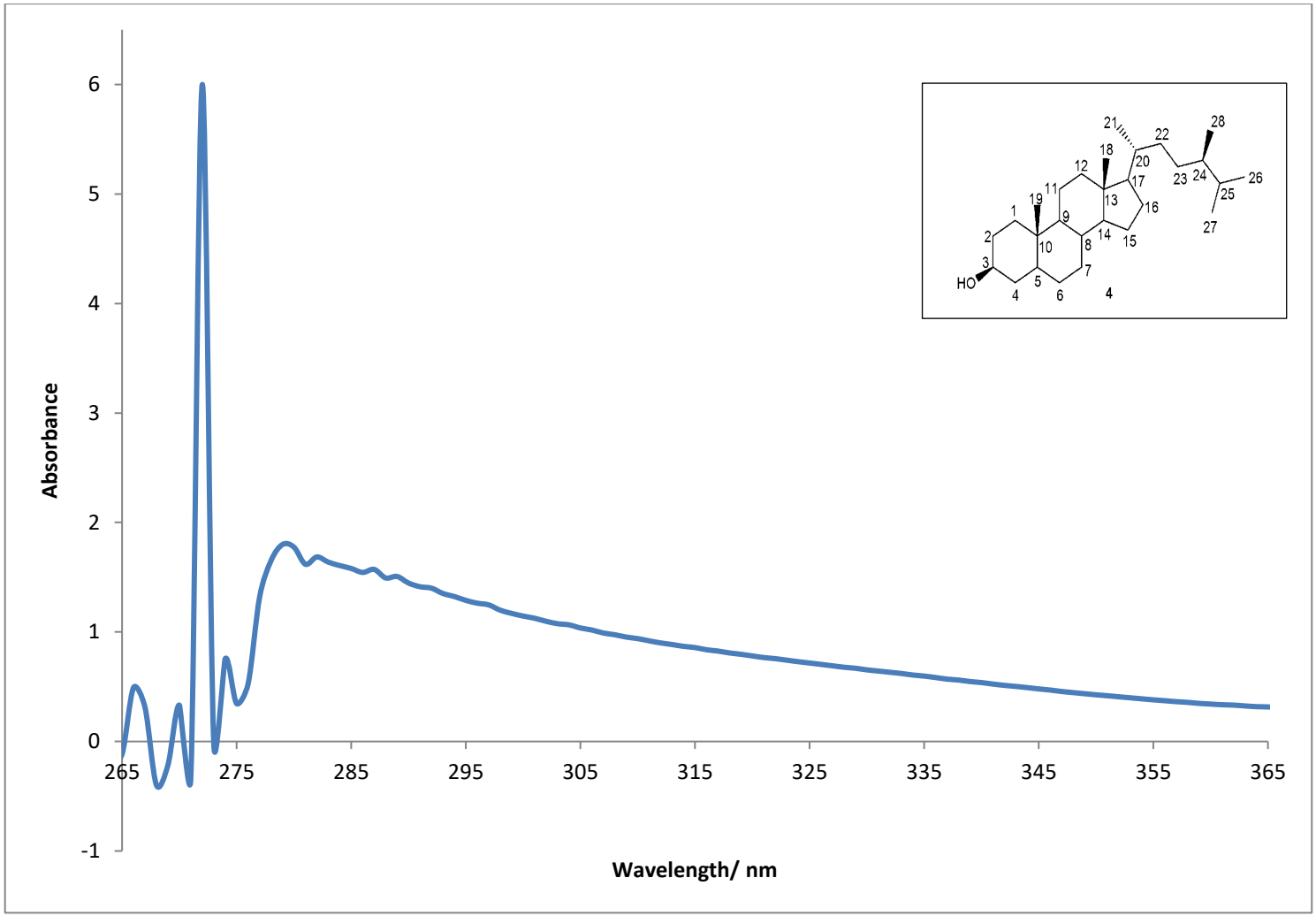

UV-Vis spectrum for Campestanol

FTIR spectra of NPs

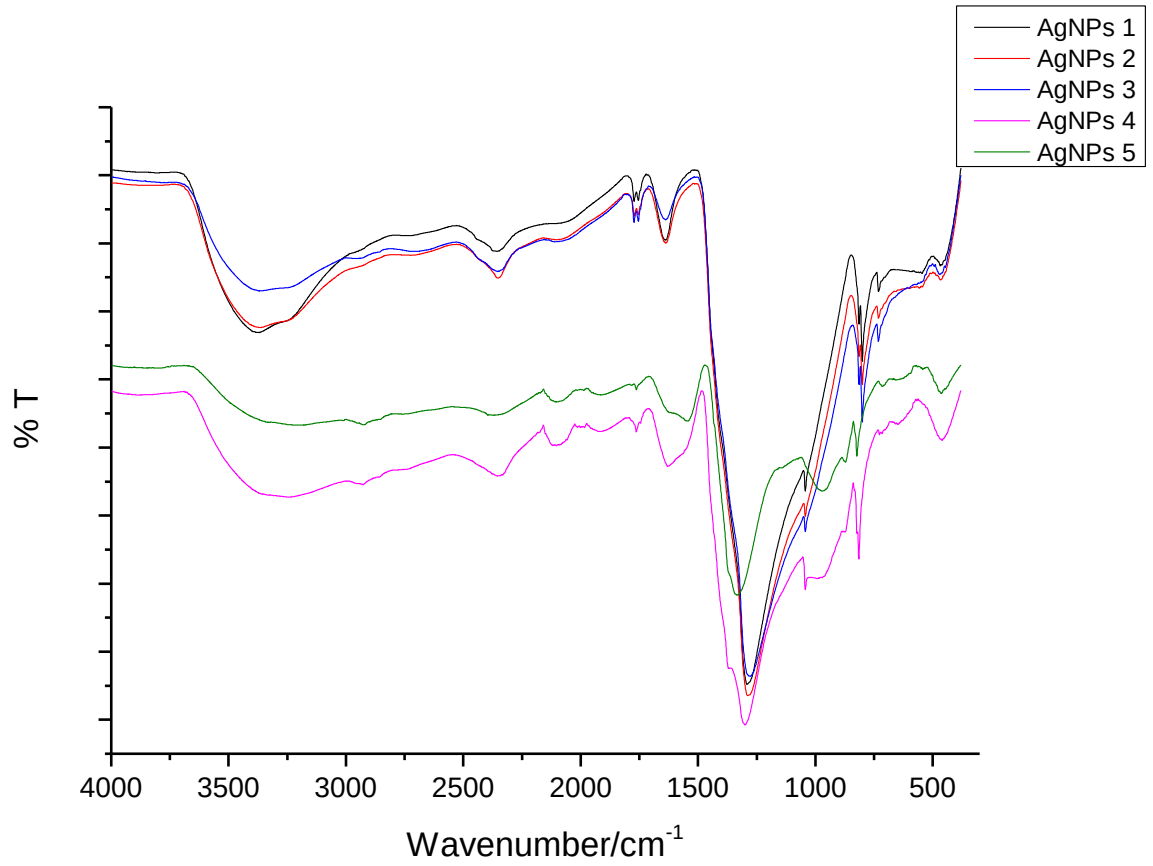

FTIR spectra of the CAgNPs synthesised from the aqueous extract (1, 2, 3, 4 and 5 represent the different concentrations)

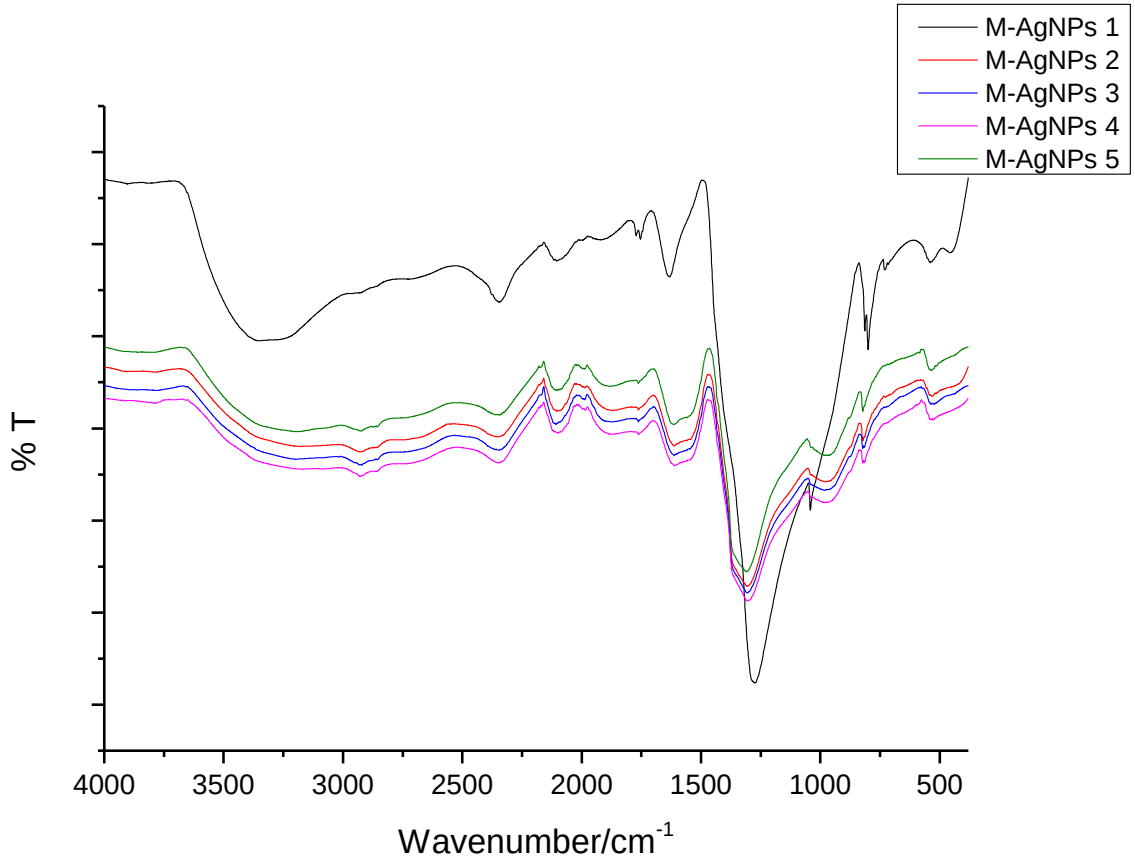

FTIR spectra of the CAgNPs synthesised from the MeOH extract (1, 2, 3, 4 and 5 represent the different concentrations)

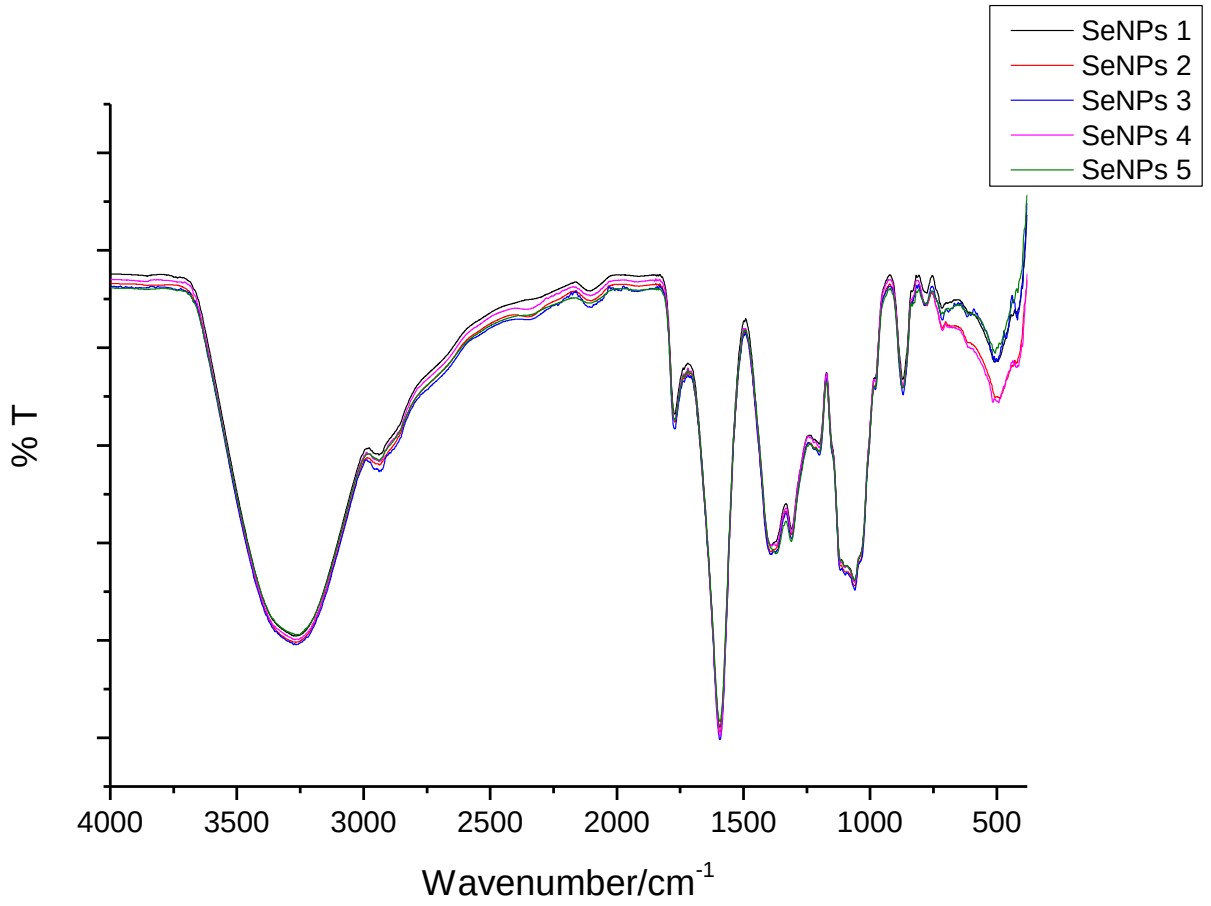

FTIR spectra of the CSeNPs synthesised from the aqueous extract (1, 2, 3, 4 and 5 represent the different concentrations)

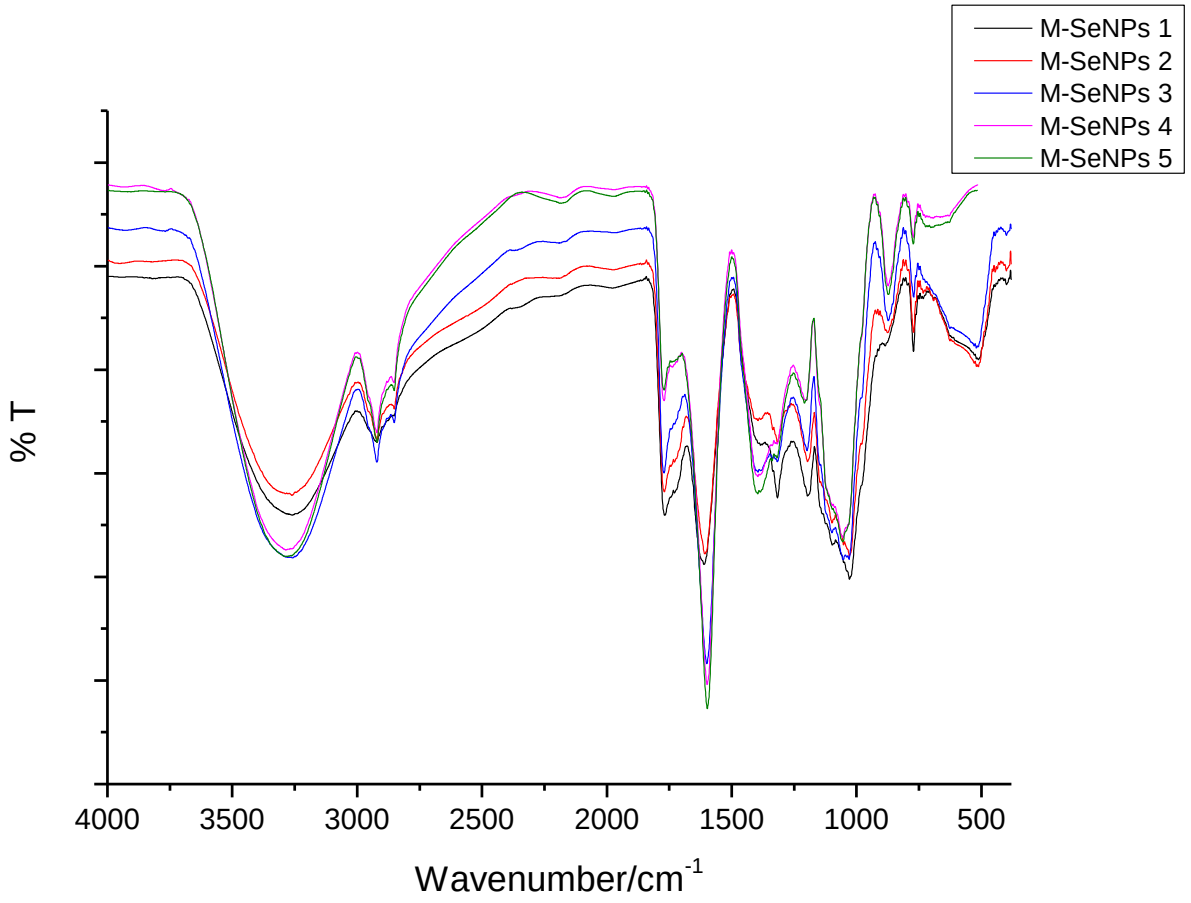

FTIR spectra of the CSeNPs synthesised from the MeOH extract (1, 2, 3, 4 and 5 represent the different concentrations)